NOVA SCHOOL OF SCIENCE & TECHNOLOGY

DEPARTAMENT OF LIFE SCIENCES

MARIA MARGARIDA FERREIRA BRÁS

BSc in Biomedical Sciences

Mechanisms of immune modulation mediated by Mesencephalic Astrocyte-derived Neurotrophic Factor

MASTER IN MOLECULAR GENETICS AND BIOMEDICINE

NOVA University Lisbon

September 2022

DEPARTAMENT OF LIFE SCIENCES

Mechanisms of immune modulation mediated by Mesencephalic Astrocyte-derived Neurotrophic Factor

MARIA MARGARIDA FERREIRA BRÁS

BSc in Biomedical Sciences

Adviser: Pedro Miguel Sousa Corado Victor
Group Leader
Instituto de Medicina Molecular | Universidade de Lisboa

Co-adviser: Paula Alexandra Quintela Videira
Assistant Professor
NOVA School of Science and Technology | NOVA University Lisbon

Examination Committee:

Chair: Maria Alexandra Núncio de Carvalho Ramos Fernandes
Assistant Professor
NOVA School of Science and Technology | NOVA University Lisbon

Rapporteur: Karine Marie Serre
Staff Scientist
Instituto de Medicina Molecular | Universidade de Lisboa

Adviser: Pedro Miguel Sousa Corado Victor
Group Leader
Instituto de Medicina Molecular | Universidade de Lisboa

MASTER IN MOLECULAR GENETICS AND BIOMEDICINE

NOVA University Lisbon
September 2022

Mechanisms of immune modulation mediated by Mesencephalic Astrocyte-derived Neurotrophic Factor

ACKNOWLEDGMENTS

This project was only possible thanks to the help, guidance, and support of many people. Therefore, I would like to express my deepest gratitude to everyone that was, somehow, involved.

Firstly, I would like to thank doctor Pedro Sousa-Victor and doctor Joana Neves for giving me the opportunity to embrace this project and for having the patience to teach and guide me throughout the whole year. It was an honour to learn from them and to work in their laboratory and at the *Instituto de Medicina Molecular.*

I would also like to express my special thanks to my colleagues at the lab and to everyone that passed through the lab during the last few months. To Neuza, for everything that she taught me and for all the help and support during the development of this project. To Inês, for taking care of the mice, for all the assistance and guidance, and all the coffee, laughs and comforting words. To Ana and Débora, for sharing with me the happiness and the difficulties of being a master's student. Thanks for always being by my side and for all the mutual help. It was truly a great pleasure to work with all of you.

A special thanks to all the facilities at IMM involved in this project. To the Bioimaging and Flow Cytometry facilities, thanks for all the help and assistance.

Then, I have to say a huge thank you to my friends that made all this challenging journey lighter and a little less stressful. To my friends in Lisbon, thank you for the most beautiful experiences here, all the laughs and the gatherings to relax and unwind. To Diana, the other half of the package, thank you for all the adventures. For all your tutorial videos, jokes, positivity, and reassuring words. To Sara, thanks for being so supportive, for all the talks, coffee breaks and nerdy jokes. You truly are amazing, and it was incredible to have you only 3 doors away. To Adriana, my roomie and bestie, thank you for welcoming me into your house, for believing in me and for being by my side over the past 10 years (10!!). Your healing hugs and croissant surprises are the best! You know that without your help this wouldn't be possible!

Finally, I have to express my deepest gratitude to my family, that always supported me and truly believed in me. A special thanks to my parents for all the late-night talks, for all the encouragement, support, love and affection. And last but not the least, to my best friend/partner in crime/personal coach, who I'm proud to call brother. Thanks for forcing me to go outside, go to concerts and experience the little things in life, but, especially, thanks for believing that I'm capable! No words will ever be enough to thank you!

Thank you all for everything!

"Terra firme só não vale
Porto seguro é não ter medo"
Terra Firme, Benjamim

ABSTRACT

Aging is characterized by a progressive decline in tissue function and integrity and an overall decline in regenerative potential. This reduction can be attributed to stem cell intrinsic dysfunctions and alterations in the local and systemic environments, including age-related immune dysfunction. The skeletal muscle is a paradigmatic model to study age-associated loss of regenerative capacity. Muscle repair depends on the precise coordination between myogenesis and the immune response and relies on the balance between pro- and anti-inflammatory signalling.

Mesencephalic Astrocyte-derived Neurotrophic Factor (MANF) is an evolutionarily conserved protein with immunomodulatory and tissue repair functions. MANF is widely expressed in the body and was found to be transiently induced during skeletal muscle regeneration, particularly by pro-repair macrophages. However, its levels are downregulated during aging, which is associated with impairments in muscle regeneration and immune responses.

In the present study, we intend to investigate the role of MANF in the process of immune modulation during skeletal muscle regeneration. Here, we demonstrate that organismal MANF loss results in a severe regenerative failure with accumulation of necrotic fibres and failure in myofibers formation. Ubiquitous loss of MANF disrupts the immune response to damage, affecting myeloid accumulation, macrophages transition towards a pro-repair state, bone marrow emergency hematopoiesis and the numbers of circulating monocytes. We further explore the specific role of MANF on macrophages, identifying a potential autocrine function in the phenotypic transition of macrophage subpopulations. In addition, we uncover intrinsic alterations in pro-repair macrophages with MANF ablation that can be associated with defective digestion of cellular debris.

This work demonstrates how a systemic immune modulator can regulate the immune response to tissue damage at multiple levels, including in the production of myeloid cells and locally during the regenerative process.

Keywords: MANF, Immunomodulation, Regeneration, Skeletal muscle, Aging, Macrophages

RESUMO

O envelhecimento é caracterizado pela redução progressiva da integridade fisiológica e por um declínio da capacidade regenerativa dos tecidos. Este fenómeno está associado a limitações intrínsecas das células estaminais e a alterações sistémicas e do nicho onde se inserem, incluindo alterações da resposta imune. O músculo esquelético é um modelo clássico utilizado no estudo da redução da capacidade regenerativa associada ao envelhecimento. A sua regeneração depende de interações altamente reguladas entre as células estaminais musculares e as células imunes e de um equilíbrio entre os sinais pro- e anti-inflamatórios.

O Fator Neurotrófico derivado de Astrócitos Mesencefálicos (MANF) é uma proteína conservada, expressa por vários tipos celulares, com funções imunomoduladoras e de reparação tecidual. Durante a regeneração muscular, o MANF é transitoriamente expresso, particularmente por macrófagos anti-inflamatórios. Porém, durante o envelhecimento, os seus níveis estão reduzidos o que se associa ao comprometimento da regeneração e da resposta imune.

Neste estudo temos como objetivo investigar o papel do MANF na regulação da resposta imune durante a regeneração muscular. Assim, demonstramos que a ausência completa de MANF resulta num severo comprometimento da regeneração, com acumulação de fibras necróticas e falha na formação de novas fibras. A perda ubíqua de MANF provoca uma falha da resposta imune, afetando a acumulação de células mieloides, a transição fenotípica dos macrófagos, o processo hematopoiético de emergência e a constituição celular do sangue. Exploramos também o papel específico do MANF nos macrófagos, identificando um possível mecanismo autócrino na transição fenotípica dos macrófagos. Por fim, identificamos alterações estruturais nos macrófagos pro-regenerativos com deleção de MANF, potencialmente associadas a falhas na digestão de material celular.

Assim, este trabalho demonstra como um modulador imune sistémico pode regular a resposta imunológica ao dano tecidual a vários níveis, incluindo na produção de células mieloides e localmente durante o processo regenerativo.

Palavras-chave: MANF, Modulação imune, Regeneração, Músculo Esquelético, Envelhecimento, Macrófagos

CONTENTS

LIST OF FIGURES ..... **XIX**

LIST OF TABLES ..... **XXI**

ACRONYMS ..... **XXIII**

1 INTRODUCTION **1**

1.1 Aging 1

1.1.1 Hallmarks of Aging 1

1.1.2 Inflammaging and Immunosenescence 2

1.1.3 Regenerative Capacity and Aging 3

1.2 The Skeletal Muscle 4

1.2.1 Skeletal Muscle Anatomy/Physiology 4

1.3 Regeneration of Skeletal Muscle 5

1.3.1 Muscle Stem cells 5

1.3.2 Myogenesis 6

1.3.3 Cells supporting myogenesis 7

1.3.4 Immune response during skeletal muscle regeneration 8

1.3.4.1 Myeloid Cells and the immune response to injury 8

1.3.4.2 Origin of immune cells: Hematopoiesis 11

1.4 Skeletal Muscle Aging 13

1.4.1 Sarcopenia 13

1.4.2 Impact of aging on MuSCs 14

1.5 Mesencephalic astrocyte-derived neurotrophic factor 15

1.5.1 MANF and Immune responses 16

1.5.2 MANF and Aging 16

1.5.3 MANF and skeletal muscle regeneration 17

1.6 Aims of the project 18

2 MATERIALS AND METHODS **19**

2.1 Animal Models 19

2.2 *In vivo* procedures 20

2.2.1 Tamoxifen intra-peritoneal injections 20
2.2.2 Muscle injury 20
2.3 Genotyping 20
2.4 Blood collection, processing, and analysis 22
2.4.1 Blood collection and processing 22
2.4.2 Blood cells Staining for Flow Cytometry and Gating Strategy 22
2.5 Bone Marrow collection, Processing and Analysis 24
2.5.1 Bone Marrow harvesting and processing 24
2.5.2 Bone Marrow Cells Staining for Flow Cytometry and Gating Strategy 24
2.6 Muscle collection, processing, and analysis 27
2.6.1 Muscle collection and storage 27
2.6.2 Histological analysis, imaging, and quantification methods 27
2.6.2.1 Hematoxylin and Eosin (H&E) staining and image acquisition 27
2.6.2.2 Immunohistochemistry, imaging, and quantification methods 27
2.6.3 Protein Analysis 28
2.6.3.1 Protein Extraction and Quantification 28
2.6.3.2 Western Blot 29
2.6.4 Muscle cell population analysis by FC or FACS 30
2.6.4.1 Muscle Cell Population Isolation 30
2.6.4.2 Muscle cells staining for Flow Cytometry and Fluorescence-Assisted Cell Sorting Analysis and Gating Strategies 30
2.7 *Ex-vivo* macrophage analysis 33
2.8 Transmission Electron Microscopy analysis of macrophages 33
2.8.1.1 Macrophages isolation and samples processing 33
2.8.1.2 TEM Images Quantification 33
2.9 Statistical Analysis 34
3 RESULTS AND DISCUSSION 35
3.1 Consequences of organismal MANF loss on skeletal muscle regenerative capacity. 35
3.1.1 Model Validation 35
3.1.2 Effects of organismal MANF loss on skeletal muscle regenerative efficiency . 37
3.1.2.1 Overall effects on skeletal muscle regeneration 37

3.1.2.2 Effects on the clearance of necrotic debris 38
3.1.2.3 Effects on the myogenic process 39
3.1.3 Effects of organismal MANF loss on the different populations involved in muscle regeneration 41
3.1.4 Effects of organismal MANF loss on the myeloid populations in the regenerating muscle 42
3.1.5 Long-term effects of organismal MANF loss on regeneration and survival 44
3.2 Causes of immune dysfunction during a regenerative pressure upon MANF ablation 46
3.2.1 Impact of MANF loss on blood circulating cells after skeletal muscle injury 46
3.2.2 Impact of MANF loss on bone marrow populations after skeletal muscle injury 48
3.2.3 Effects of MANF loss in the phenotypic transition of macrophages 50
3.2.4 Pro-repair macrophages alterations upon MANF ablation 53
4 CONCLUSIONS 57
4.1 Future Perspectives 58
REFERENCES 59
A APPENDIX 67

LIST OF FIGURES

Figure 1.1 - Myogenic process during skeletal muscle regeneration 7

Figure 1.2 - Timeline of the inflammatory response triggered after an injury and the myogenic phase associated. 9

Figure 1.3 - Schematic illustration of the hematopoietic process in the bone marrow. 13

Figure 2.1 - Flow cytometry gating strategy to analyse immune cell populations in mouse peripheral blood..... 23

Figure 2.2 - Flow cytometry gating strategy to analyse bone marrow hematopoietic cell populations..... 26

Figure 2.3 - Flow cytometry gating strategy used to analyse the different populations involved in muscle regeneration 32

Figure 2.4 - Flow cytometry and FACS gating strategies used to analyse and isolate the immune cell populations in the regenerating skeletal muscle 32

Figure 3.1 - Validation of MANF deletion on the Rosa26$^{CRE-ERT/+}$Manf$^{fl/fl}$ mouse model by PCR 36

Figure 3.2 - MANF expression levels in injured muscles from Rosa26$^{CRE-ERT/+}$Manf$^{fl/fl}$ mouse model at 3dpi..... 37

Figure 3.3 - Histological analysis of the impact of MANF loss in the regeneration process at 4 dpi by H&E 38

Figure 3.4 - Impact of MANF loss on necrotic fibres clearance at 4 dpi 39

Figure 3.5 - Impact of MANF loss on the formation of new myofibers (eMHC^{pos}) at 4 dpi 40

Figure 3.6 - Effects of organismal MANF loss on the different populations involved in muscle regeneration analysed by Flow Cytometry..... 42

Figure 3.7 - Effects of organismal MANF loss on the myeloid populations involved in muscle regeneration evaluated by Flow Cytometry..... 43

Figure 3.8 - Long-term effects of organismal MANF loss on survival and regeneration. 45

Figure 3.9 - Impact of organismal MANF loss on the blood cell populations analysed by Flow Cytometry. 47

Figure 3.10 - Impact of organismal MANF loss on the bone marrow cell populations analysed by Flow Cytometry. 49

Figure 3.11 - Impact of conditional MANF deletion on the phenotypic transition of cultured macrophages, assessed by Flow Cytometry 52

Figure 3.12 - Impact of MANF supplementation on the phenotypic transition of cultured MANF-deficient macrophages analysed by Flow Cytometry 53

Figure 3.13 - Impact of MANF ablation in pro-repair macrophages evaluated by TEM 54

LIST OF TABLES

Table 2.1 - Sequences of the primers used for genotyping PCR. 20

Table 2.2 - PCR program conditions for *Manf*^{fl} amplification 21

Table 2.3 - Fluorochrome conjugated antibodies used for blood cell analysis by flow cytometry 22

Table 2.4 - Fluorochrome conjugated antibodies used for bone marrow cell population analysis by flow cytometry 25

Table 2.5 - Fluorochrome conjugated antibodies used for muscle cell population analysis by flow cytometry. 31

ACRONYMS

$BaCl_2$: Barium Chloride

BM: Bone Marrow

bp: base pairs

BSA: Bovine Serum Albumin

BV: Brilliant Violet

$CaCl_2$: Calcium dichloride

CCL2: CC-chemokine ligand 2

CCR2: C-C chemokine receptor type 2

CD11b: Integrin alpha-M

CD14: Custer of differentiation 14

CD150 (SLAM): cluster of differentiation 150 (signalling lymphocyte activation molecule)

CD16: Cluster of differentiation 14 / Fc gamma receptor IIIa

CD31: Platelet endothelial cell adhesion molecule

CD34: Cluster of Differentiation 34

CD3e: Cluster of differentiation 3 epsilon

CD45: lymphocyte common antigen

CD48: cluster of differentiation 48

CLPs: common lymphoid progenitors

CMPs: common myeloid progenitors

CSA: cross-sectional area

CX3CR1: Chemokine C-X3-C motif receptor 1

CXCL1: CXC-chemokine ligand 1

DAMPs: damaged-associated molecular patterns

DAPI: 4′,6-diamidino-2-phenylindole

DMEM: Dulbecco's Modified Eagle's Medium

DNA: Deoxyribonucleic acid

dpi: days post injury

ECM: Extracellular Matrix

EDTA: Ethylenediaminetetraacetic acid

eMHC: embryonic Myosin Heavy Chain

ER: Endoplasmic reticulum

FA: formaldehyde

FACS: Fluorescent-ctivated cell sorting

FAPs: Fibro-adipogenic progenitors

FBS: Fetal Bovine Serum

FC: Flow cytometry

FcγR: Fc gamma receptor

fl: floxed

FSC: forward scatter

GMPs: granulocyte-macrophage progenitors

H&E: Hematoxylin and Eosin

HRP: horseradish peroxidase

HS: Horse Serum

HSCs: hematopoietic stem cells

IGF-1: Insulin-like growth factor 1

IL-10: Interleukin 10

IL1β: Interleukin 1 beta

IL-6: interleukin 6

iMM: Instituto de Medicina Molecular

kDa: kilodalton

loxP: locus of X-over P1

LT-HSC: Long-term hematopoietic stem cells

Ly6C: lymphocyte antigen 6 complex, locus C

Ly6G: Lymphocyte antigen 6 complex, locus G

MANF: Mesencephalic astrocyte-derived neurotrophic factor ()

MEPs: megakaryocyte-erythrocyte progenitors

MPPs: Multipotent progenitors

MRF4: Myogenic regulatory factor 4

MuSCs: Muscle Stem Cells

Myf5: Myogenic regulatory factor 5

MyoD: Myogenic Differentiation Protein 1

Neg: Negative

NFkB: Nuclear factor kappa B

NTFs: neurotrophic factors

P/S: Penicillin-Streptomycin

Pax7: Paired box transcription factor 7

PB: phosphate buffer

PBS: Phosphate-buffered saline

PBS-T: Phosphate-buffered saline 0.1% Tween20

PCR: Polymerase Chain Reaction

PDGF: Platelet-derived growth factor VEGF: vascular endothelial growth factor

PDGFRα: platelet-derived growth factor receptor alpha

PFA: Paraformaldehyde

Pos: Positive

QC: Quadriceps

RBC: Red Blood Cell

rMANF: recombinant MANF

ROS: Reactive Oxygen Species

RT: Room Temperature

SASP: Senescence-associated secretory phenotype

Sca1: stem cells antigen-1

SCs: Stem Cells

SDS-PAGE: Sodium Dodecyl Sulfate Polyacrylamide Gel Electrophoresis

SEM: standard error of the mean

SSC: Side scatter

ST-HSC: Short-term hematopoietic stem cells

TA: Tibialis anterior

TAE: Tris-Acetate-Ethylenediaminetetraacetic acid

Tam: Tamoxifen

TBS: Tris-buffered saline

TBS-T: Tris-buffered saline-0.1% Tween20

TEM: Transmission Electron Microscope

TGFb: Transforming growth factor beta

TNFa: Tumor Necrosis Factor alpha

WT: Wild-type

1

INTRODUCTION

1.1 Aging

World´s population aging is a worldwide phenomenon that reflects, in large part, the advances in public health and scientific, technological, and socioeconomic development[1,2]. In 2019, approximately 703 million people were 65 years old or more and the elderly population is expected to more than double in the next 30 years, reaching more than 1.5 billion in 2050[1].

Nowadays, all societies are experiencing an increment in life expectancy. This, associated with the decline of fertility, contributes to an increasing elderly population at a faster pace than before. This ongoing fast demographic shift is accompanied by socioeconomic and health challenges since aging represents a major risk factor for debilitating and life-threatening diseases, all of which are increasing in prevalence[1,2].

At a biological level, aging is a complex process characterized by a progressive decline of integrity and function of most tissues, which leads to increased cell and tissue damage and vulnerability to diseases[3,4]. Despite being an extremely heterogeneous process, that depends on genetic inheritance and physical and social environments, aging is associated with many conditions including chronic, degenerative, metabolic, cardiovascular, pulmonary, immune, and musculoskeletal diseases/disorders[5,6]. Moreover, older people are more likely to experience comorbidities and geriatric syndromes[6].

Therefore, a better understanding of the aging process and its role in such diseases is crucial to prevent disease development and progression and to improve the quality of life of the elderly.

1.1.1 Hallmarks of Aging

A series of interrelated processes, known as hallmarks of aging, are considered the fundamental mechanisms underlying aging. These hallmarks may have different contributions to cellular and tissue damage among different people, so collectively, they define the aging phenotype[3]. They can be divided into different categories. Processes that can be direct causes of damage are considered primary hallmarks and include genomic instability (accumulation of mutations throughout life), epigenetic changes, telomeric attrition and loss of proteostasis. On the other hand, mitochondrial dysfunction, senescence, and deregulation of nutrient sensing are recognized as antagonistic hallmarks since, at

low levels, they are positive responses to damage but over time, when exacerbated, become detrimental and damaging. Lastly, integrative hallmarks arise from accumulated damage induced by the previous hallmarks and are ultimately responsible for the phenotype. These include stem cell exhaustion (reduction and dysfunction) and alterations in intercellular communications[3].

Taken all together, these hallmarks contribute to one of the most evident characteristics of aging: the decline of the overall regenerative capacity of the organism[3].

1.1.2 Inflammaging and Immunosenescence

An important age-related alteration at the intercellular communication level is known as inflammaging. This is described as a chronic, sterile, and low-grade state of inflammation that progresses with age[3] and is characterized by increased basal levels of pro-inflammatory markers, including interleukin 1 beta (IL-1β), interleukin 6 (IL-6), tumor necrosis factor-α (TNFα) and C-reactive protein. Inflammaging has been associated with the etiology and progression of numerous age-related diseases and with increased vulnerability, morbidity, and mortality in the elderly[7].

This persistent inflammatory state can have multiple causes[3] involving the exacerbation of pro-inflammatory signalling. The diversity of stimuli triggering inflammaging usually converges on a few mechanisms and pathways such as overactivation of the nuclear factor kappa B (NFkB) signalling and activation of NLRP3 inflammasome[3,7,8].

Accumulation of cellular debris due to increased production and/or deficient clearance, mitochondrial dysfunction and dysfunctional autophagic responses may lead to this aged-associated phenotype[3,4,7]. Moreover, the accumulation of senescent cells associated with aging can contribute to inflammaging. These cells exhibit severe alterations in their secretome, described as senescence-associated secretory phenotype (SASP) that is characterized by the enrichment of pro-inflammatory cytokines, chemokines, and extracellular matrix (ECM) metalloproteinases[3,9].

Notably, during chronological aging, the immune system also undergoes remarkable alterations that lead to impaired immune responses, which contribute to inflammaging[7]. This is described as immunosenescence and affects both innate and adaptive immunity. This process results in increased vulnerability to infections and diseases and may result in chronic systemic inflammation[8,9].

The impact of aging on adaptive immunity has been well studied and it is established that its function declines with age[7,8]. On the other hand, innate immunity alterations due to aging have been associated with a defective and dysregulated response, with either loss or gain of function (hyperactivity)[7,9]. For instance, old monocytes/macrophages remain in a chronically activated state, with more and persistent expression of inflammatory molecules[10]. These cells have a dysfunctional activity, exhibiting an impaired phagocytic capacity[9,11].

As further explained in the next sections, healthy macrophages have a crucial role in inflammatory initiation and resolution, being able to switch from pro-inflammatory to anti-inflammatory phenotypes. This event may also be impaired with aging[12,13].

Taken together, these age-related immune alterations result in an imbalance between anti-inflammatory and pro-inflammatory signalling/responses[4], which contributes to tissue dysfunction and frailty and may be associated with deficient regenerative capacity[7,11].

1.1.3 Regenerative Capacity and Aging

Regeneration refers to the ability to replace and reconstitute lost/damaged cells, tissues, and structures. This comprises tissue turnover and responses to injuries. All organisms have some regenerative potential, which is essential for survival. However, this capacity varies greatly among species and tissues and throughout life[14,15].

Contrasting with other organisms, mammals have a very limited regenerative capacity, which relies on tissue-resident stem cells[15,16]. The healing process after an injury in mammals differs, depending on the nature and the extent of the injury and on the regenerative potential of the tissue involved[14,16].

Tissues with high regenerative ability, like skeletal muscle, liver and skin, can completely regenerate after an injury. These tissues can restore the normal and functional structure of the tissue by proliferation and differentiation of local stem cells. However, most tissues are incapable of complete regeneration, often leading to scar formation at the expense of tissue structure and function. Notably, very severe tissue damage often results in incomplete restoration and fibrotic scarring, even in tissues with high regenerative potential[14,16].

During aging, the regenerative potential declines, which is associated with tissue loss of function and structure and correlates with the general organismal decay[15]. Given the central role of stem cells in the regeneration process throughout life, aged-associated alterations in these cells, which are considered a hallmark of aging, contribute to compromised tissue maintenance and regeneration[4,15]. Alterations in stem cells include loss of self-renewal ability, functional and potency decline and alterations in proliferative behaviour[3,15].

In addition to intrinsic alterations in stem cells, changes in extrinsic factors during aging can also contribute to this age-related regenerative decay. These include alterations in the stem cell niche (where they reside) and in the systemic environment, for instance, in the immune system[4,15]. It is known that successful regeneration requires an effective biphasic immune response, that involves a first wave of pro-inflammatory signalling and a second wave of anti-inflammatory and pro-repair activity[17]. This response is precisely coordinated with stem cell activity and function, optimizing tissue clearance and remodelling. The balance between pro-inflammatory and anti-inflammatory signalling can affect the

regeneration outcome, which is particularly relevant during aging, as this process is characterized by inflammaging and immunosenescence, as previously mentioned[15].

Addressing the factors and mechanisms underlying the age-related regenerative decline provides insights into major roadblocks to effective tissue regeneration, which has potential high clinical relevance, especially, for regenerative medicine. This branch of medicine aims to develop therapies that restore and rejuvenate tissues using endogenous stem cells or exogenous cells derived from stem/progenitor cells. However, these interventions require a good understanding of the limitations imposed by the aging environment. Considering the collective role of intrinsic and extrinsic factors on regeneration potential, new approaches targeting them are emerging to improve stem cell-based therapies in old organs [4,11,15].

1.2 The Skeletal Muscle

A paradigmatic example of regeneration capacity is the skeletal muscle.

Skeletal muscle is considered one of the most abundant tissues in the body[18] and represents approximately 40% of total body mass[19,20]. This tissue is controlled by the somatic nervous system and is essential for several different and vital functions, namely voluntary and reflex movement, postural support, breathing, etc. It also controls thermogenesis[20,21] and energy demands by regulating hormones and energy reserves[20,22]. This tissue is characterized by high plasticity and adaptive capacity to physiological demands. It has a remarkable regeneration potential, allowing the formation of new fibres and tissue repair after severe injuries[20,23].

In addition to the striking regenerative and plasticity capacity, skeletal muscle is a very accessible tissue and there is a diversity of experimental models that could be used to compromise the muscle tissue and induce a regenerative pressure. This way, skeletal muscle is a classic and excellent model to study tissue regeneration[22].

Importantly, the regenerative capacity of skeletal muscle also undergoes marked decay with age, highlighting the importance of this tissue in regenerative and aging studies[17].

1.2.1 Skeletal Muscle Anatomy/Physiology

Skeletal muscle is composed of cylindrical and multinucleated fibres, known as myofibers, surrounded by connective tissue mainly composed of collagen fibrils. The entire muscle is encircled by an outer layer of dense connective tissue denominated epimysium. This layer is connected to the tendon, or in some cases, directly to the periosteum of bones, allowing muscle contraction while maintaining its structural integrity[22]. Within the muscle, myofibers are arranged in parallel bundles called fascicles, each one involved in another connective tissue layer designated perimysium. Inside each fascicle, myofibers are surrounded by a thin layer named endomysium. This whole connective tissue network provides

support to the muscle and allows vascularization and innervation necessary to the tissue[20,21,24]. Besides the endomysium, myofibers are encircled, more internally, by a basal lamina and a plasma membrane called sarcolemma. Each myofiber is a long contractile cell that has a high-protein synthesis demand. Within each cell, proteins are organized in myofibrils composed of myofilaments, namely, actin and myosin. These, alongside other regulatory and structural proteins, are highly arranged in groups, forming the sarcomeres, which are considered the basic functional/contractile unit of skeletal muscle[21].

Importantly, several different cell types reside in the skeletal muscle allowing its maintenance throughout life, including muscle stem cells (MuSCs), mesenchymal stem cells, fibroblasts, and resident immune cells[20].

1.3 Regeneration of Skeletal Muscle

Skeletal muscle is prone to different injuries throughout life, including mechanical trauma, myotoxic agents, degenerative diseases, ischemia, exposure to hot or cold temperatures, etc. These injuries disrupt myofibers integrity triggering a regenerative process[25,26].

The high regenerative potential of this tissue is, in large part, mediated by muscle stem cells (MuSCs), also known as satellite cells, that are able to engage the myogenic program and give rise to new myofibers. Nonetheless, the regulation of this process involves the cooperation of numerous other cell types and molecular components, being a tightly coordinated process[26].

Thus, the regeneration process is characterized by a sequence of interlinked events that include necrosis of injured myofibers, inflammation, MuSCs proliferation/differentiation, maturation of the newly formed fibres and remodelling of the restored tissue[14,23]. The regeneration phases are similar following different causes of injury, though the kinetics and amplitude of each may vary depending on the nature and extent of the injury[27]. The immune response and myogenesis are precisely coordinated, highlighting the pivotal role of both responses in muscle tissue regeneration[14,28].

1.3.1 Muscle Stem cells

MuSCs lie underneath the basal lamina, along the entire length of muscle fibres and in close proximity to them[20,23]. They represent 2.5%–6% of nuclei of a given muscle fibre, however, the proportion of MuSCs depends on several factors including muscle type, age, and species[20]. Like other stem cells found in adult tissues, MuSCs are characterized by their self-renewal and multipotency capacity. Thus, these cells can both replicate themselves, ensuring the stem cell pool maintenance, and generate progeny of committed progenitors capable of generating myofibers and restoring the damaged tissue[20].

Considering that skeletal muscle is a low turn-over tissue with reduced homeostatic renewal, MuSCs aren’t constantly active throughout life. Instead, MuSCs remain in a quiescent state and become

activated upon a regenerative pressure[11]. They express different surface and nuclear markers such as α7-integrin and paired box transcription factor 7 (Pax7)[20].

MuSCs reside in a niche, which is considered any cell population, tissue, or ECM in direct contact or close to the MuSCs, influencing their activity and function. MuSCs activity and fate depend on dynamic interactions between non-myogenic cells (immune and stromal cells) and ECM components[29].

1.3.2 Myogenesis

Under normal resting conditions, MuSCs are in a quiescent state and are characterized by the high and continuous expression of the Pax7, that is essential for their maintenance. In this state, MuSCs are in a G0 phase, exhibiting a reduced metabolism rate[20,23,30].

After an injury and tissue damage, several different extracellular signals such as growth factors and pro-inflammatory cytokines are released and stimulate the MuSCs' reentry into the cell cycle and therefore, its activation[20,23,31]. Activated MuSCs proliferate and migrate to the site of injury, originating myogenic progenitors, or myoblasts, that are characterized by the expression of the early myogenic commitment markers: myogenic regulatory factor 5 (Myf5) and/or myogenic differentiation protein 1 (MyoD)[23]. These, together with myogenin and myogenic regulatory factor 4 (MRF4), are myogenic regulatory factors that are sequentially expressed to control the myogenic program[31].

MyoD plays a key role in the proliferation and subsequent differentiation phase of myoblasts. It facilitates the cell cycle's exit through the induction of cell cycle inhibitors and enables the transition to the differentiation phase through the upregulation of myogenin. This last is an important differentiation factor since it activates genes implicated in contractility such as myosin heavy chain and troponin. MRF4 also plays an important role in late differentiation[20,31].

Once myoblasts start to differentiate, they become myocytes with an elongated shape[23] and begin to fuse with each other giving rise to new multinucleated fibres (myotubes), or fuse with the damaged fibres to repair them[20,31]. Newly formed myofibers, then, need to mature and develop all the proteins and organelles necessary to become completely functional. Thereafter, the function and structure of muscle tissue can be fully repaired[20].

It is important to mention that a subgroup of MuSCs withstand this myogenic process through the downregulation of MyoD, to maintain the MuSCs pool[23].

Myogenesis (Figure 1.1) can be characterized and identified by a series of morphological/histological alterations in skeletal muscle tissue. New myofibers are identified by their small calibre and centrally

located nuclei. They are also characterized by the expression of embryonic myosin heavy chain (eMHC), a protein that otherwise would only be present during embryonic development[23,31].

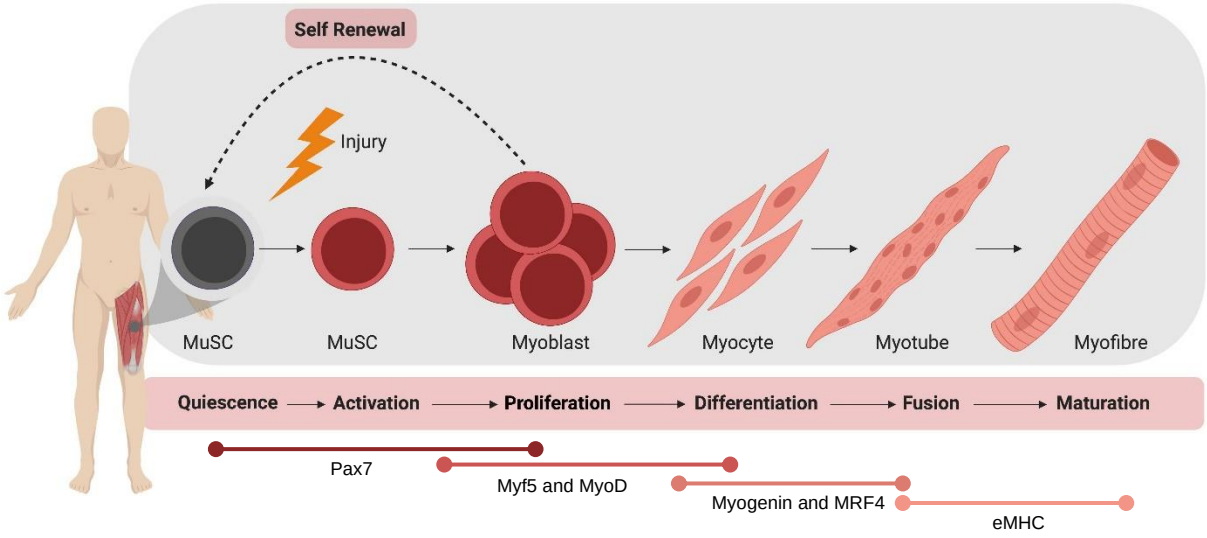

Figure 1.1 - Myogenic process during skeletal muscle regeneration
Upon an injury, quiescent muscle stem cells (MuSCs) become activated and proliferate originating myoblasts, that differentiate into elongated myocytes. These cells then fuse and mature, giving rise to new myofibers. During this process, MuSCs also sustain the maintenance of the stem cell pool producing undifferentiated progeny (self-renewal). Myogenic cells express different key modulators during the different stages of myogenesis. Quiescent and activated MuSCs express the paired box transcription factor 7 (Pax7). Myoblasts are characterized by the expression of myogenic regulatory factor 5 (Myf5) and/or myogenic differentiation protein 1 (MyoD). During differentiation, myocytes express myogenin and myogenic regulatory factor 4 (MRF4). New fibres express embryonic myosin heavy chain (eMHC). *Adapted from reference* [99].

1.3.3 Cells supporting myogenesis

The muscle regeneration process is supported not only by MuSCs but also by other resident and infiltrating cell types, that play important regulatory functions[30,32]. Immune cells, endothelial/vascular cells and fibro-adipogenic progenitors (FAPs) are among the non-myogenic cells that contribute to effective muscle repair.

FAPs are a bipotent mesenchymal cell type present in the interstitial space of the myofibers that can differentiate into fibroblasts and adipocytes and are characterized by the expression of platelet-derived growth factor receptor-α (PDGFRa) and stem cells antigen-1 (Sca1)[23,32,33]. Upon an injury, FAPs also became activated, having an important role in supporting myogenesis[32]. These cells secrete different proteins and molecules such as growth factors and cytokines that remodel the ECM and contribute to MuSCs commitment and differentiation. For instance, these undifferentiated FAPs can secrete molecules like IL-6, Insulin-like growth factor 1 (IGF-1) and Wnt1 that stimulate the differentiation of myoblasts[32,33].

During regeneration, vascular cells also dynamically interact with MuSCs, which is essential for revascularization but also for MuSCs regulation. Particularly, endothelial cells promote MuSCs growth by secreting a diversity of growth factors including IGF-1, platelet-derived growth factor (PDGF) and

vascular endothelial growth factor (VEGF). Endothelial cells also secrete cytokines that promote the recruitment of immune cells to the injury site [28,29].

1.3.4 Immune response during skeletal muscle regeneration

The immune system plays a crucial and complex role in tissue repair since the immune cells are involved in multiple stages of the regeneration process and interact dynamically with other cells, which ultimately determines the fate of the damaged tissue. Whether immune activation leads to complete regeneration and reconstitution of functional tissue or to scarring and fibrosis is determined by numerous factors including age, species, availability and status of the stem-cell pool[34]. Importantly, muscle healing outcome also depends on the balance between pro-inflammatory and anti-inflammatory signalling[27].

Upon severe injury and consequent tissue damage, a complex inflammatory response is triggered. This response is characterized by two main phases: a pro-inflammatory one, where leukocytes infiltrate the lesion site and contribute to the inflammatory state, and an anti-inflammatory or restorative phase, during which the tissue is reconstituted, and the inflammation is resolved. This shift in the immune response is mandatory for muscle healing[35].

1.3.4.1 Myeloid Cells and the immune response to injury

The innate immune system is considered one of the first lines of defence of the organism and is the most conserved component of immunity across species, even though the complexity differs significantly. Innate immune activity is readily activated in response to trauma or infection, being rapid but fairly non-specific[9]. Components of innate immunity perform essential functions during the regeneration process, and this involves both resident and infiltrating immune cells[20].

Tissue-resident immune cells, located within the interstitial space of the muscle, include resident macrophages, dendritic cells, mast cells, a subset of patrolling monocytes, among others. These cells act as sentinels, patrolling and sensing any alteration in tissue homeostasis[20,36].

Upon an injury, the sarcolemma of myofibers becomes compromised and cellular components are released into the extracellular space, triggering an immune response. This tissue-resident immune cells became readily activated, in particular, by damaged-associated molecular patterns (DAMPs) released by the necrotic myofibers. These DAMPs comprise nucleic acids, proteins, lipids, and other metabolites. Resident activated leukocytes, then, release a burst of cytokines and chemokines that facilitates the infiltration of circulating immune cells into the lesion site[20].

The first non-resident cells to be recruited within 1-3 hours after injury, are granulocytes, especially, neutrophils (Figure 1.2). These cells respond to DAMPs and chemotactic signals such as CC-chemokine ligand 2 (CCL2) and CXC-chemokine ligand 1 (CXCL1), secreted by resident cells.

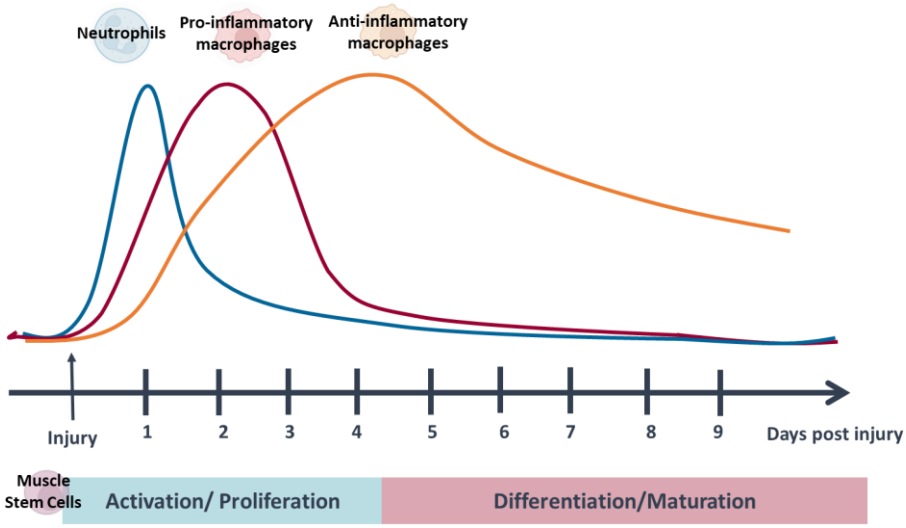

Figure 1.2 - Timeline of the inflammatory response triggered after an injury and the myogenic phase associated.
Upon an injury, a complex immune response is initiated, and neutrophils are the first non-resident cells to invade the tissue, reaching a maximum at 12-24h post-injury. Subsequently, circulating monocytes invade the tissue and differentiate into pro-inflammatory macrophages, peaking around 2 days post-injury. In this pro-inflammatory phase, factors secreted by the immune cells influence the myogenic process and stimulate the activation and proliferation of the muscle stem cells. Then, macrophages transit towards an anti-inflammatory pro-repair state. Consequently, the number of pro-inflammatory macrophages declines while the number of anti-inflammatory increases. This anti-inflammatory phase occurs within 4-8 days post-injury and facilitates the differentiation of the myogenic cells and the fusion and maturation of the myofibers. Original image, based on reference[36].

Neutrophils are essential for the initial removal of necrotic debris and further recruitment of more immune cells since they have a high phagocytic capacity and release several pro-inflammatory cytokines, chemokines, and enzymes/proteases[14,37]. Their large contribution to the pro-inflammatory microenvironment also influences the myogenic process[20]. During their activity, however, neutrophils produce large amounts of Reactive Oxygen Species (ROS) and oxidative byproducts[25,37]. Although ROS may activate important signalling pathways for muscle repair, overproduction and consequent excessive oxidative stress can contribute to further tissue damage[25,37,38]. Therefore, early invasion of neutrophils is an indispensable response to muscle damage, but their activity must be limited[36,38]. Neutrophil excessive recruitment and accumulation may exacerbate damage. In mice, these cells are typically identified by the expression of lymphocyte antigen 6 complex, locus G (Ly6G) and high levels of integrin alpha-M (CD11b)[36].

The infiltration of neutrophils peaks around 12-24h post-injury and decreases over a period of 2-4 days[14,36]. Following neutrophils, circulating monocytes are recruited to the site of injury.

In mice, two subpopulations of circulating monocytes can be distinguished based on the expression levels of lymphocyte antigen 6 complex, locus C (Ly6C), C-C chemokine receptor type 2 (CCR2) and Chemokine C-X3-C motif receptor 1 (CX3CR1)[39]. The non-classical monocytes have low expression of Ly6C (Ly6C^{Low}) and CCR2 and high levels of CX3CR1 and are known as patrolling monocytes. On the

other hand, the classical inflammatory monocytes are identified by the high expression of Ly6C (Ly6C^{High}) and CCR2 and low levels of CX3CR1[14,39]. Also in humans, monocytes can be divided into different categories. These subsets are identified according to the expression level of CD14 and CD16 and resemble, to some extent, the previously mentioned monocyte groups in mice. Mouse Ly6C^{High} monocytes are correlated with the human CD14^{High} / CD16^{Neg} monocytes whereas mouse Ly6C^{Low} monocytes correspond, at some level, to human CD14^{Low} / CD16^{High} [40].

Among the two subpopulations of mice's monocytes, Ly6C^{High} monocytes are the ones recruited to the injured muscle, in a process mainly dependent on CCL2/CCR2 interaction, and once in the tissue, they differentiate into Ly6C^{High} macrophages[39,40].

Macrophages are a highly heterogenic population with high phenotypic plasticity, which means these cells can adapt and adjust their phenotype and function accordingly to tissue necessities. Therefore, they have crucial roles in homeostasis and tissue repair. These cells are considered central players in the complex tissue response to injury, acting like both orchestrators and effectors of immune responses[14,26].

One of the major functions of macrophages is phagocytosis, which is essential for efficient muscle repair. These cells accumulate in the damaged site within a few days after an injury and remove necrotic myofibers and debris by phagocytosis. According to the literature, when the influx of macrophages to the injury site is blocked, debris accumulates in the tissue, which contributes to an impaired regeneration process[41]. Moreover, macrophages are also capable of neutrophils' clearance, which may contribute to the resolution of the pro-inflammatory phase and accelerate the transition to an anti-inflammatory stage. Clearance of cellular debris avoids continuous deleterious effects and chronic activation of inflammation[28,41].

Besides being responsible for clearance and phagocytosis, macrophages mediate inflammation, angiogenesis, remodelling of the ECM, fibrosis and regulate MuSCs activity through secretion of cytokines, growth factors and other molecules[14].

Macrophages express the surface marker F4/80 and two main subpopulations can be discriminated by the Ly6C expression levels. Ly6C^{High} macrophages exhibit a pro-inflammatory phenotype while the Ly6C^{Low} population express higher levels of anti-inflammatory cytokines[14,26].

In the initial phase of the immune response, Ly6C^{High} monocytes/macrophages clear the injury site through phagocytosis and release pro-inflammatory cytokines such as TNFa and IL-1B. These support MuSCs activation and proliferation and delay the differentiation phase[14,42]. This pro-inflammatory phase has a peak around 2 days post-injury (dpi)[36].

Then, as the inflammatory response proceeds, macrophages undergo a phenotypic transition towards an anti-inflammatory state, altering their cytokine profile. Macrophages reduce the secretion of pro-

inflammatory cytokines and enhance the expression of anti-inflammatory molecules. During this phenotypic switch, macrophages decrease their levels of Ly6C and start to express CX3CR1[14,26].

These Ly6C^{Low} Cx3Cr1^{High} macrophages, originated from the Ly6C^{High} population, secrete high levels of anti-inflammatory cytokines such as Transforming growth factor β (TGFβ) and Interleukin 10 (IL-10) allowing immune resolution. These cells support the myogenic commitment, differentiation of MuSCs, fusion and maturation of myofibers. For that reason, this population of macrophages is also described as pro-repair macrophages[14]. This phase occurs within 4-8 days after injury[36].

The crucial role of macrophage subsets in the regulation of MuSCs and myoblasts during myogenesis had been highlighted/validated by several *in vitro* and *in vivo* studies[42,43].

The phenotypic transition and the consequent immune resolution are essential for effective regeneration and restoration of the muscle tissue structure and function. The immune response is tightly orchestrated, both timely and spatially. If the pro-inflammatory signalling persists or the anti-inflammatory phase begins prematurely, the regeneration process becomes impaired and muscle tissue may not be fully recovered[14,44].

Importantly, tissue-resident and recruited macrophages play important but fairly distinct roles in skeletal muscle following injury. Local macrophages act as primary sensors, whereas recruited macrophages intensify and regulate the inflammatory response. Furthermore, these can be developmentally distinct. Macrophages originate, as mentioned, from circulating monocytes produced in the bone marrow but tissue-resident macrophages may also self-proliferate in situ from macrophages early developed during embryogenesis[28,37].

1.3.4.2 Origin of immune cells: Hematopoiesis

Following an injury, resident and infiltrating immune populations are recruited to the injured site and contribute to the immune response. Nonetheless, the vast majority of immune cells that accumulate within the damaged muscle are originated and recruited from the bone marrow (BM) and do not result from the proliferation of resident populations[45].

Thus, during a muscular regenerative pressure, circulating immune cells that are produced in the BM of adult mammals through a process known as hematopoiesis adhere to the blood vessels and migrate to the injured muscle, invading the damaged tissue [28,45].

Hematopoiesis is responsible for the generation of all blood cells and is a highly regulated process that can be influenced by a diversity of signals, enabling adaptation to body requirements (which is essential for an efficient immune response)[46,47]. Models of hematopoiesis have changed over the years and are constantly being revised as new discoveries emerge[46]. However, it is established that this process is initiated from hematopoietic stem cells (HSCs), that are characterized by their high self-renewal and

multipotency capacity[46,48]. These cells can produce all types of blood cells including cells from myeloid and lymphoid lineages (Figure 1.3). Currently, HSCs are considered a highly heterogenic population with different behaviours and lineage biases[46] and can be divided into long-term (LT-HSC) and short-term (ST-HSC). LT-HSC are a rare and generally quiescent population, with high self-renewal potential, with only a small role in the homeostatic generation of blood cells[46,48]. They can differentiate into ST-HSCs, which are more transient, and that, subsequently, give rise to multipotent progenitors (MPPs)[46]. In adult mice, all these cells are considered Lin-Sca1+cKit+ (LSK cells), meaning that they express the molecular markers Sca-1 and c-kit but lack lineage markers (Lin) present in mature lymphoid and myeloid cells[49].

MPPs maintain high lineage differentiation potential but have a restrict or non-detectable self-renewal ability[50,51]. This population is also extremely heterogeneous regarding lineage bias and fates, immunophenotype, cell cycle state and bone marrow frequency and can be divided into four categories: MPP1, MPP2, MPP3 and MPP4[49,50]. The first group share similarities with ST-HSC and are likely to give rise to the other MPPs[49]. These last ones lack self-renewal capability and are more proliferative and lineage-bias [49,50].

MPP2/3 are myeloid biased, even though MPP2 produces higher levels of platelets being a megakaryocyte/erythroid-biased subset. Both are functionally different from MPP4, which are primed to lymphoid lineage. Although they exhibit this lineage tendency, MPP fate is not fixed and can be redirected under particular circumstances and signals[50,52]. Moreover, it is known that MPP2/3 produce low levels of lymphocytes and MPP4 generates low levels of myeloid cells[50]. MPPs sustain hematopoiesis and originate lineage-restricted progenitors, including common myeloid progenitors (CMPs) and common lymphoid progenitors (CLPs). CMPs further give rise to bipotent granulocyte-macrophage progenitors (GMPs) and megakaryocyte-erythrocyte progenitors (MEPs). Subsequently, GMPs generate granulocytes and monocytes, MEPs originate megakaryocytes/erythrocytes and CLPs give rise to lymphocytes B and T, Natural Killer cells and dendritic cells[50,53].

All these populations of cells, in distinct differentiation states, co-exist in the bone marrow niche with other non-hematopoietic cells that support this process. These cells include endothelial cells, fibroblast, osteoblast and adipocytes, among others. Given the multicellular complexity of this microenvironment, the BM is highly vascularized and innervated, which allows continuous communication between the bloodstream and peripheral tissues[46].

This way, BM cell populations, including HSCs, progenitor cells and non-hematopoietic cells from the niche, can sense/detect several environmental cues including inflammatory signals and adjust accordingly, increasing proliferation, lineage skewing and immune cell production, and, ultimately, contributing to an efficient inflammatory response[46,54].

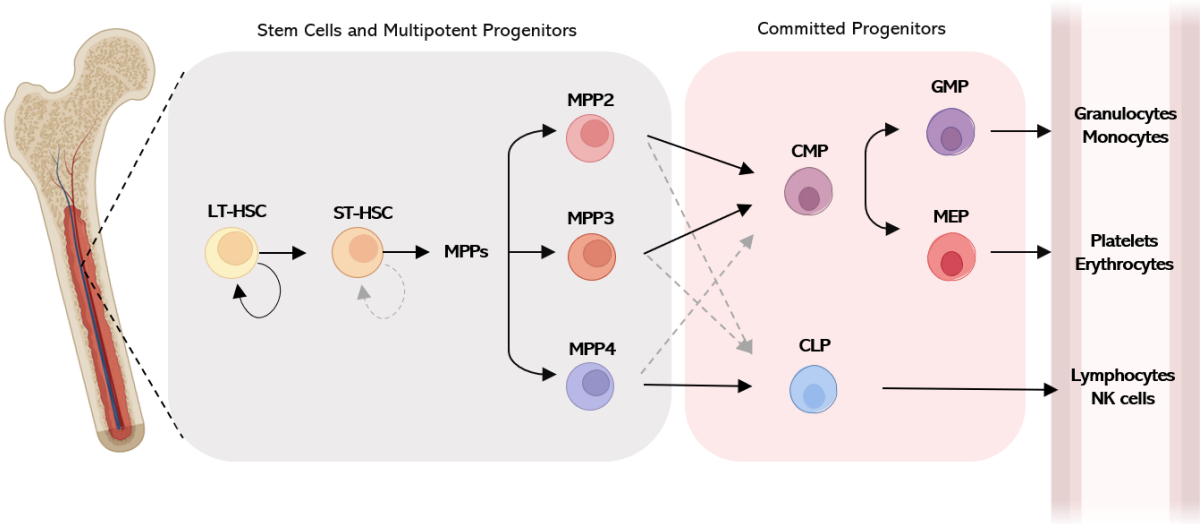

Figure 1.3 - Schematic illustration of the hematopoietic process in the bone marrow.

Long-term hematopoietic stem cells (LT-HSCs) have high self-renewal potential and can differentiate into short-term hematopoietic stem cells (ST-HSCs), with less self-renewal ability. These, in turn, differentiate into multipotent progenitors (MPPs) with very restricted renewal ability. MPP can be divided into the lineage-biased MPP2, 3 and 4. MPP2 and MPP3 are myeloid-biased originating higher levels of common myeloid progenitors (CMPs) and MPP4 are lymphoid-biased, giving rise to common lymphoid progenitors (CLPs). However, MPPs can originate cells from both lineages. CMP and CLP are committed progenitors. CMP can generate granulocyte-macrophage progenitors (GMPs) and megakaryocyte-erythrocyte progenitors (MEPs). GMPs give rise to granulocytes and monocytes (and further macrophages), MEPs differentiate into megakaryocytes/platelets and erythrocytes and CLPs originate lymphocytes and NK cells. Cells generated in the bone marrow are then released into the bloodstream. *Original image, based on reference* [50].

1.4 Skeletal Muscle Aging

1.4.1 Sarcopenia

Skeletal muscle is a paradigmatic model to study regeneration but also tissue aging. With increased age, skeletal muscle undergoes several structural and functional alterations, that ultimately lead to sarcopenia, an aged-associated condition characterized by a generalized and progressive loss of skeletal muscle mass and function. This muscle atrophy and loss of strength that define sarcopenia are associated with increased vulnerability, physical disabilities, falls and fractures, poor quality of life and even mortality[2]. In addition, sarcopenia has been associated with other age-related diseases such as dementia, diabetes mellitus, obesity, and cardiovascular and respiratory diseases, being extremely common in individuals with these conditions[15,55,56]. Thus, sarcopenia represents a public health problem of the elderly, and its prevalence is expected to rise, as a result of the world's population aging[2].

The gradual loss of mass characteristic of skeletal muscle aging and sarcopenia is mainly attributed to the reduction in the number and size of myofibers. In addition, skeletal muscle aging is also characterized by accumulation of intermuscular adipocytes, enhanced fibrosis, and muscle stiffness. With advanced age, there is also gradual loss of innervating motor neurons and vessels in the skeletal muscle, which, altogether, contribute to progressive loss of power and endurance[55,57].

During aging, skeletal muscle also undergoes a significant reduction in the regenerative potential, which may be associated with sarcopenia. The failure to replace damaged fibres and restore the muscle tissue may contribute to gradual loss of mass and strength[58].

Skeletal muscle aging phenotype is influenced by intrinsic and extrinsic factors such as immune and metabolic alterations, hormonal imbalances and diet and nutrition[58].

1.4.2 Impact of aging on MuSCs

During aging, the regenerative potential of skeletal muscle declines and this is largely associated with an age-related reduction in MuSCs functionality and number.

Aged-linked defects in MuSCs occur due to cell-autonomous and environmental alterations that influence their behaviour[17]. As a consequence, aged MuSCs have a reduced capacity for activation and proliferation upon an injury, producing insufficient progeny to sustain the regeneration process. Moreover, the MuSCs progeny show limited differentiation capacity and lineage skewing. Aged MuSCs also reveal a reduced ability to self-renew and replenish the stem cell pool, which partly explains the substantial decrease of MuSCs numbers in aged muscle[17,58].

Quiescent MuSCs undergo intrinsic age-associated alterations that compromised their responses to regenerative cues. Altered proteostasis, deficient protein quality control mechanisms, mitochondrial dysfunction, altered autophagic response, telomeric attrition, changes in metabolic pathways, and consequent, epigenetic alterations are all mechanisms that can drive MuSCs' decline of function[11,58]. Furthermore, resting MuSCs become irreversibly pre-senescent, losing their quiescent reversible state, as demonstrated in geriatric mice. This state leads to complete senescence upon a regenerative pressure[59].

MuSCs aging is also driven by alterations in the systemic and local environments. These include modifications in the inflammatory signals, growth factors and extracellular matrix. Signals from circulation can influence MuSCs directly or induce changes in the niche[17].

The importance of the systemic factors is supported by heterochronic parabiosis studies, where the circulatory systems of young and old mice are joint, allowing the exchange of circulating factors and cells. These experimental interventions had shown that impaired regenerative capacity found in old muscles can be reversed after exposure to a young systemic environment. On the other hand, the MuSCs function and regenerative capacity of young skeletal muscle are worsened after exposure to an old systemic milieu[60–62].

These studies highlight that the modulation of circulating factors in the elderly has an important effect on regenerative capacity and the identification of such factors can be clinically important for rejuvenating strategies in regenerative medicine. Evidence from this type of studies suggests that molecules

implicated in immune modulation may be within the factors that contribute to tissues' altered regenerative potential[11].

Given the immune system's role in muscle regeneration, aged-related alterations in immune cells may contribute to a disrupted inflammatory signalling in old muscle, impairing MuSCs and myoblasts' function[17]. Bone marrow transplantations between young and old mice demonstrate that transplanted BM cells from old donors were sufficient to impair MuSCs function in young mice and promoted conversion towards a fibrogenic phenotype, highlighting the influence of the immune system on muscle aging[63].

Multiple interventions have been suggested in the literature to restore the regenerative potential of aged skeletal muscle. Considering the synergistic effects of intrinsic and extrinsic factors on the aged MuSCs function, rejuvenating strategies are likely to depend on approaches that target both[17]. Therefore, potential interventions include stem cell-based therapies (involving ex vivo stem-cell approaches and transplantation), niche-specific strategies, and systemic approaches[17,64]. Taking into account the negative impact of immune dysregulation (characteristic of aging) on MuSCs function, immune modulation has been considered a potential strategy to counteract or limit the regenerative capacity decay[11,64].

1.5 Mesencephalic astrocyte-derived neurotrophic factor

Mesencephalic astrocyte-derived neurotrophic factor (MANF) is a highly evolutionarily conserved protein found not only in vertebrates but also in invertebrate species such as *Drosophila melanogaster and Caenorhabditis elegans*[65–67].

This protein was initially identified as a selectively protective factor for dopaminergic neurons in an astrocyte-conditioned medium and, for that reason, classified as a neurotrophic factor (NTF)[68]. NTFs are essential secreted proteins expressed in the nervous system that promote neuronal differentiation, growth, survival, and plasticity[66]. However, despite its neuroprotective activities, MANF protein is structurally different from the classical NTFs. Moreover, it has a largely unknown signalling mechanism and receptor, and its physiological functions are not limited to the nervous system[66,69].

MANF is widely expressed by most tissues in the human and mouse body[69,70]. High levels of MANF have been especially detected in secretory tissues, including salivary gland and pancreatic endocrine beta cells and exocrine acinar cells, which may suggest an important role of MANF in cells with high rates of protein synthesis and secretion. Low levels of MANF were detected in homeostatic skeletal muscle. This protein has also been detected in human blood[69,71,72].

Manf gene has 4 exons and is located on mouse chromosome 9 and human chromosome 3[73,74]. MANF is a highly soluble 18 kilodalton (kDa) protein with a dual functional location. Its primary protein sequence

contains an N-terminal signal peptide targeting the intracellular MANF to the endoplasmic reticulum (ER), where it acts as an ER-stress response protein[67,69].Thus, MANF expression and secretion are induced and enhanced by ER stress[67]. When the signal peptide is cleaved, MANF can be released in the extracellular space and execute their extracellular functions[67,69].

1.5.1 MANF and Immune responses

Cytoprotective MANF activities have been demonstrated in several studies, not only in neurological and neurodegenerative conditions, such as Parkinson's disease and cerebral ischemia but also in pancreatic b-cells, cardiomyocytes, and retinal cells[72,75–77]. Besides this biological function, recent studies have suggested an important role of MANF in the regulation of immune responses. MANF protein is expressed in immune cells and, although the mechanism involved remains relatively unexplored, several studies have supported the idea that its activity is associated with negative regulation of inflammation[76,78,79]. MANF acts as an immunomodulator in an autocrine manner, inhibiting pro-inflammatory signalling/phenotype[66,76,79].

This MANF role was particularly demonstrated in the context of retinal tissue damage in flies and mice. In response to damage, MANF was transiently induced in immune cells (hemocytes in flies and macrophages in mice) and this was found to be essential for tissue repair. Moreover, in this study, MANF supplementation was sufficient to delay retinal degeneration, highlighting its conserved neuroprotective function. In this study, MANF proved to be essential for its neuroprotective and tissue repair promoting activities in the retina[76].

In another study, that used a rabbit model of arthritis, MANF was found particularly expressed by fibroblast-like synoviocytes, one of the main inflammatory cell types in the synovium tissue, and its functions were also associated with the inhibition of inflammatory signalling[79].

Heterozygous carriers of the *Manf* null allele mice, that exhibit half levels of MANF in circulation and tissues, revealed signs of chronic inflammation with increased expression of pro-inflammatory cytokines and accumulation of activated macrophages in several organs[78].

Thereby, MANF proved to have cytoprotective and immunomodulatory functions, which, synergistically, may contribute to more efficient tissue recovery and regeneration[66].

1.5.2 MANF and Aging

MANF expression is altered by aging. Systemic MANF levels decrease with age in flies, mice, and humans, which contributes to loss of tissue homeostasis, at least, in mice and flies[78].

A 2019 heterochronic parabiosis study suggested that MANF may be one of the factors in young blood that contributes to the rejuvenating effects of these interventions in old animals. In this study, old wild-

type mice were exposed to the circulatory system of young heterozygous carriers of the MANF null allele mice. The rejuvenating effects of heterochronic parabiosis were significantly impaired, indicating that MANF is essential for complete liver rejuvenation. Moreover, MANF supplementation in old mice was sufficient to ameliorate age-related inflammation and reduce age-associated tissue damage in the liver[78].

These experiments support the notion that MANF is a systemic factor important for immune regulation in the context of aging and tissue homeostasis.

1.5.3 MANF and skeletal muscle regeneration

As previously mentioned, MANF proved to be an immunomodulator whose effects improved immune homeostasis in old animals, limited liver tissue damage and promoted retinal tissue repair. However, it has been suggested that these beneficial effects of MANF are not limited to these tissues[78].

In a previously study from the group, it was demonstrated that MANF expression is transiently induced during skeletal muscle regeneration in young mice, peaking at 3-4 days post-injury and progressively declining afterwards. This expression is particularly induced in anti-inflammatory/pro-repair macrophages. However, MANF production upon injury is affected by aging, since aged muscles did not reveal a significant induction of MANF after injury[80].

In addition, old animals exhibit a blunted myeloid recruitment and an impairment/delay in the phenotypic transition from pro-inflammatory to pro-repair macrophages, during the regenerative process. This was associated with the decline in regenerative capacity and may be related to the reduction in MANF expression.

Interestingly, a mouse model with conditional ablation of MANF in anti-inflammatory macrophages, that mimics the age-related decline in MANF production, was able to recapitulate several phenotypes seen in aged animals, including the defects in immune response during a regenerative pressure and the impairment in skeletal muscle regeneration. MANF loss of function in anti-inflammatory macrophages leads to an inflammatory crisis, formation of smaller myofibers and reduced MuSCs number[80].

This study supports the hypothesis that MANF expression is involved in the muscle regeneration process, in particular, in the regulation of the macrophages' phenotypic transition towards an anti-inflammatory profile. Moreover, it suggests that aged-related MANF decline in macrophages is associated with a reduction in regenerative capacity[80].

Ultimately, this work highlights the relevance of MANF in immune modulation and skeletal muscle regeneration and introduces this protein as a potential candidate for rejuvenating strategies for skeletal muscle regeneration. However, the precise mechanism underlying MANF activity during the immune response to injury remains unclear. Additionally, considering MANF's widespread expression, it is not

clear whether MANF originated from other cell types are compensating the MANF knockdown in pro-repair macrophages, which is a limitation to fully evaluate the consequence of MANF loss for regenerative success.

1.6 Aims of the project

In this project, we aim to expand the studies on the immunomodulatory functions of MANF during skeletal muscle regeneration, characterizing the consequences of its ubiquitous loss for skeletal muscle regenerative response. Additionally, we will explore the specific role of MANF in macrophages and its association with the modulation of immune phenotypes during skeletal muscle regeneration. Thus, the particular goals of this project are to:

- Characterize the consequences of ubiquitous MANF loss for regenerative efficiency (short and long-term effects) and for the immune responses associated with muscle recovery.
- Characterize the consequences of ubiquitous MANF loss for the different cell populations involved in skeletal muscle regeneration.
- Uncover the mechanism causing immune dysfunction in conditions of MANF loss of function.
- Identify intrinsic defects in the MANF-deficient pro-repair population of macrophages

2

MATERIALS AND METHODS

2.1 Animal Models

In this project, three different genetic mouse models with MANF knockout in distinct cell populations were used. All animals were housed and bred in an accredited rodent facility at *Instituto de Medicina Molecular (iMM).* The experimental protocols and procedures were conducted accordingly to European animal welfare policies and guidelines/regulations and approved by the iMM Animal Care and Ethical Committees (iMM-ORBEA).

For this study, a genetic mouse model with inducible and ubiquitous MANF knockout, identified as **Rosa26$^{CRE-ERT/+}$Manf$^{fl/fl}$,** was generated. Mice carrying the Rosa26$^{CRE-ERT}$ allele were purchased from The Jackson Laboratory (004847). These mice have a tamoxifen (tam) inducible Cre-recombinase sequence fused to a modified version of the mouse estrogen receptor ligand binding domain, located in the GT(ROSA)26Sor locus, that is ubiquitously expressed. Manf$^{fl/fl}$ mice were previously described[78]. In the Rosa26$^{CRE-ERT/+}$Manf$^{fl/fl}$, Cre recombinase expressed in all cells upon tamoxifen induction recognizes the locus of X-over P1 (loxP) sites that flank the *Manf* gene, allowing MANF ablation in all cells.

This project also includes experiments on the **Cx3cr1$^{CRE-ER/+}$, Manf$^{fl/fl}$** mouse model, whose generation was formerly described[78]. In this model, the Cre recombinase gene is fused to an estrogen receptor ligand binding domain placed in exon 1 of the Cx3cr1 locus. This way, this model allows the conditional ablation of MANF in Cx3CR1 positive macrophages upon tamoxifen induction, enabling a temporal control of the loxP-flanked *Manf* gene expression. Cx3cr1$^{CRE-ER/+}$ were purchased from The Jackson Laboratory (021160).

Lastly, **LysM$^{CRE/+}$Manf$^{fl/fl}$,** a genetic model that allows the MANF ablation in macrophages in a tamoxifen-independent manner was also used in this study. Manf$^{fl/fl}$ mice were crossed with the LysM^{CRE} driver mice, that were purchased from The Jackson Laboratory (004781) and have a Cre recombinase inserted in the lysozyme 2 gene expressed in myelomonocytic cells[81]. Manf$^{fl/fl}$ mice littermates were used as controls.

2.2 *In vivo* procedures

2.2.1 Tamoxifen intra-peritoneal injections

Cre activity on both Rosa26$^{CRE-ERT/+}$Manf$^{fl/fl}$ and Cx3cr1$^{CRE-ERT/+,}$ Manf$^{fl/fl}$ models was induced through daily intra-peritoneal injections of tamoxifen (T5648-1G – Sigma) in sterile corn oil (20 mg/ml) at a dose of 75mg/Kg of body weight. Control animals were littermates, with the same genotype, that received the equivalent volume of only corn oil (sham injections) or Manf$^{fl/fl}$ mice that also received tamoxifen.

The tamoxifen/oil treatment began one day before the injury induction to allow MANF deletion before the initiation of the regenerative process. The treatment continued the following days after injury to ensure MANF ablation during this process. For survival analysis following muscle damage, tamoxifen injections were given only before the injury.

2.2.2 Muscle injury

To stimulate the regeneration process, muscle injuries were conducted using a chemical method, namely, barium chloride ($BaCl_2$) injections that induce myofibers degeneration. For this procedure, mice were, firstly, anesthetized through isoflurane inhalation. Then, mice received intramuscular injections of sterile 1.2% $BaCl_2$ (Sigma: 342920) in saline solution (0.9% NaCl, B. BRAUN) into one of the hindlimb tibialis anterior (TA, 40µl) or quadriceps (QC, 50µl) muscle, depending on the experiment.

2.3 Genotyping

MANF deletion was confirmed by polymerase chain reaction (PCR) based genotyping. Primers (Invitrogen) used permit de amplification of *Manf*^{fl} allele and the sequences are listed in Table 2.1.

.

Table 2.1 - Sequences of the primers used for genotyping PCR.
The forward and reverse primers listed were used to amplify the *Manf*$^{fl/fl}$ gene

Allele	Forward Primer	Reverse Primer
Manf ^{fl}	5´-TGAAGCAAGAGGCAAAGAGAATCGG-3´	5'- CCATGGTGATGCTGTAACTGTCACG -3'

This MANF knockout confirmation method is based on the fact that the length of the amplicons obtained by PCR differs depending on whether *Manf*^{fl} was excised or not. Cre recombinase, when active in cells, induces recombination and excision between the LoxP sites that flank the gene exon 3. Therefore, intact *Manf*^{fl} lead to an amplicon with more than 1000 base pairs (bp), whereas excised *Manf*^{fl} results in an amplicon of 786 bp.

DNA used for PCR protocol was extracted from fractions of the mice ear, collected after mice sacrifice. For genomic DNA extraction, 50µl of DNA extraction mix from Xpert direct Xtract PCR Kit (Grisp) were added to each sample. This mix contains 10µl of Xpert directXtract Buffer A, 5µl of Xpert directXtract Buffer B and 35µl of RNAse-free water. After guaranteeing that all tissue was submerged in the extraction solution, samples were incubated at 75ºC for 10 minutes to induce cell lysis and protein denaturation. Then, samples were incubated for another 10 minutes at 95ºC, for additional denaturation and inactivation of the mix. Next, RNAse-free water was added to the extracted DNA at a 1:5 dilution. DNA samples were kept at -20 ºC until PCR analysis.

Each PCR reaction required a 25µl mixture containing 1µl of the extracted DNA, the forward and the reverse primers in a final concentration of 0.4uM, RNAse-free water and 1x Xpert Fast Hotstart Mastermix with dye (Grisp). This Mastermix comprises DNA polymerase, $MgCl_2$, and deoxyribonucleotide triphosphates (dNTPs) necessary for each reaction.

PCR was carried out in a thermal cycler (C1000 Touch PCR thermal, BIO-RAD) according to the conditions described below (Table 2.2). Then, the PCR products were analysed in 2% (w/v) agarose gels prepared in 0.5x Tris-Acetate-Ethylenediaminetetraacetic acid (TAE; 20mM Tris, 10nM acetic acid and 0.5mM Ethylenediaminetetraacetic acid (EDTA), pH 8.0). The nucleic acid stain GreenSafe Premium (Nzytech) was added to the agarose solution (7µl/100ml solution) to enable the observation of the PCR products during electrophoresis.

After gel polymerization, the molecular weight marker NZYDNA ladder V (Nzytech) and the PCR products were loaded into the gel and run at 95 V for 45min, in 0.5x TAE solution. Electrophoresis was performed in Wide Mini-Sub Cell GT Cell (Bio-rad) tanks using the PowerPac ^{HC} (Bio-rad) as the power supply. Results were visualized using the ChemiDoc XRS and the Gel Imaging System (Bio-rad).

Table 2.2 - PCR program conditions for *Manf*^{fl} amplification

Time	Temperature (ºC)	Number of cycles
5 min	94	-
15 sec	94	10X (*Reduction of 1ºC/cycle)
30 sec	55-65*	
40 sec	72	
15 sec	94	30x
30 sec	55	
40 sec	72	
5 min	72	-
∞	4	-

2.4 Blood collection, processing, and analysis

2.4.1 Blood collection and processing

For blood collection, animals were lethally anesthetized, and blood was collected by heart puncture in EDTA-coated tubes and kept on ice. Then, blood was transferred into a 15ml tube filled with 2 ml of 1x Red Blood Cell (RBC) lysis buffer (Santa Cruz Biotechnology) and incubated for 15 minutes at room temperature (RT) with periodic inversions. Samples were centrifuged for 5 minutes at 500g, resuspended in 2 ml of 1x RBC lysis buffer and incubated once again for 15 minutes with regular inversions. After a 5 minutes centrifugation at 500g, samples were resuspended in 1ml of Phosphate-buffered saline (PBS) containing 2% Fetal Bovine Serum (FBS) and counted using a hemacytometer.

2.4.2 Blood cells Staining for Flow Cytometry and Gating Strategy

The characterization of blood cell populations was accomplished by flow cytometry (FC), which relies on the presence of specific cell markers stained with fluorescent antibodies.

After cell counting, 500 000 blood cells from each animal were incubated in viability dye Zombie Aqua (Biolegend) diluted at 1:1000 in PBS for 15 minutes on ice. After a 5 minutes centrifugation at 500g, cells were incubated for another 15 minutes on ice with a Fc receptor block mix that consists of anti-mouse CD16/32 FcγR (Biolegend) diluted at 1:250 in Brilliant Violet (BV) buffer. BV buffer is 1x Brilliant Stain Buffer Plus (BD Biosciences) in PBS-2%FBS. CD16/CD32 are Fcγ III/II receptors expressed on a variety of immune cells including monocytes/macrophages, B cells, NK cells, and granulocytes, among others[82]. Therefore, this blocking step allowed saturation of these receptors prior to staining, avoiding background or false positives in the following analysis. Subsequently, 50µl of BV Buffer containing the antibodies mentioned in Table 2.3 were added to the blood cell solution and cells were incubated with the antibodies for 30 minutes at 4ºC, covered from the light.

Table 2.3 - Fluorochrome conjugated antibodies used for blood cell analysis by flow cytometry
Enumeration of the antibodies and associated fluorochromes, respective populations recognized, source and dilution applied.

Antibodies and conjugated fluorochromes	Cell population identified	Source	Dilution
PE anti-mouse **F4/80**	Macrophages	Biolegend (123110)	1/50
APC anti-mouse **Ly6C**	Monocytes/Macrophages	eBioscience (17-5932-82)	1/200
FITC anti-mouse **Ly6G**	Neutrophils	Biolegend (127606)	1/400
APC-eFluor® 780 anti-mouse **CD11b**	Myeloid cells	eBioscience (47-0112-82)	1/200
BV421 anti-mouse **CD45R/B220**	B cells	Biolegend (103240)	1/20
BV785 anti-mouse **CD3e**	T cells	Biolegend (100355)	1/50

After immunostaining, cold PBS was added, and the cell suspension was centrifuged for 5 minutes at 500g. Cells were fixed with intracellular (IC) Fixation buffer (Invitrogen) in PBS 2%FBS for at least 1h. Then, cells were centrifuged at 500g for 5 minutes, resuspended in PBS 2%FBS and filtered through a 5 ml Polystyrene Round-Bottom tube with a cell-strainer cap (Falcon) (herein named FACS tubes) for FC analysis.

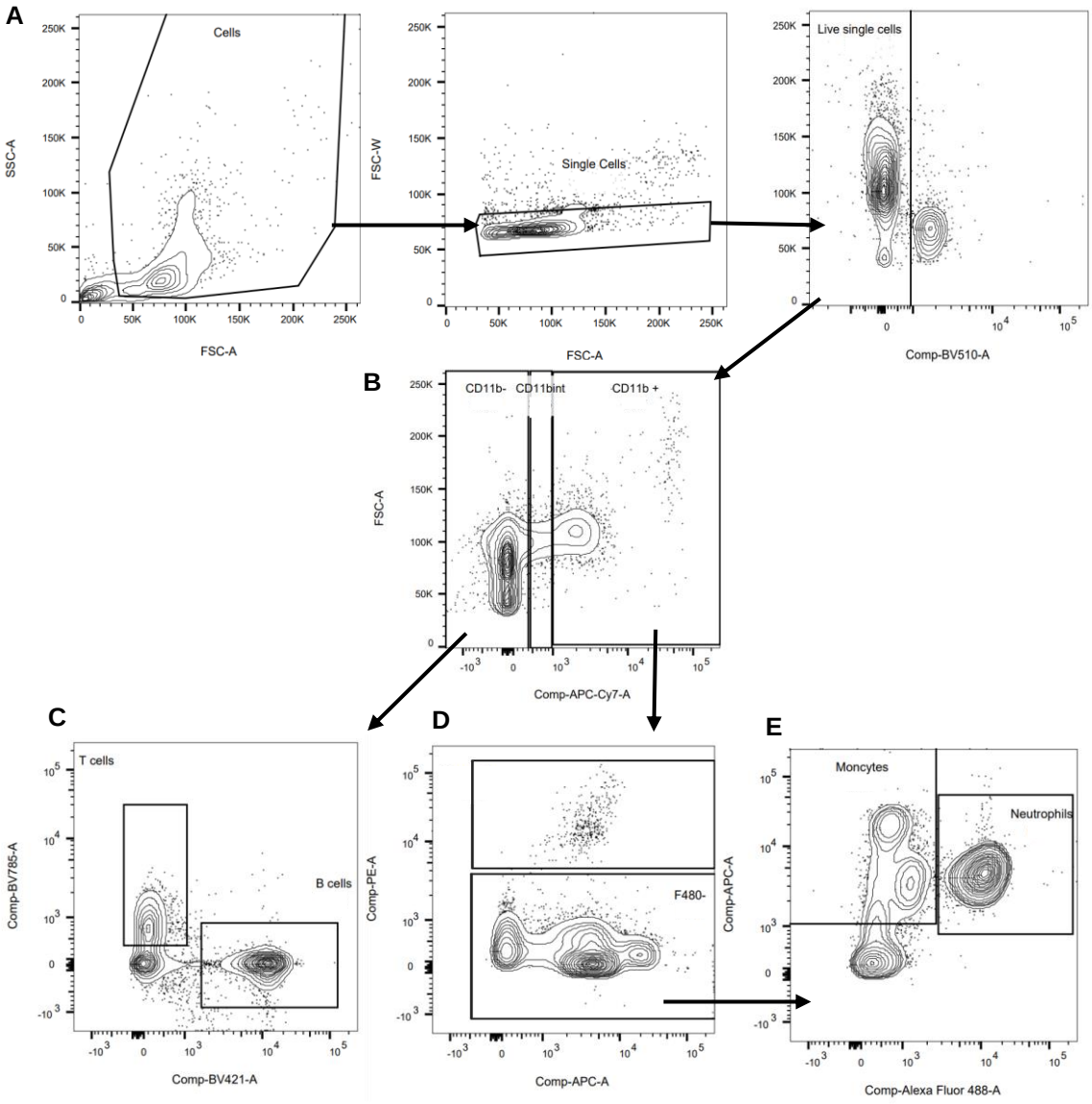

Figure 2.1 - Flow cytometry gating strategy to analyse immune cell populations in mouse peripheral blood **A.** Firstly, cells were selected by plotting the forward scatter (FSC) vs. side scatter (SSC), excluding cell debris. FSC indicates relative differences in the cell size and SSC gives information about relative differences in cell complexity or granularity. Front Scatter Width (FSC-W) vs. Area (FSC-A) plot was used to discriminate between single cells and doublets. From the single cell population, the viable cells were selected. From here, the following gates allowed the isolation of blood cells according to their specific markers. **B.** Discrimination between myeloid cells ($CD11b^{Pos}$) and non-myeloid cells ($CD11b^{Neg}$) from the live cell population. **C.** Identification of T cells ($CD3e^{Pos}$) and B cells ($CD45R^{Pos}$) from the $CD11b^{Neg}$ population. **D.** Distinction between $F4/80^{Pos}$ and $F4/80^{Neg}$ population and **E.** selection of monocytes ($Ly6C^{Pos}$) and neutrophils ($Ly6G^{Pos}$) from the $F4/80^{Neg}$ population.

The gating strategy used is described in Figure 2.1. Initially, cell debris and doublets were excluded, and viable cells were discriminated. From live single cells, myeloid cells were selected based on the CD11b marker. Monocytes were identified as F4/80^{Neg}Ly6G^{Neg}Ly6C^{Pos} while neutrophils were selected as F4/80^{Neg} Ly6G^{Pos}. On the other hand, T and B cells were selected based on the expression of CD3e and CD45R, respectively, from the CD11b^{Neg} gate. Importantly, all gates in FC experiments were defined using single colours controls, which allowed the correction of spectral overlaps through the compensation method. FC analysis was performed on the cell analyser LSRFortessa X-20 (BD Bioscience), using the FACSDiva 8.0 software. FC data were further analysed using the FlowJo (BD Biosciences) software.

2.5 Bone Marrow collection, Processing and Analysis

2.5.1 Bone Marrow harvesting and processing

To isolate BM, mice were euthanized through cervical dislocation and one leg of each mouse was collected. The skin and the muscle attached were removed using a scalpel, and the femur was individualized and kept on ice in sterile PBS. Then, each bone was placed on a plate with 2ml of PBS 2%FBS and both edges of the bone were cut. Subsequently, the bone marrow was flushed out onto a plate using a 1ml syringe with a 26G needle filled with PBS 2%FBS. This process was repeated twice on each side of the bone. Red blood cell clumps were mechanically disrupted using the syringe, and the cell suspension was collected and filtered through a 70µm filter. Then, the cell suspension was centrifuged at 500g for 5 minutes at 4ºC, resuspended in 1 ml of 1x RBC lysis buffer and incubated at RT for 5 minutes. Cells were centrifuged and washed with 5ml of PBS. After another centrifugation at 500g for 5 minutes, cells were resuspended in 5ml of PBS 2% FBS and counted using a hemacytometer.

2.5.2 Bone Marrow Cells Staining for Flow Cytometry and Gating Strategy

The characterization of BM cell populations was performed through FC. 5 000 000 cells were incubated with the viability dye Zombie Aqua, as described. Upon a 500g centrifugation for 5 minutes, cells were incubated for 15 minutes on ice with the block mix containing APC conjugated Anti-CD16/32 FcgR (Biologend) (1:300) in BV buffer. Subsequently, BM cells were incubated in BV Buffer with the fluorochrome-conjugated antibodies displayed in Table 2.4, at a density of 1x10^6 cells/100µl for 1h at 4ºC, protected from the light. After the incubation period, the following steps were similar to the ones mentioned in the blood protocol until FC analysis.

The gating strategy is explained in Figure 2.2. From live single cells, cells that lack specific lineage markers (Lin^{neg}) were selected, excluding erythrocytes, myeloid, T and B cells from the following analysis. Then, LSK cells were selected as Lin^{neg} Sca-1^{pos} c-Kit^{pos} and within this population, it was possible to identify LT-HSCs, ST-HSCs and MPPs based on the differential expression of the CD150(SLAM), CD48 and Flk2 surface markers. On the other hand, the CMPs, MEP and GMPs were

isolated from the Lin^{neg}Sca-1^{neg}c-Kit^{pos} population according to the expression of CD34 and CD16/32. FC data were analysed as previously mentioned.

Table 2.4 - Fluorochrome conjugated antibodies used for bone marrow cell population analysis by flow cytometry.
Enumeration of the antibodies and fluorochromes associated, respective populations recognized, source and dilution applied.

Antibodies and conjugated fluorochromes	Cell population identified	Source	Dilution
APC-Cy7 anti-mouse **CD5**	T cells and B cells subset	Biolegend (100650)	1/200
APC-Cy7 anti-mouse **CD4**	T cells CD4+	Biolegend (100414)	1/40
APC-Cy7 anti-mouse **CD8a**	T cells CD8+	Biolegend (100714)	1/40
APC-Cy7 anti-mouse **CD3e**	T cells	Biolegend (100330)	1/100
APC-Cy7 anti-mouse **CD45R/B220**	B cells	Biolegend (103224)	1/200
APC-Cy7 anti-mouse **Ter119**	Erythroid cells	Biolegend (116223)	1/200
APC-eFluo780 anti-mouse **CD11b**	Myeloid Cells	eBioscience™ (47-0112-82)	1/200
APC-Cy7 anti-mouse **Gr-1(L6-6G/Ly-6C)**		Biolegend (108424)	1/200
BV785 anti-mouse **CD48**	Hematopoietic cells	Biolegend (103449)	1/50
PE-Cy7 anti-mouse **CD150 (SLAM)**		Biolegend (115914)	1/40
PE anti-mouse **Sca-1**		Biolegend (108108)	1/50
PerCP anti-mouse **c-Kit**		Biolegend (105822)	1/40
BV421 anti-mouse **Flk-2(CD135)**		Biolegend (135315)	1/50
FITC anti-mouse **CD34**		BD Biosciences (553733)	3/25

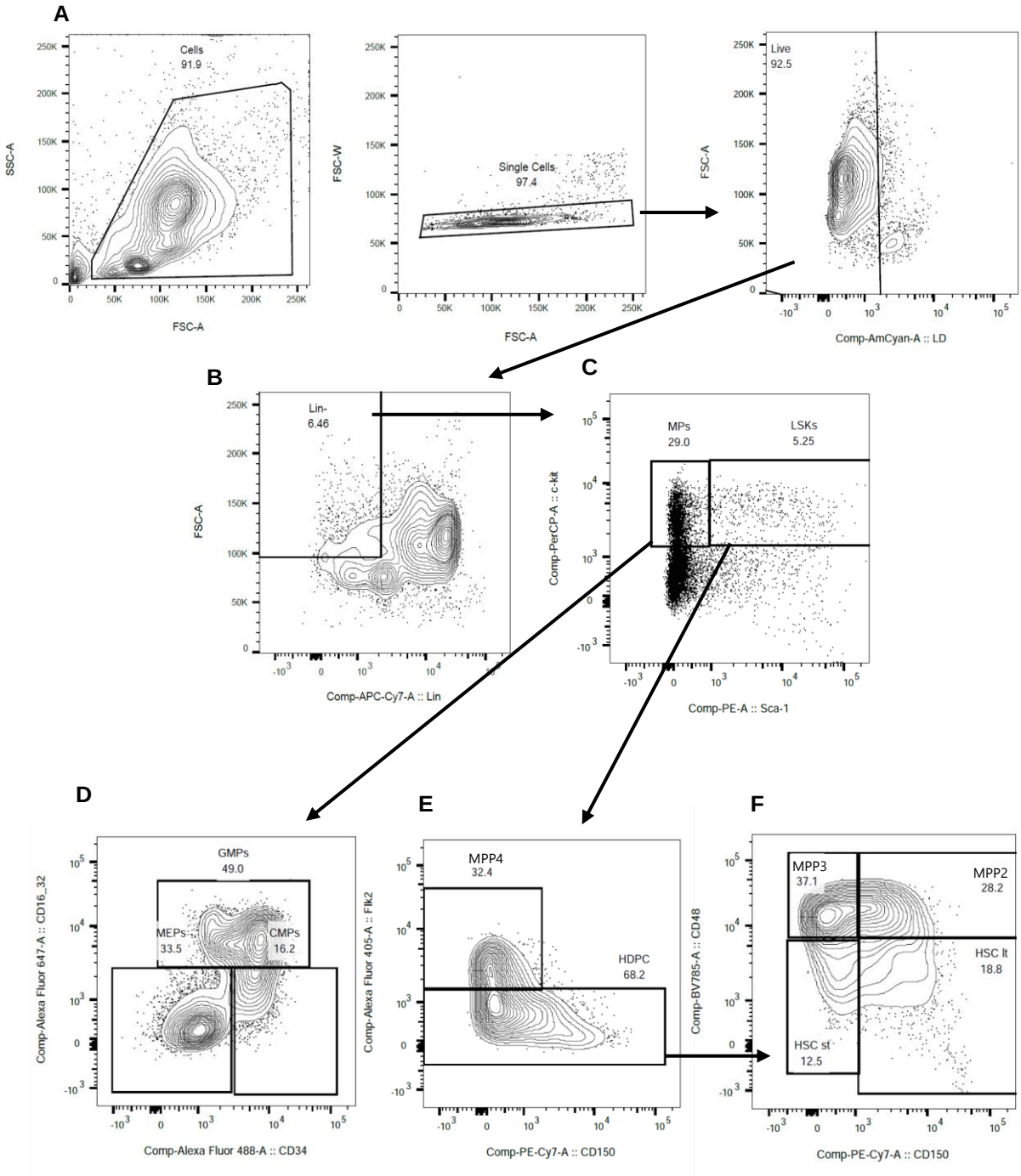

Figure 2.2 - Flow cytometry gating strategy to analyse bone marrow hematopoietic cell populations
A. Live single cells were initially selected as in the Figure 2.1. **B.** Selection of cells that lack lineage commitment markers (Lin^- cells), that is, negative selection of myeloid, erythroid, T and B cells, from the live single cells gate; **C**. Identification of LSK cells ($Lin^{Neg}Sca1^{Pos}cKit^{Pos}$) and MPs ($Lin^{Neg}Sca1^{Neg}cKit^{Pos}$), from the Lin^- population, **D.** Identification of GMPs ($CD16/32^{Pos}$), CMPs ($CD34^{Pos}CD16/32^{Neg}$), and MEPs ($CD34^{Neg}$ $CD16/32^{Neg}$) from de MPs gate, **E.** Within the LSK population, MPP4 are selected as $CD150^{Neg}$ $Flk2^{Pos}$ **F.** From the $Flk2^{Neg}$ gate, MPP2, MPP3, ST-HSC, and LT-HSC were selected based on the expression of the markers CD150 and CD48. Myeloid progenitors (MPs); common myeloid progenitors (CMPs), granulocyte-macrophage progenitors (GMPs); megakaryocyte-erythrocyte progenitors (MEPs); Multipotent progenitors (MPP 2/3/4); long-term (LT-HSC) and short-term (ST-HSC) hematopoietic stem cells.

2.6 Muscle collection, processing, and analysis

2.6.1 Muscle collection and storage

To study the skeletal muscle regeneration process, mice were euthanized at chosen timepoints after an injury, as previously described, and tibialis anterior or quadricep muscles were dissected/collected.
Muscle tissue was harvested for different purposes including histological analysis, protein analysis and cell population study by FC or fluorescent-activated cell sorting (FACS). For **histology studies**, dissected muscles were positioned vertically in a 1% (w/v) tragacanth gum (G1128-100G– Sigma - recipe in Appendix A.1) and frozen for 17 seconds in isopentane (VWR), previously cooled in liquid nitrogen, to minimise ice crystals generation. Frozen tissue was, then, stored at -80ºC and subsequently cryosectioned on a cryostat (LEICA CM 3050S). Ten-µm thickness cross-sectioned tissue was collected in Superfrost microslides and again stored at -80ºC until analysis. Muscles collected for **protein analysis** were snap frozen in cryovials by immersing them in liquid nitrogen after dissection and stored at -80ºC. Injured muscles used for **cell population analysis** by FC or FACS were immediately processed.

2.6.2 Histological analysis, imaging, and quantification methods

2.6.2.1 Hematoxylin and Eosin (H&E) staining and image acquisition

Cryosectioned muscle tissue was stained with Hematoxylin and Eosin (H&E) for histological characterization. Hematoxylin exhibits a dark blue/purple colour and stains nucleic acids, while eosin has a pink colour and stains proteins in a non-specifical manner[83].

Slides containing muscle cryosections were defrosted at RT for 10 minutes. Then, slides were immersed in distilled water for 5 minutes, stained with Harris Hematoxylin (05-06004E – Enzifarma) for 3 minutes and washed under running water for 5 minutes. Next, slides were dipped once on ethanol 70%, and four times on Eosin Y (HT110132-1L- Sigma). After staining, the samples were gradually dehydrated. For that, stain tissue was serially immersed in 70%, 95%, 100%, and again 100% ethanol for 30 seconds each. Lastly, slides were left in xylene (Leica Microsystems) for at least 10 minutes and mounted with microscope cover glass No. 1.5H (Marienfeld) using Micromount Mounting Medium (Leica Microsystems). Digital images of the H&E-stained sections were obtained using a digital slide scanner NanoZoomer SQ (HAMAMATSU) with an objective of 20x magnification.

2.6.2.2 Immunohistochemistry, imaging, and quantification methods

In this project, eMHC and necrotic myofibers immunohistochemistry were performed in the cryosectioned muscle. Slides containing tissue cryosections were thawed at RT for 10 minutes and permeabilized with 4% Paraformaldehyde (PFA) in PBS in a wet dark chamber for 10 minutes at RT. Fixed tissue was then washed with PBS 0.1% Tween20 (PBS-T) and boiled in Citrate Buffer (10Mm Citric Acid, 0.05%Tween20, ph 6.0) during 45 minutes for antigen retrieval. Slides were again washed

with PBS-T for 10 minutes and incubated for 2h in a wet chamber with Mouse-on-Mouse Blocking Reagent (R&D Systems) in PBS-T at a 3:100 dilution.

For **eMHC immunostaining**, samples were then rinsed in PBS-T and incubated overnight at 4ºC in a humidified chamber with non-diluted primary antibody against mouse eMHC (D.S.H.B). On the second day, slides were washed 4 times with PBS-T for 10 minutes minimum and incubated with the secondary antibody anti-mouse IgG alexa555 (Abcam) diluted at 1:400 in 10% Horse serum in PBS-T for 2h and 30 minutes in a humidified chamber at RT. Next, samples were washed 5 times with PBS-T for at least 10 minutes and stained with 300 nM 4′,6-diamidino-2-phenylindole (DAPI) in PBS for 5 minutes, protected from light. After rinsing in PBS, slides were mounted using microscope cover glass No. 1.5H (Marienfeld) and mowiol mounting media.

For **necrotic fibres immunostaining,** after blocking, samples were incubated for 2h30min at RT in a wet chamber directly with the secondary antibody anti-mouse IgG coupled to Alexa-647 diluted at 1:400 in 10%HS in PBS-T, without the overnight incubation with primary antibody. The secondary antibody was retained within the necrotic myofibers. Slides were washed 5 times with PBS-T for 10 minutes and stained with DAPI in PBS for 5 minutes, protected from light. Slides were rinsed in PBS and mounted as described.

Immunostained tissues were imaged using a motorized inverted fluorescence widefield microscope, Zeiss Axiovert 200M, provided with a CCD camera (Photometrics CoolSNAP HQ CCD). For image acquisition, the Metamorph 7.7.9.0 software was used. Images were obtained using a 20x objective and different filter sets considering the immunostaining performed. DAPI was observed using a filterset that enables excitation at 330-385nm and emission at > 397 nm; IgG alexa555 (Rhodamine) using one with excitation at 540-552 nm and emission at 575-640 nm; IgG alexa647 (FarRed) using a filterset with excitation at 608-648 nm and emission around 672-712 nm. Complete sections were reconstructed with a 10% image overlay. Images' analysis and quantifications were performed using the ImageJ software, after scale normalization. Total muscle section area and the number and cross-sectional area (CSA) of eMHC-positive fibres were determined to evaluate muscle regeneration success. The number of necrotic fibres in the whole muscle sections was quantified using the cell counter plugin of ImageJ.

2.6.3 Protein Analysis

2.6.3.1 Protein Extraction and Quantification

For protein analysis, whole protein extracts were obtained from the collected muscle. Half-frozen TA or QC were fully submerged in immunoprecipitation buffer (150Mm NaCl, 50Mm Tris ph7.5, 5mM EDTA, 0.5%NP-40, 1% Triton, in Mili-Q Water) supplemented with proteinase inhibitors and phosphatase inhibitors and maintained on ice. The muscle was disrupted into small pieces with scissors and further disaggregated using a disruptor. Disaggregated samples were rotated for 45 minutes at 4ºC and then

centrifuged at 4ºC for 15min at 12000g. The supernatant was recovered and used for further protein analysis.

Protein quantification was performed using the Bradford assay. The necessary calibration curve was obtained using the standard solution Bovine Serum Albumin (BSA; Pierce™ Bovine Serum Albumin Standard Ampules, 2 mg/mL). Bradford Reagent (VWR) was used and absorbance at 595 mm was measured with Microplate Reader TECAN INFINITE M200.

2.6.3.2 Western Blot

Protein Analysis was performed through western blotting. This technique involves protein separation through Sodium Dodecyl Sulfate Polyacrylamide Gel Electrophoresis (SDS-PAGE), membrane transferring, blocking and immunodetection.

For sample preparation, the loading buffer 1x Laemmli sample buffer (Bio-Rad) was added to 30/50 µg of protein from the protein extracts and then incubated for 5min at 95ºC. Protein samples and molecular weight marker PageRuler Prestained protein ladder were loaded in a 12% polyacrylamide gel composed of a separation gel 12% and a stacking gel (recipes in Appendix A.1). Proteins were separated according to the molecular size by electrophoresis at a 75-100mV of voltage for 1h and 30 minutes immersed in running buffer (3.5 mM SDS, 25 mM Tris base (ph8.3), 192 mM glycine). This was performed using the Mini-PROTEAN® Tetra System (Bio-rad) and PowerPac™ HC (Bio-rad).

After SDS-PAGE, proteins were transferred into a nitrocellulose membrane of 0.2µm (Amersham) using the Trans-Blot Turbo Transfer system (Bio-Rad), for 30 minutes at 25V (Standard protocol). Protein gel, filter paper and nitrocellulose membrane were embedded in transfer buffer (25 mM Tris (pH 8.3), 221 mM glycine, 20% methanol) for semi-wet transfer conditions. Subsequently, membranes were washed with Tris-buffered saline-0.1% Tween 20 (TBS-T). To validate the presence of equal amounts of protein between samples, membranes were incubated for 10-20 minutes in Ponceau S solution (Sigma) and washed twice with TBS-T to remove excess. Next, membranes were washed again with TBS-T to remove all remains of Ponceau S solution and blocked for, at least, 1h at RT with 5% milk in TBS-T, to prevent antibody unspecific binding. After washing with TBS-T, membranes were incubated overnight with primary antibody against MANF (SAB3500384 -Sigma) at 4ºC, diluted at 1:1000 in TBS-T 1% milk.

On the next day, membranes were washed with TBS -T four times for, at least, 10 min and incubated for 1h with horseradish peroxidase (HRP)-conjugated anti-rabbit secondary antibody (1:10000; Abcam) in TBS-T 1%milk. Membranes were again washed 5 times with TBS-T and twice with TBS for a minimum of 10 minutes. Revelation was performed using Pierce ECL Western blotting substrate (ThermoScientific) and the following chemiluminescence detection and image acquisition was achieved using Amersham Imager 680 blot (Amersham).

2.6.4 Muscle cell population analysis by FC or FACS

2.6.4.1 Muscle Cell Population Isolation

For isolation of muscle cell populations for FC or FACS, dissected muscles were processed into a single cell suspension using the same protocol. Initially, half or whole TA or QC was mechanically disrupted in a petri dish using scissors and scalpels and then enzymatically digested in a 50 ml tube with 5ml of a collagenase solution containing Dulbecco's Modified Eagle's Medium (DMEM; Corning®) media with 1% Penicillin-Streptomycin (P/S; Gibco), 0.2%(w/v) of collagenase B (Roche) and Calcium dichloride ($CaCl_2$) 0.5 mM for 1h at 38ºC, shaking it every 10 minutes. Then, the digested muscle was decanted and filtered through a 70µm cell strainer into a 50ml tube and washed twice with DMEM media containing 10% FBS and 1% P/S (complete media), and centrifuge at 670g for 10 minutes at 4ºC to remove the remains of collagenase. After centrifugation, cells were resuspended in 500ml of 1x RBC lysis buffer and incubated on ice, covered from light for 10 minutes. Next, cells were washed with DMEM 1% P/S, centrifuged at 670g for 10min at 4ºC and resuspended in 1ml of DMEM 10% FBS 1% P/S. Cells were counted using a hemacytometer.

2.6.4.2 Muscle cells staining for Flow Cytometry and Fluorescence-Assisted Cell Sorting Analysis and Gating Strategies

After cell counting, cells obtained from the previous protocol were incubated in PBS containing 5% Horse Serum (HS) (FACS buffer) with specific antibodies at a density of $1x10^6$ cells/100µl, for 30 minutes at 4ºC, protected from light. The antibodies used for two different analyses are listed in Table 2.5. After the incubation period, cells were centrifuged for 5 minutes at 500g, resuspended in FACS buffer, and filtered through the mentioned 5 ml FACS tubes for FACS and FC analyses.

In this project, different immune cells present in the regenerating muscle and MuSCs and other non-myogenic cells were evaluated. The gating strategy used to analyse the MuSCs, infiltrating hematopoietic cells, endothelial cells, and FAPS within the muscle is shown in Figure 2.3. Viable cells were selected considering the signal from LIVE/DEAD. Infiltrating hematopoietic/immune cells and endothelial cells were isolated from the viable population using the markers CD45 and CD31, respectively. The cell surface markers α7-integrin and Sca-1 were used to identify the population of MuSCs and FAPs, respectively, upon negative selection of the previous markers.

The gating strategies used for immune cell isolation/quantification are described in Figure 2.4. Two different strategies were used, depending on the purpose of the experiment. In FC and FACS analysis, the myeloid population was selected using the CD11b marker. The F4/80 and Ly6G marker were used to distinguish the neutrophil population. Ly6C was used to select the different subpopulations of macrophages. In some cases, only the $Ly6C^{High}$ and $Ly6C^{Low}$ populations were considered. For specific analyses of macrophages phenotype, macrophages with intermediate levels of Ly6C were also isolated.

Table 2.5 - Fluorochrome conjugated antibodies used for muscle cell population analysis by flow cytometry.

Antibodies are grouped according to the different cell populations analyses performed. Enumeration of the antibodies and fluorochromes associated and respective populations recognized, source and dilution.

	Fluorophore conjugated Antibodies /Dyes	Cell population identified	Source	Dilution
MuSC and non-myogenic cells analysis	AF488 anti-mouse **CD31**	Endothelial Cells	Biolegend (102513)	1/50
	PE-Cy5 anti-mouse **CD45**	Hematopoietic cells	Biolegend (103109)	1/100
	PE-Cy7 anti-mouse **Sca-1**	Mesenchymal stem cells	Biolegend (108113)	1/100
	PE anti-mouse **a7integrin**	Muscle stem cells	Miltenyibiotec (130-120-812)	1/40
	APC anti-mouse **F4/80**	Macrophages	Biolegend (123115)	1/100
	LIVE/DEAD™ FixableNear-IR Dead Cell StainLive	Live/Dead cells	Invitrogen (L34975A)	1/1000
Immune cells analysis	PE anti-mouse **F4/80**	Macrophages	Biolegend (123110)	1/50
	APC anti-mouse **Ly6C**	Monocytes/ Macrophages	eBioscience (17-5932-82)	1/200
	FITC anti-mouse **Ly6G**	Neutrophils	Biolegend (127606)	1/400
	APC-eFluor® 780 anti-mouse **CD11b**	Myeloid cells	Bioscience (47-0112-82)	1/200

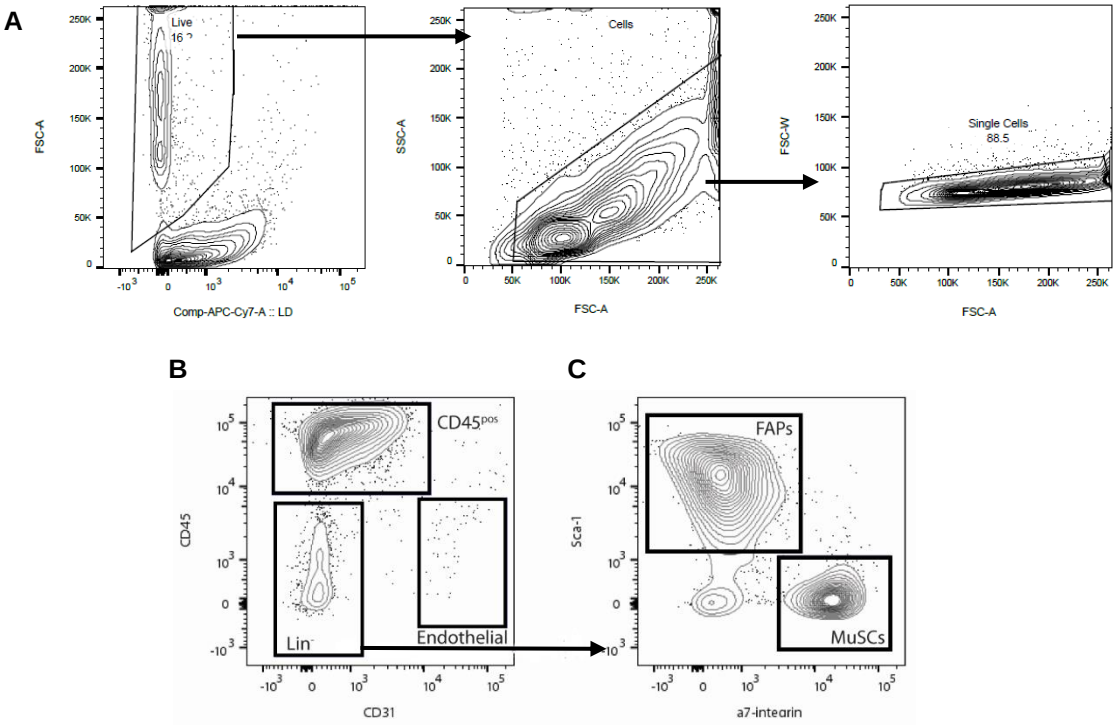

Figure 2.3 - Flow cytometry gating strategy used to analyse the different populations involved in muscle regeneration
A. Single live cells selection. Viable cells were identified based on the LIVE/DEAD stain. Within the viable cell population, cells and single cells were selected. **B.** From the live single cells gate, infiltrating hematopoietic cells ($CD45^{pos}$) and endothelial cells ($CD31^{pos}$) were isolated. **C**. From the population with negative signal for both these markers ($CD45^{neg}CD31^{neg}$), FAPs ($Sca\text{-}1^{pos}$) and MuScs ($a7\text{-}integrin^{pos}$) were discriminated.

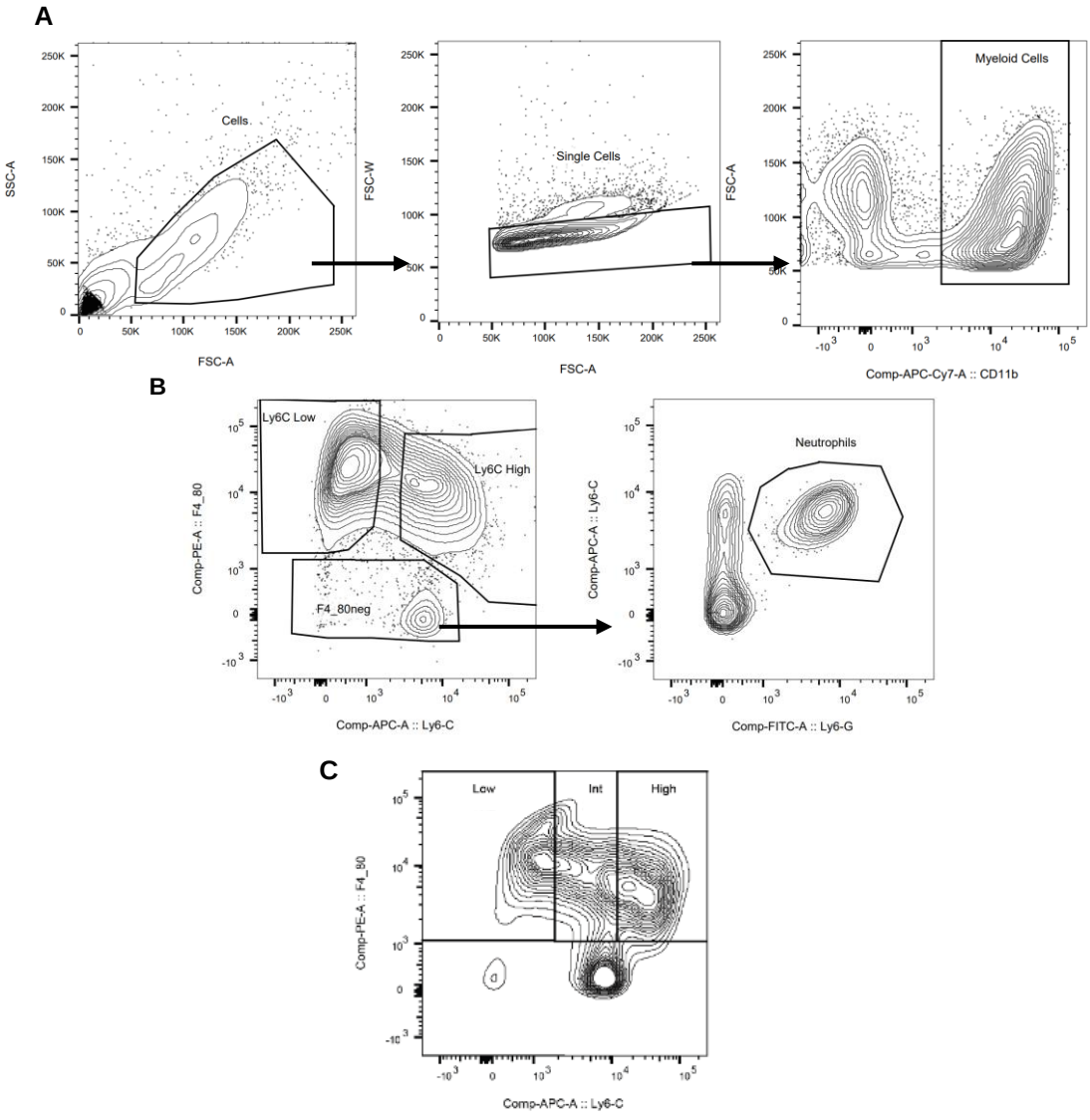

Figure 2.4 - Flow cytometry and FACS gating strategies used to analyse and isolate the immune cell populations in the regenerating skeletal muscle
A. Cells were selected by plotting the forward scatter (FSC) vs. side scatter (SSC), excluding cell debris. Single cells were selected from the previous gate based on Front Scatter Width (FSC-W) vs. Area (FSC-A). From the single cells, the myeloid population ($CD11b^{pos}$) was isolated. From this gate, two different strategies were used, considering the purpose of the experiment. **B.** Selection of pro-inflammatory ($F4/80^{pos}/Ly6C^{High}$), and anti-inflammatory macrophages ($F4/80^{pos}/Ly6C^{Low}$) and neutrophils ($F4/80^{neg}/Ly6G^{pos}$). This strategy was used in FC and FACS analysis. **C.** Selection of macrophages ($F4/80^{pos}$) with Low, Intermediate and High levels of Ly6C within the myeloid cell population previously selected.

2.7 *Ex-vivo* macrophage analysis

Two days post-injury quadriceps from LysM^{CRE}Manf$^{fl/fl}$ and Manf$^{fl/fl}$ mice were isolated and processed into a single cell suspension as formerly described. For each animal, 500 000 cells were collected at 0h and other 500 000 cells were cultured in FACS tubes and collected after 16h. Cells were incubated in suspension at 37ºC in SF medium (Corning® SF Medium, with L-glutamine and 1 g/L BSA) supplemented with 10% FBS and 1% P/S. To assess MANF supplementation effects, other 500 000 cells per animal were incubated in suspension for 16h with recombinant MANF (rMANF) (P-101-100, Icosagene) at a concentration of 10µg/ml. Cells collected at 0h and 16h were immunostained for FC analysis as described above for muscle immune cell populations.

2.8 Transmission Electron Microscopy analysis of macrophages

2.8.1.1 Macrophages isolation and samples processing

Pro-repair macrophages from Cx3cr1$^{CRE-ER/+}$Manf$^{fl/fl}$ and Manf$^{fl/f}$ mice were isolated by FACS as formerly described. Sorted macrophages were plated on 12 mm sterile coverslips inserted in a 24-well plate with complete media and incubated at 37ºC for 2h allowing them to adhere. Cells were then fixed on ice for 45 minutes with 2% formaldehyde (FA) and 2.5% Glutaraldehyde in 0.1M phosphate buffer (PB) and subsequently fixed overnight with 1% FA in PB at 4ºC. The remaining processing and imaging protocols were performed at the Electron Microscopy facility at Instituto Gulbenkian de Ciênca (Lisbon, Portugal). Overnight fixed cells were washed twice on the following day with PB and post-fixed with 1% osmium in PB for 1h on ice. Cells were again washed twice in PB and then in water and stained with 1% tannic acid for 20 minutes on ice. Next, cells were washed 2x in water, stained with 0.5% in Uranyl acetate for 1h at RT and serial dehydrated in increasing concentrations of ethanol. Coverslips with cells were mounted on top of EPON capsules and baked at 60ºC overnight. Sections of 70 nm were obtained using a UC7 Ultramicrotome (Leica), stained with uranyl acetate and lead citrate for 5 minutes each. Images of single macrophages were acquired on a Tecnai G2 Spirit BioTWIN Transmission Electron Microscope (TEM) from FEI operating at 120 keV and equipped with an Olympus-SIS Veleta CCD Camera.

2.8.1.2 TEM Images Quantification

Quantifications of individual pro-repair macrophages from Cx3cr1$^{CRE-ER/+}$Manf$^{fl/fl}$ and Manf$^{fl/f}$ mice, analysed by TEM were performed using the ImageJ software, after scale normalization. Intracellular vesicles were manually surrounded, and the number and area were determined. In addition, the area of each individual cell was calculated. The number and length of protrusions were also determined using the *freehand line* tool of the software.

2.9 Statistical Analysis

Data representation and statistical analysis were performed using the GraphPad 8.0.2 software. Quantitative results are presented in the graphics as mean ± standard error of the mean (SEM).
To determine statistical significance between two groups, the unpaired two-tailed Student's t-test was carried out, except for the ex vivo experiment with MANF supplementation comparison, where the paired two-tailed Student's t test was applied. For survival curves comparison, the log-rank (Mantel-cox) test was used. P-values < 0.05 were considered statistically significant.

3

RESULTS AND DISCUSSION

3.1 Consequences of organismal MANF loss on skeletal muscle regenerative capacity

MANF protein was identified as an immunomodulator and has been associated with the phenotypic transition of macrophages during an immune response to injury, likely contributing to effective tissue repair[76,80]. This protein was found to be transiently expressed during the skeletal muscle regeneration process, particularly by pro-repair macrophages[80]. Nonetheless, MANF is expressed and secreted by multiple cell types[69], other than macrophages, which possibly influences the regeneration process as well.

During aging, MANF induction by pro-repair macrophages after an injury is impaired, which correlates with defects in the associated immune response and regenerative capacity of aged muscle[80]. However, it is unclear if MANF from other cellular sources can influence the regenerative process while counteracting the effects of MANF loss in this particular cell type. Moreover, the precise mechanism underlying MANF activity during the immune response to injury remains unclear. So, in this project, we aim to further investigate the consequences of MANF loss for muscle regeneration and the causes of such effects.

To explore the consequences of impaired MANF signalling for muscle regeneration, we generated the Rosa26$^{CRE\text{-}ERT/+}$Manf$^{fl/fl}$ mouse model, which allows the inducible and ubiquitous MANF deletion in adult mice upon tamoxifen administration. Tamoxifen allows the temporal control of MANF loss, enabling its deletion only in adult life. In this case, this is extremely important since embryonic ubiquitous MANF ablation is lethal[76].

3.1.1 Model Validation

Rosa26$^{CRE\text{-}ERT/+}$Manf$^{fl/fl}$ mouse model carries a copy of the inducible-*Cre* recombinase allele and two copies of the *Manf^{fl}* allele, which has loxP sequences flanking the exon 3 of the *Manf* gene. Upon tamoxifen induction, Cre becomes active in all cell populations and induces recombination and excision of the third exon of the *Manf* sequence. This results in the ubiquitous ablation of the functional *Manf* gene.

Thus, in the current study, tamoxifen injections in Rosa26$^{CRE-ERT/+}$Manf$^{fl/fl}$ mice were used to induce full MANF deletion in adulthood. Control conditions were obtained using: (1) Rosa26$^{CRE-ERT/+}$Manf$^{fl/fl}$ mice that received sham injections with the vehicle corn oil; (2) tam-treated Manf$^{fl/fl}$ mice that don't carry any copy of the inducible-*Cre* recombinase allele.

Confirmation of MANF deletion in the tam-injected Rosa26$^{CRE-ERT/+}$Manf$^{fl/fl}$ mice was performed by genotyping PCR since the length of the *Manf*^{fl} amplicons varies accordingly to the genotype and treatment received.

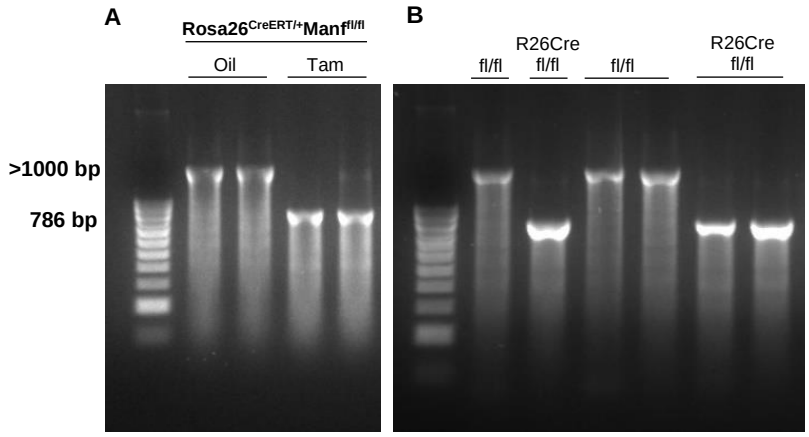

Figure 3.1 - Validation of MANF deletion on the Rosa26$^{CRE-ERT/+}$Manf$^{fl/fl}$ mouse model by PCR
Representative genotyping results after PCR reaction: **A.** Agarose gel of the PCR products from Rosa26$^{CRE-ERT/+}$Manf$^{fl/fl}$ mice that received oil or tamoxifen (Tam) injections. **B.** Agarose gel of the PCR products from tam-treated Manf$^{fl/fl}$ mice (herein identified as fl/fl) and tam-treated Rosa26$^{CRE-ERT/+}$Manf$^{fl/fl}$ mice (here referred as R26Cre fl/fl). Complete *Manf*^{fl} allele originates an amplicon with >1000 base pairs (bp) (upper band), whereas the amplicon of excised *Manf*^{fl} allele has 786bp (lower band).

Tam-treated Rosa26$^{CRE-ERT/+}$Manf$^{fl/fl}$ mice have an excised *Manf*^{fl} allele, exhibiting a smaller amplicon, with only 786 bp (lower band). On the other hand, oil-treated mice, that preserve the functional *Manf* gene, revealed an amplicon with more than 1000bp (upper band) (Figure 3.1A). The same result was seen in Manf$^{fl/fl}$ mice treated with tamoxifen (Figure 3.1B).

Moreover, to ensure MANF ablation in the regenerating tissue of the Rosa26$^{CRE-ERT/+}$Manf$^{fl/fl}$ mice upon tamoxifen injections, MANF protein levels were also analysed in the injured muscle at 3dpi by Western blotting. Ponceau S staining was used as a loading control, to confirm the amount of protein within each sample. This technique was applied since typical housekeeping genes, including β-actin, may differ among different conditions, due to different cellular constitution of the tissue[84]. Results revealed that tamoxifen treatment in Rosa26$^{CRE-ERT/+}$Manf$^{fl/fl}$ mice led to a complete loss of MANF protein in the muscle tissue, whereas oil-treated mice maintained MANF protein expression (Figure 3.2).

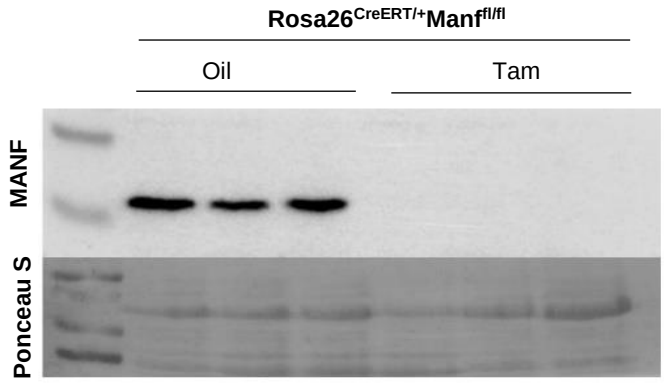

Figure 3.2 - MANF expression levels in injured muscles from Rosa26$^{CRE\text{-}ERT/+}$Manf$^{fl/fl}$ mouse model at 3dpi
Western blot analysis of MANF levels in protein extracts from Rosa26$^{CRE\text{-}ERT/+}$Manf$^{fl/fl}$ mice injected with Oil or Tam at 3dpi. Ponceau S staining was performed to verify equivalent protein loading in each sample. MANF protein size is 18 kilodalton (kDa). The molecular weight marker PageRuler Prestained protein ladder is shown.

These results ensured MANF deletion only in the tamoxifen-treated Rosa26$^{CRE\text{-}ERT/+}$Manf$^{fl/fl}$ mice, validating this mouse model to study the effects of total MANF loss.

3.1.2 Effects of organismal MANF loss on skeletal muscle regenerative efficiency

To assess the effects of organismal MANF loss on the muscle regeneration process, histological analyses of injured muscle from tam-treated Rosa26$^{CRE\text{-}ERT/+}$Manf$^{fl/fl}$ mice were performed. Both controls previously described were used.

3.1.2.1 Overall effects on skeletal muscle regeneration

H&E staining of muscle cryosections provided an overview of the impact of MANF deletion during regeneration. With this stain, nuclei exhibit a dark blue/purple colour whereas cytoplasm and ECM are stained with different tones of pink.

At 4dpi, both tamoxifen-treated Manf$^{fl/fl}$ mice and oil-treated Rosa26$^{CRE\text{-}ERT/+}$Manf$^{fl/fl}$ used as controls revealed a high number of mononucleated inflammatory cells within the injured area and few damaged myofibers, that weren't yet eliminated. Moreover, it was possible to observe blank rounded spaces at the injured site which indicates that necrotic myofibers are being cleared and eliminated by the immune cells, leaving empty spots in their places (Figure 3.3A-B). These histological features are consistent with the normal regeneration process described in the literature[26,27].

On the other hand, analysis of injured muscles from tam-treated Rosa26$^{CRE\text{-}ERT/+}$Manf$^{fl/fl}$ mice revealed defects in the muscle regeneration process (Figure 3.3C). At 4dpi, it was possible to observe an accumulation of necrotic fibres within the injured muscle, which indicates impairments in debris clearance. MANF knockout mice showed immune cells infiltration into the injured tissue. However,

compared to controls, the immune response appears to be weaker, as indicated by a reduced number of immune cells in the regenerating tissue.

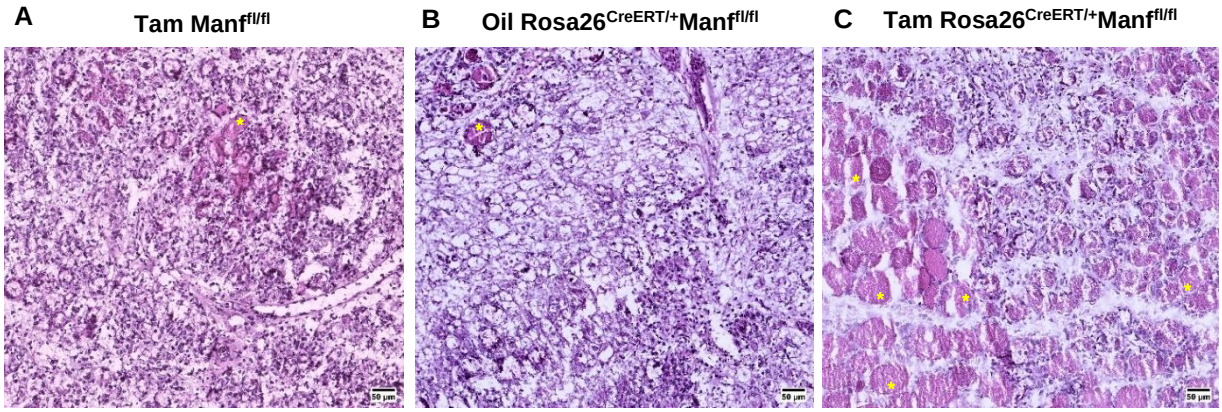

Figure 3.3 - Histological analysis of the impact of MANF loss in the regeneration process at 4 dpi by H&E
A-C. Representative images of H&E staining in cryosections of regenerating TA muscles from (A) tam-treated Manf$^{fl/fl}$ mice, (B) oil-treated Rosa26$^{CRE-ERT/+}$Manf$^{fl/fl}$ mice and (C) tam-treated Rosa26$^{CRE-ERT/+}$Manf$^{fl/fl}$ mice at 4dpi. Representative necrotic fibres are indicated in each image (asterisks). Scale bar, 50µm.

3.1.2.2 Effects on the clearance of necrotic debris

The persistence of necrotic fibres within the tissue was further evaluated through mouse IgG immunohistochemistry in regenerating TA muscles. The staining of necrotic myofibers using IgG as a marker is based on the fact that myofibers become permeable during necrosis allowing the passive uptake of IgG proteins, trapping them[85].

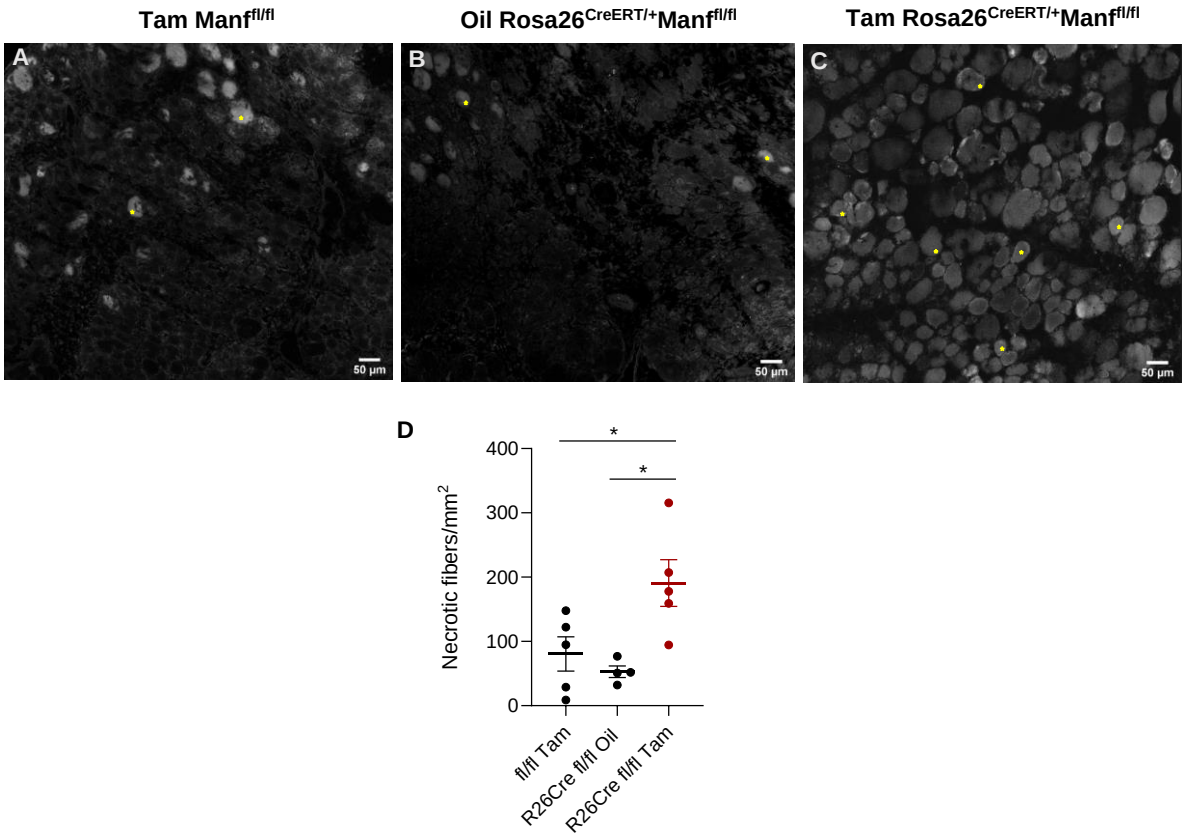

Figure 3.4 - Impact of MANF loss on necrotic fibres clearance at 4 dpi
A-C. Representative images of muscle cryosections immunostained with mouse IgG of regenerating TA from (A) tam-treated $Manf^{fl/fl}$ mice, (B) oil-treated $Rosa26^{CRE\text{-}ERT/+}Manf^{fl/fl}$ mice and (C) tam-treated $Rosa26^{CRE\text{-}ERT/+}Manf^{fl/fl}$ mice at 4dpi. Representative necrotic fibres are indicated in each image (asterisks). Scale bar, 50µm. **D.** Quantification of the number of necrotic fibres per mm^2 of damage area in regenerating TA from tam-treated $Manf^{fl/fl}$ (herein shown as fl/fl Tam) (n=4), oil-treated $Rosa26^{CRE\text{-}ERT/+}Manf^{fl/fl}$ (herein shown as R26Cre fl/fl Oil) (n=4) and tam-treated $Rosa26^{CRE\text{-}ERT/+}Manf^{fl/fl}$ (herein shown as R26Cre fl/fl tam) (n=5) mice at 4dpi. Data is shown as mean± SEM and each point represents one animal. *p<0.05

At 4dpi, it was possible to observe a high accumulation of degenerating myofibers in tam-treated $Rosa26^{CRE\text{-}ERT/+}Manf^{fl/fl}$ mouse muscle, while control animals visibly exhibited less necrotic fibres (Figure 3.4A-C). Quantification analysis of IgG^{pos} fibres (Figure 3.4D) confirmed this persistence of necrotic myofibers within the regenerating tissue of MANF deficient mice. The number of necrotic myofibers per square millimetre of muscle tissue was significantly higher, more than doubling when compared to both control conditions.

These results reinforce that MANF loss during muscle regeneration impairs debris elimination.

3.1.2.3 Effects on the myogenic process

Following skeletal muscle damage, MuSCs become activated and give rise to new myofibers, that are small at the early stages and gradually increase in size as myoblasts fuse. Newly formed fibres are valuable indicators of skeletal muscle regeneration success and are specially characterized by central nuclei and the expression of eMHC[23].

Thus, the impact of MANF deletion on regeneration was also evaluated through eMHC immunostaining of skeletal injured muscle, which is a useful method to analyse the progression of the myogenic process.

At 4dpi, it was already possible to identify eMHC positive centrally nucleated myofibers in both controls and in MANF deficiency conditions, which indicate recently regenerating myofibers (Figure 3.5A-C). However, the density of nascent myofibers was significantly reduced in tam-treated $Rosa26^{CRE\text{-}ERT/+}Manf^{fl/fl}$ mice when compared to both controls (Figure 3.5D). Moreover, the cross-sectional area (CSA) of new myofibers at 4dpi was significantly lower in MANF ablated muscles. (Figure 3.5E). Considering the frequency distribution of new fibres' CSA in each condition, more than 20% of total new myofibers from tam-treated $Rosa26^{CRE\text{-}ERT/+}Manf^{fl/fl}$ mice were approximately 75µm^2, whereas the area of nascent fibres of control animals was more frequent around 275µm^2 (Figure 3.5F).

These results indicate that MANF ablation impairs the myogenic process preventing normal myofiber formation and leading to fewer and smaller fibres.

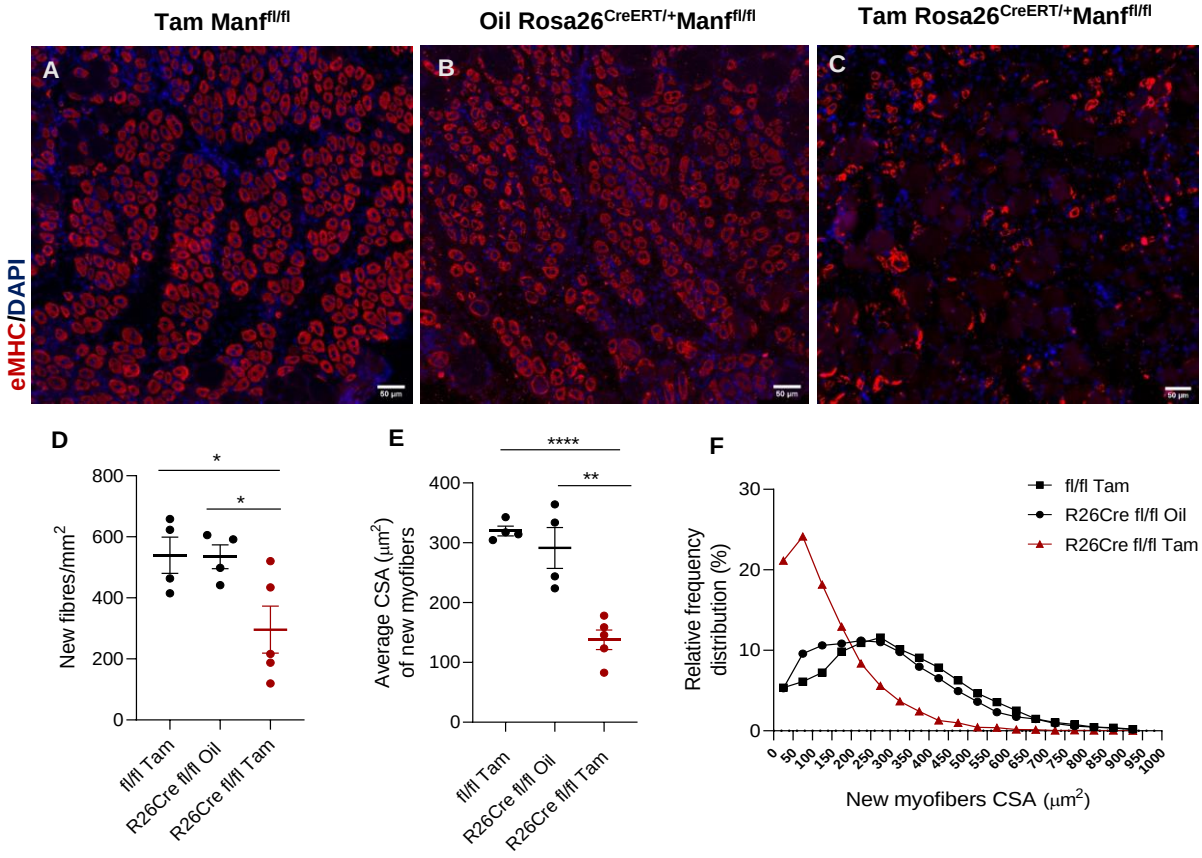

Figure 3.5 - Impact of MANF loss on the formation of new myofibers (eMHC^{pos}) at 4 dpi
A-C. Representative images of eMHC (red) and DAPI (blue) staining in muscle cryosections of regenerating TA from (A) tam-treated Manf$^{fl/fl}$ mice, (B) oil-treated Rosa26$^{CRE-ERT/+}$Manf$^{fl/fl}$ mice and (C) tam-treated Rosa26$^{CRE-ERT/+}$Manf$^{fl/fl}$ mice at 4dpi. eMHC marker is used to identify newly formed fibres in the regenerating tissue and DAPI is used for nuclei detection. Scale bar, 50µm. **D-E**. Quantification of (D) the density of eMHC^{pos} fibres per mm^2 of damage area and (E) the average eMHC^{pos} cross sectional area (CSA; µm^2) within the whole damaged area for tam-treated Manf$^{fl/fl}$ mice (herein shown as fl/fl Tam) (n=4), oil-treated Rosa26$^{CRE-ERT/+}$Manf$^{fl/fl}$ mice (shown as R26Cre fl/fl Oil) (n=4) and tam-treated Rosa26$^{CRE-ERT/+}$Manf$^{fl/fl}$ mice (shown as R26Cre fl/fl Tam) (n=5) at 4dpi. Results are represented as mean± SEM and each point represents one animal. *p<0.05, **p<0.01 and ****p<0.0001. **F.** Relative frequency distribution (%) of eMHC^{pos} fibres cross sectional area (CSA; µm^2) in each condition.

Taken together, all referred histological analyses allowed the identification of important regenerative failures when MANF is ubiquitously ablated. MANF loss impaired the clearance of damaged fibres and affected myofiber formation resembling the phenotype observed in mice with MANF deletion in pro-repair macrophages[80]. Importantly, the magnitude of the phenotype observed was much higher in this model of ubiquitous MANF deletion.

These results support the notion that MANF is indeed an essential factor for muscle regeneration and that MANF from different sources may influence the regeneration phenotype. This will be further discussed in the next chapters.

Importantly, literature shows that defects in the phagocytic removal of cellular material are associated with delayed regeneration[34,42]. The necrotic myofibers that remain in the regenerating tissue may influence the formation of new fibres by acting as physical barriers, preventing contact of myoblasts[28,41].

Whether degenerating fibres also suppress myoblast growth by acting as atrophic factors remains unclear.

Furthermore, both impaired processes are dependent on the immune response triggered after injury. Debris clearance depends on the phagocytic activity of the myeloid cells promptly recruited to the injury site, including neutrophils and macrophages[14]. Several studies demonstrate that when the infiltration of macrophages in the regenerating tissue is defective, cellular debris accumulates within the injured muscle impairing the repair process[86,87]. Moreover, the formation of new fibres and the multiple steps of the myogenic process depend on a biphasic response of macrophages[42]. Hence, since MANF is an immunomodulator that had been already associated with the myeloid recruitment and macrophages phenotypic transition, the regeneration defects here identified in its absence may be associated with more severe alterations in immune responses.

The formation of myofibers also depends on the presence and activity of MuSCs at the injury site and other non-myogenic cells such as FAPS and endothelial cells[28]. So, alterations in these populations in complete absence of MANF may also be related to the regenerative impairments seen.

3.1.3 Effects of organismal MANF loss on the different populations involved in muscle regeneration

Taking into account the previous results, we evaluated the impact of MANF loss on the different populations involved in the muscle regeneration process. Muscle cell populations were isolated from QC and analysed by FC 3 days after injury. In this analysis, only oil-treated Rosa26$^{CRE\text{-}ERT/+}$Manf$^{fl/fl}$ mice were used as controls.

Muscle-resident and infiltrating cell populations can be identified by their distinct surface markers. Infiltrating hematopoietic cells, endothelial, and mesenchymal progenitor cells such as FAPS, are respectively CD45^{pos}, CD31^{pos}, and CD45^{Neg}CD31^{Neg}Sca-1^{pos}. The identification of MuSCs by FC depends on the exclusion of these cell populations and subsequent selection of the one positive for α7-Integrin.

Animals treated with tamoxifen and with consequent MANF ablation displayed significantly reduced numbers of MuSCs and CD45^{pos} immune cells compared to animals who received oil treatment. On the other hand, no alterations in the populations of FAPs (CD45^{Neg}CD31^{Neg}Sca-1^{pos}) and endothelial cells (CD31^{pos}) were detected (Figure 3.6).

Muscle regeneration is an extremely coordinated process that depends on dynamic interactions between MuSCs and infiltrating immune cells and both populations showed to be reduced in the absence of MANF. Impairments in MuSCs activation and proliferation may lead to reduced numbers of MuSCs and consequently defects in myofibers formation and incomplete restoration of the muscle tissue. The immune cells that accumulate within the tissue secrete important signals that modulate

MuSCs activity and function[36,42]. Thus, defects in immune cells recruitment and response may impact MuSCs numbers and function and affect the outcome of muscle repair.

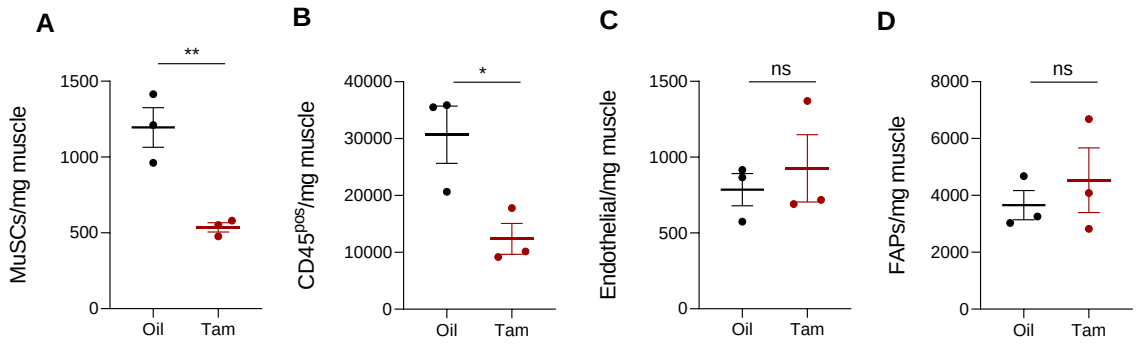

Figure 3.6 - Effects of organismal MANF loss on the different populations involved in muscle regeneration analysed by Flow Cytometry
Quantification by flow cytometry of (A) MuSCs, (B) $CD45^{pos}$ immune cells (C) endothelial cells ($CD31^{pos}$) and (D) FAPs ($CD45^{Neg}CD31^{Neg}Sca\text{-}1^{pos}$) in regenerating quadriceps (QC) of oil-treated $Rosa26^{CRE\text{-}ERT/+}Manf^{fl/fl}$ mice (n=3) and tam-treated $Rosa26^{CRE\text{-}ERT/+}Manf^{fl/fl}$ mice (n=3) at 3dpi. Normalization was performed considering muscle mass (mg). Data is shown as mean ± SEM and each point represents one animal. *p<0.05, **p<0.01 and ns= not significant.

3.1.4 Effects of organismal MANF loss on the myeloid populations in the regenerating muscle

One of the most immediate cellular responses triggered by muscle injury is the activation of innate immunity and consequent infiltration of myeloid cells into the injured muscle[36]. These cells have a fundamental role in debris clearance and phagocytosis of dead fibres, a process that is impaired in the absence of MANF. Moreover, these cells help modulate the myogenic process, which is also compromised in this condition. This way, we focused our investigation on the myeloid response to muscle injury.

Neutrophils and macrophages are among the main myeloid cells enriched in the regenerating muscle, thus being analysed more closely in this study. The different populations were isolated based on the expression of specific surface markers. Myeloid cells are positive for CD11b, and neutrophils are $F4/80^{neg}$ and $Ly6G^{pos}$. Macrophages are identified by the expression of F4/80 and their subpopulations can be distinguished based on the expression levels of Ly6C. Pro-inflammatory and pro-repair populations of macrophages are isolated as $Ly6C^{High}$ and $Ly6C^{Low}$, respectively.

FC analysis showed that tam-treated $Rosa26^{CRE\text{-}ERT/+}Manf^{fl/fl}$ mice had a 66,5% reduction in the number of $CD11b^{pos}$ cells at 3dpi compared to the control condition, implying a defect in the myeloid cells' accumulation at the injury site (Figure 3.7A). This reduction is associated with an 84% decline in the number of pro-repair macrophages ($F4/80^{pos}Ly6C^{Low}$) and a less pronounced decrease in the pro-inflammatory population of macrophages, although not statistically significant (Figure 3.7B-C). No significant differences were detected regarding the population of neutrophils (Figure 3.7D).

The overall reduction in the macrophage population may be explained by the blunted accumulation of myeloid cells following injury. However, there is an imbalance in macrophage subpopulations. While anti-inflammatory pro-repair ($Ly6C^{Low}$) macrophages have a striking reduction, the pro-inflammatory population ($Ly6C^{High}$) displayed a non-significant decrease.

These results might indicate that the pro-inflammatory macrophages are not transiting towards the anti-inflammatory phenotype in the absence of MANF, accumulating at the expense of the $Ly6C^{Low}$ population. To better visualize this, we use the ratio $Ly6C^{Low}/Ly6C^{High}$, which represents the ratio between pro-repair and pro-inflammatory macrophages (Figure 3.7E). Since $Ly6C^{Low}$ macrophages arise in the regenerating muscle from the $Ly6C^{High}$ population, this ratio increases as more transition occurs and more pro-repair macrophages emerge. The ratios obtained for tam-treated mice were significantly diminished compared to controls, reinforcing the idea that MANF ablation leads to impairments in the phenotypic transition.

Thus, this analysis revealed that full MANF deletion results in an inflammatory crisis with defective myeloid accumulation and impaired phenotypic transition.

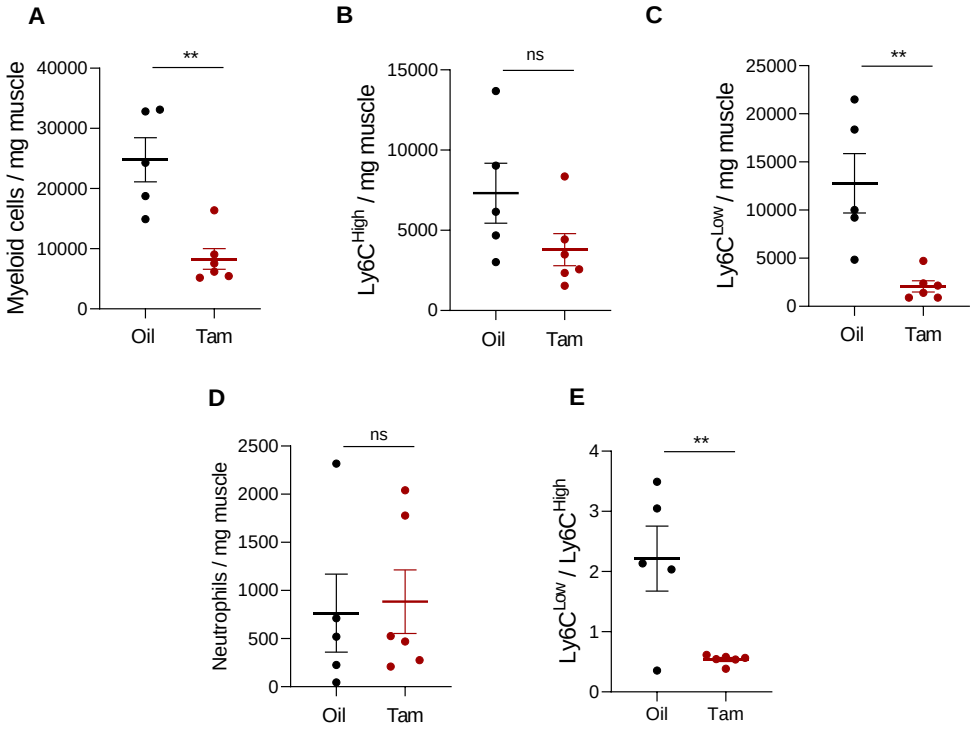

Figure 3.7 - Effects of organismal MANF loss on the myeloid populations involved in muscle regeneration evaluated by Flow Cytometry.
A-D. Quantification by flow cytometry of (A) Myeloid Cells ($CD11b^{pos}$), (B) $Ly6C^{High}$ pro-inflammatory macrophages (C) $Ly6C^{Low}$ anti-inflammatory macrophages and (D) Neutrophils ($F4/80^{Low}Ly6G^{High}$) in regenerating quadriceps (QC) of oil-treated $Rosa26^{CRE\text{-}ERT/+}Manf^{fl/fl}$ mice (n=5) and tam-treated $Rosa26^{CRE\text{-}ERT/+}Manf^{fl/fl}$ mice (n=6) at 3dpi. Normalization was performed considering muscle mass (mg). **E.** Ratio of pro-repair $Ly6C^{Low}$ to pro-inflammatory $Ly6C^{High}$ macrophages quantified by flow cytometry in single cells suspensions isolated from QC muscles. Data is presented as mean ± SEM and each point represents one animal. **p<0.01 and ns= not significant.

The phenotype observed regarding myeloid cell numbers is possibly explained by impairments in their recruitment to the damaged site shortly after the injury. This may be due to a defect in the recruitment mechanism or alterations in the immune cell pool available in circulation. Alternatively, it is also possible that cells are dying within the tissue. Hence, the cause of such a defect will be explored later in this study.

MANF function has already been associated with the immune cells phenotypic shift towards an anti-inflammatory state, acting in an autocrine manner[76]. Moreover, previous results from the group have demonstrated that MANF ablation in the pro-repair population resulted in less pronounced defects in immune accumulation and macrophages' transition during muscle regeneration, resembling the phenotype observed in aging[80].

Nevertheless, the increased severity of the regenerative and immune impairments in the full MANF knockout mice observed in the present study highlights the impact of MANF secreted by other cell types on the muscle regeneration phenotype. This suggests that, despite working in an autocrine manner, other sources of MANF may impact the regeneration process.

MANF was found to be induced in skeletal muscle, particularly by pro-repair macrophages[80]. However, MANF is widely expressed in the organism. One possible explanation for the presented results is that MANF knockdown in pro-repair macrophages can result in a compensatory up-regulation of MANF in other cell types limiting the effects observed in that condition. Thus, when MANF is fully ablated, the other cell types cannot proceed with such a cellular compensatory mechanism resulting in a more severe phenotype.

On the other hand, it is also possible that MANF expressed by other cells in the muscle, such as MuSCs, influence the regeneration process in normal conditions. This hypothesis should be tested in the future, for instance with conditional ablation of MANF in MuSCs.

3.1.5 Long-term effects of organismal MANF loss on regeneration and survival

Considering the defects identified in the regeneration process on the following days of the muscle injury, we assessed if the MANF loss at the moment of the injury had long-term effects on the animals' tissue recovery.

For that, tam-injected $Rosa26^{CRE\text{-}ERT/+}Manf^{fl/fl}$ and $Manf^{fl/fl}$ mice were monitored for 14 days after an injury. On the 14th day, animals that survived were euthanized, and subsequent H&E histological analysis was performed on the cryosectioned muscles. Throughout the experiment, it was possible to detect a high mortality rate of the $Rosa26^{CRE\text{-}ERT/+}Manf^{fl/fl}$ mice, so a survival analysis was also performed.

The results obtained showed that only 25% of $Rosa26^{CRE\text{-}ERT/+}Manf^{fl/fl}$ mice survived, while 80% of tam-treated $Manf^{fl/fl}$ mice were still alive after 14 days. Mice with MANF ablation appear to have an increased

tendency to die compared to animals that preserved MANF levels throughout the whole experiment (Figure 3.8A), although not statistically significant.

Given the several functions of MANF described in the literature[70], it is possible that ubiquitous MANF loss, at the organismal level, before an injury induces a systemic response that may be lethal to animals. However, it would be important to increase the number of animals per condition in this study. Further pathology analysis must be performed to better understand the causes of death.

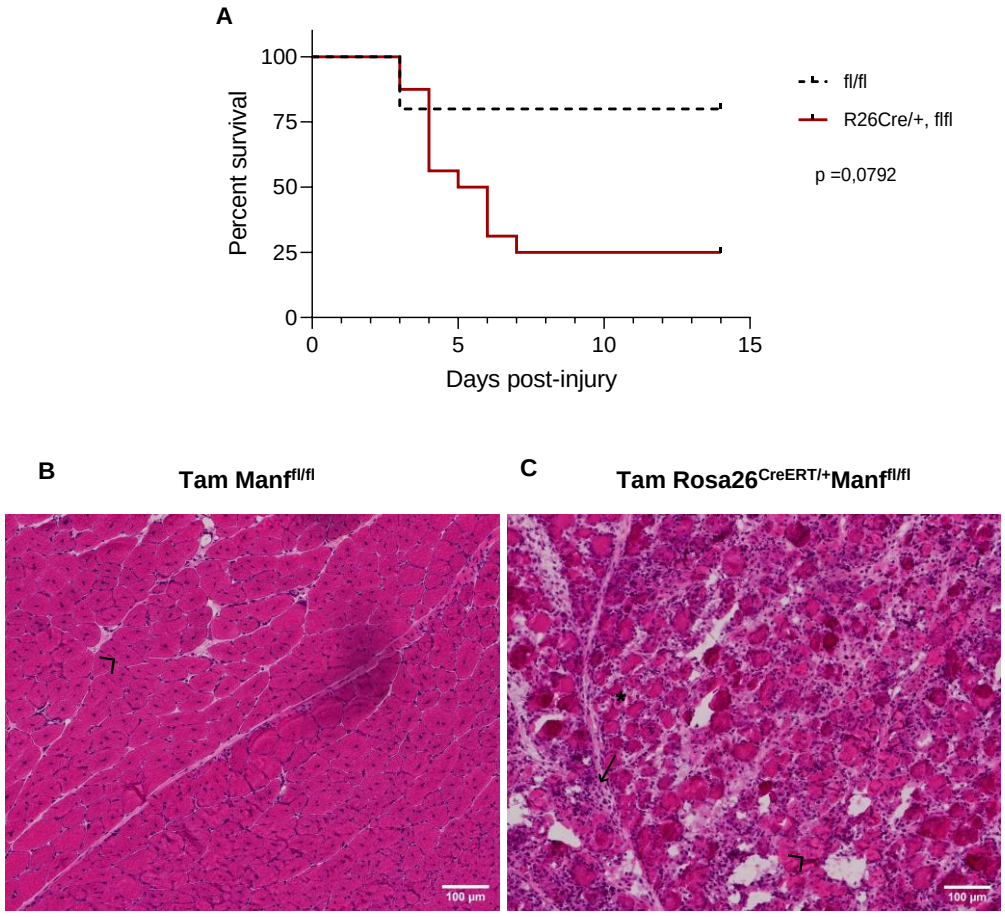

Figure 3.8 - Long-term effects of organismal MANF loss on survival and regeneration.
A. Kaplan-Meier survival curves of the tamoxifen-treated Rosa26^{CreER}Manf$^{fl/fl}$ (n=16) and Manf$^{fl/fl}$ (n=5) mice for 14 days. **B-C.** Representative images of H&E staining in muscle cryosections of regenerating QC from (B) tam-treated Manf$^{fl/fl}$ mice, and (C) tam-treated Rosa26$^{CRE-ERT/+}$Manf$^{fl/fl}$ mice at 14dpi. Representative new centrally nucleated fibres (>), necrotic fibres (*), and mononucleated inflammatory cells (→) are indicated in the images Scale bar, 100µm.

Regarding tissue analysis after 14 days of injury, Rosa26$^{CRE-ERT/+}$Manf$^{fl/fl}$ mice that survived revealed unsuccessful tissue regeneration which is strikingly different from what is observed in the Manf$^{fl/fl}$ mice.

Muscles at 14 dpi from tam-treated Manf$^{fl/fl}$ (Figure 3.8B) exhibited a high density of big centrally nucleated myofibers, homogenously organized in the whole muscle section, indicating effective

myofibers formation. By day 14, immune cells were not detected indicating that inflammation was resolved. These results are consistent with the normal regeneration process of skeletal following intramuscular $BaCl_2$ injury described in the literature[26].

On the other hand, tam-treated Rosa26$^{CRE-ERT/+}$Manf$^{fl/fl}$ revealed an accumulation and persistence of mononucleated inflammatory cells and necrotic myofibers. Few small centrally nucleated myofibers could be identified (Figure 3.8C).

Thus, this descriptive analysis points to long-term defects in the repair process in the absence of MANF, suggesting that, in these conditions, the immune response cannot be resolved, the myogenic process cannot progress, and necrotic fibres accumulate, within 14 days.

The impaired recruitment and the disruption of a spatiotemporally regulated response of macrophages are likely to contribute to these alterations. Macrophages' activities are associated not only with debris clearance but also with the regulation of both MuSCs and FAPs activity[26,28]. Thus, if the biphasic response of macrophages becomes dysfunctional, these cells cannot properly regulate the myogenic process.

Importantly, considering that alterations in the immune system may affect MuSC and stimulate a shift towards a fibrogenic phenotype[63] and impact FAPs, it would be of great interest to analyse the fibrotic tissue within the regenerating muscle through a specific technique such as Masson's Trichrome stain[88].

3.2 Causes of immune dysfunction during a regenerative pressure upon MANF ablation

The previous results supported the notion that loss of MANF disrupts the immune response to muscle damage, affecting the myeloid cells accumulation rapidly triggered after injury and the crucial phenotypic transition of macrophages. These consequences are related to impaired tissue clearance and defective myogenesis. However, the causes of such inflammatory defects remain unknown.

Therefore, we looked into the origin of the inflammatory crisis, exploring, initially the defects in myeloid accumulation and then focusing on the effects of MANF loss specifically on macrophages.

3.2.1 Impact of MANF loss on blood circulating cells after skeletal muscle injury

Tam-treated Rosa26$^{CRE-ERT/+}$Manf$^{fl/fl}$ mice exhibit a blunted myeloid accumulation in response to skeletal muscle injury. Most leukocytes present in the regenerating muscle are recruited from the bloodstream[28,37]. So, impairments in this process may impact the blood constitution or vice versa. The origin of the recruitment defect is unclear, but it may be associated with the pool of cells in circulation available to be recruited upon an injury.

To better understand the defective accumulation of immune cells upon an injury when MANF is ablated, blood circulating leukocytes from tam-treated Rosa26$^{CRE-ERT/+}$Manf$^{fl/fl}$ mice were analysed by FC 3 days after injury. Manf$^{fl/fl}$ mice that received tamoxifen injections were used as controls.

Live single cells were selected based on the viability dye Zombie Aqua. Myeloid cells are identified as CD11b^{pos} cells. Within this population, monocytes and neutrophils are distinguished within the F4/80^{neg} population based on the expression of Ly6C and Ly6G, respectively. In addition to the myeloid cells, T and B cells were also quantified, using the corresponding surface markers CD3e and CD45R.

Compared to the control condition, MANF knockout mice displayed a significant 70% reduction in the number of monocytes per microliter (µl) of blood (Figure 3.9B). The number of B cells per µl is also significantly reduced in the MANF loss mouse model (Figure 3.9D). Although no significant differences were detected regarding total myeloid cells, neutrophils, and T cells, these populations tend to be decreased when MANF is deleted (Figure 3.9A,C,E).

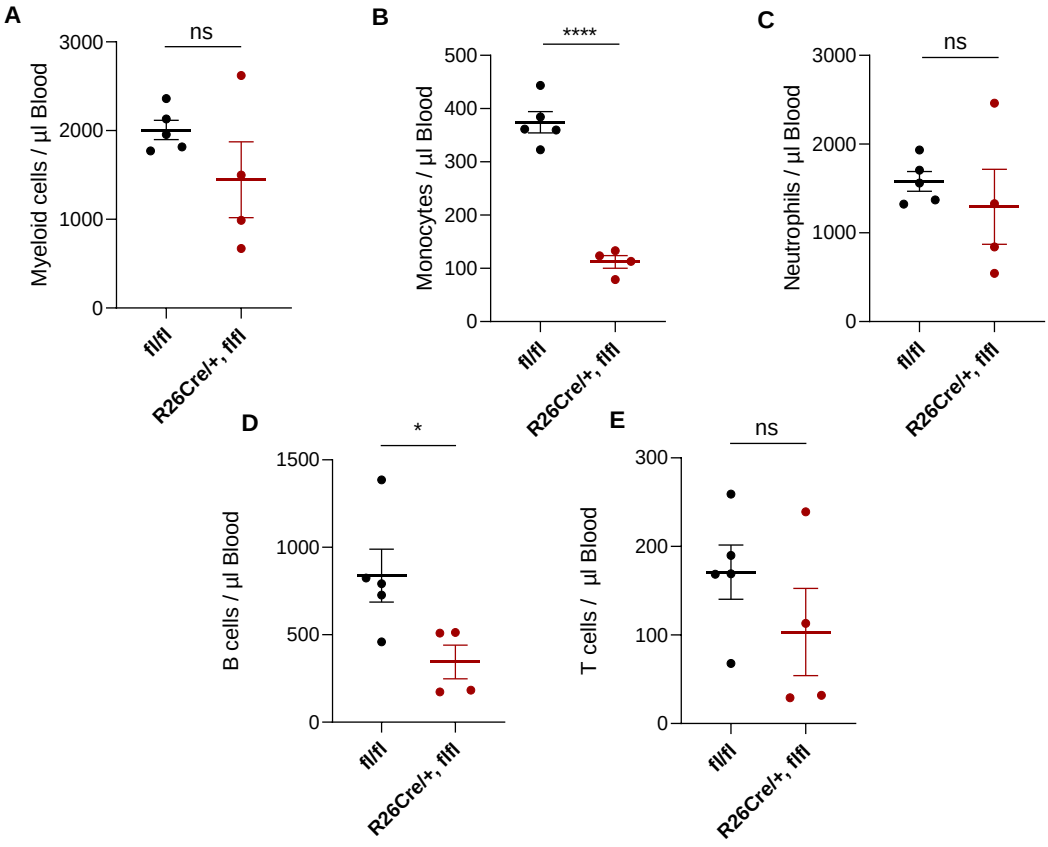

Figure 3.9 - Impact of organismal MANF loss on the blood cell populations analysed by Flow Cytometry. A-E. Quantification by flow cytometry of (A) Myeloid (CD11b^{pos}) cells, (B) Monocytes (F4/80^{Neg}Ly6C^{pos} cells), (C) Neutrophils (F4/80^{Neg}Ly6G^{pos} cells) (D) B cells (CD45R^{pos}) and (E) T cells (CD3e^{pos}) per microliter of blood collected from tam-treated Manf$^{fl/fl}$ mice, here identified as fl/fl (n=5) and tam-treated Rosa26$^{CRE-ERT/+}$Manf$^{fl/fl}$ mice (n=4) at 3dpi. Data is shown as mean ± SEM and each point represents one animal. *p<0.05, ****p<0.0001 and ns= not significant.

Usually, muscle damage induces a robust infiltration of blood-derived immune cells. However, in the absence of MANF, this process is blunted/impaired, and fewer immune cells infiltrate the tissue. The blood analysis demonstrated that cells are not accumulating in the blood but appear to be also reduced in the bloodstream, in particular, monocytes, that are involved in the myeloid response, and B cells.

Usually, circulating Ly6C^{high} monocytes infiltrate the injury site shortly after neutrophils and differentiate into pro-inflammatory macrophages. Thus, the reduced number of monocytes in the blood may be responsible for the altered levels of macrophages within the injured area.

These results suggest that the recruitment defect identified when MANF is lost may be associated with changes in circulating immune cell numbers. One potential explanation is the existence of defects in the production of immune cells in the bone marrow.

3.2.2 Impact of MANF loss on bone marrow populations after skeletal muscle injury

The former results suggested an alteration in the circulating numbers of immune cells, particularly monocytes and B cells. Given that immune cells are constantly produced in adult life in the bone marrow and that the primary source of inflammatory cells in the regenerating muscle is the BM[45], defects in the hematopoietic process may alter the cell numbers entering the blood and the muscle tissue following injury.

This way, we focused our study on the hematopoietic process and, particularly on myeloid cells production. To assess the effect of MANF deficiency on hematopoiesis, we identified and analysed the bone marrow populations by FC 3 days after the injury.

LSK cells are considered the Sca-1^{pos}c-Kit^{pos} hematopoietic progenitor cells that lack specific lineage markers (Lin^{neg}) and, thus, are not yet fully committed to any blood cell line. These include LT-HSCs, ST-HSCs and MPPs. Among these populations, only ST-HSCs cells were significantly elevated in tam-treated Rosa26$^{CRE-ERT/+}$Manf$^{fl/fl}$ mice when compared to control Manf$^{fl/fl}$ mice. However, the numbers of all LSK populations reveal a tendency to be increased when MANF was ablated (Figure 3.10A-F).

By contrast, all myeloid progenitors in bone marrow were significantly reduced in animals with MANF deletion. In this analysis, MPs were considered the Lin^{Neg} Sca-1^{Neg}c-Kit^{Pos} population and comprised the common myeloid progenitors (CMP), megakaryocytic/erythroid progenitors (MEP) and granulocyte/macrophage progenitors (GMP), all of which reduced in MANF loss conditions. We observed that the CMPs from tam-treated Rosa26$^{CRE-ERT/+}$Manf$^{fl/fl}$ mice experienced an 83% reduction and GMPs a 78% decline in their numbers, compared to control animals (Figure 3.10G-J).

Importantly, the present results imply a defect in the hematopoietic process in conditions of MANF deficiency. Early-stage multipotent cells, especially, ST-HSCs, appear to be accumulating at the expense of the committed progenitors, leading to reduce numbers of the following CMPs, GMPs and MEPs. The decline in myeloid progenitors correlates with the strikingly reduced numbers of monocytes

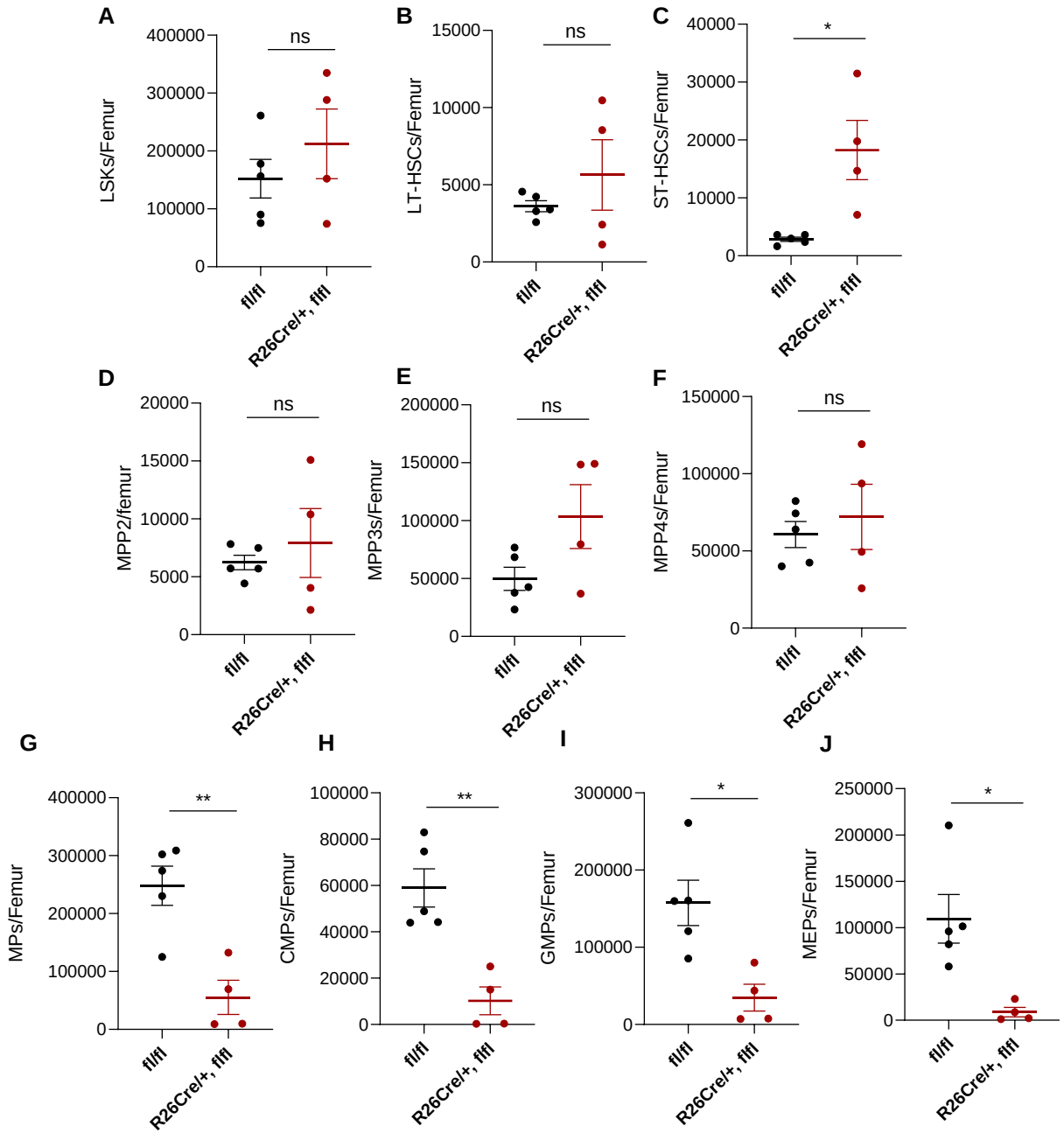

Figure 3.10 - Impact of organismal MANF loss on the bone marrow cell populations analysed by Flow Cytometry.
A-J. Quantification by flow cytometry of (A) overall LSK cells, including (B) LT-HSCs, (C) ST-HSCs and (D-F) MPPs; and (G) overall committed myeloid progenitors, comprising (H) CMPs, (I) GMPs and (J) MEPs present in a femur bone marrow from tam-treated $Manf^{fl/fl}$ mice, here identified as fl/fl (n=5), and tam-treated $Rosa26^{CRE-ERT/+}Manf^{fl/fl}$ mice (n=4) at 3dpi. Data is shown as mean ± SEM and each point represents one animal. *p<0.05, **p<0.01 and ns= not significant.

in the bloodstream since they are derived from GMPs. In turn, this may be associated with the defective recruitment identified at the injury site.

Given that lymphocytes also appear to be reduced in the blood, it is not likely that hematopoietic cells are skewing towards the lymphoid lineage, although this must be further confirmed looking into the CLPs numbers.

Literature reported that after severe injury, the high demand for leukocytes and, particularly, myeloid cells stimulates an emergency hematopoietic response[54]. This process is associated with the expansion of the HSCs, MPPs and higher numbers of myeloid skewed progenitors[54,89].

However, in the absence of MANF, the BM does not seem able to respond effectively and generate sufficient progeny necessary for a successful immune response to muscle damage. The current results unveiled a potential correlation (direct or indirect) between MANF activity and the hematopoietic process, at least during a regenerative pressure, and showed that its loss may originate defects in the formation of immune cells. This potential role of MANF in hematopoiesis may be due to MANF in HSCs or in the environment that controls these cells.

It remains unclear whether these findings are in some way related to the aged-associated defects in myeloid recruitment following a muscle injury identified in old mice[80].

The aging process is known to affect the hematopoietic system, directly impacting on HSCs and the BM niche. HSCs functionality is known to be reduced during aging, which leads to immune dysregulations and intrinsic alterations in myeloid lineage cells[90]. In turn, the numbers of HSCs are increased in aging, possibly to counteract their loss of function[91]. Hematopoietic aging has also been associated with HSCs and progenitors' lineage skewing and differentiation towards the myeloid lineage, having less differentiation potential to lymphoid cells in homeostasis[92–94]. Nevertheless, the impact of aging in hematopoiesis during a regenerative pressure remains unexplored. Thus, to our knowledge, it is not described if aged BM is able to efficiently respond to the immune challenge imposed by muscle injury.

This way, it is imperative to further analyse the hematopoietic populations of young and old mice after muscle injury. The characterization of young animals would facilitate the comprehension of the emergency hematopoietic response following muscle injury, while the study of old animals' hematopoiesis upon injury would clarify if the defects here identified in the absence of MANF have any similarity to the aging phenotype.

3.2.3 Effects of MANF loss in the phenotypic transition of macrophages

Macrophages' infiltration and their biphasic response within the damaged tissue are essential for successful skeletal muscle restoration[26]. These cells are a source of MANF after injury[76,80] and the loss of this protein is associated with a defective myeloid infiltration and a delay in the phenotypic transition

of macrophages after skeletal muscle injury. Thus, to better understand the causes of immune dysfunction during regeneration upon MANF loss, we next focus our study on the role of this protein on macrophages.

To assess the specific role of MANF in phenotypic transition, independently of the myeloid recruitment, we developed an *ex vivo* experiment where we eliminate the recruitment confounding factor and follow the phenotypic transition of macrophages.

In this assay, we used a different mouse model - LysM$^{CRE/+/}$Manf$^{fl/fl}$ mice - where MANF is ablated in all populations of macrophages in a tamoxifen-independent manner. With this model, we focused on the specific role of MANF in macrophages and the consequences of its particular loss. Similar to Rosa26 mice, this model exhibits myeloid alterations during the immune response to injury, having reduced numbers of myeloid cells within the regenerating tissue and defects in the phenotypic transition (unpublished data). Importantly, this model has the advantage over the Cx3cr1$^{CRE-ER/+,}$ Manf$^{fl/fl}$ model of eliminating the need to administer tamoxifen in culture to sustain MANF elimination in transitioning cells.

For this experiment, single-cell suspensions isolated from 2dpi muscles were cultured for 16h and the distribution of the macrophage populations was determined by FC at 0h and 16h. Macrophages were identified as F4/80^{pos} cells, and the different subsets were identified based on the expression levels of Ly6C. Macrophages with high, intermediate, and low levels of Ly6C were evaluated.

Importantly, cultured control macrophages were able to maintain their phenotypic transition capacity, recapitulating the phenotypic switch observed *in vivo*. Looking into the FC plots of Manf$^{fl/fl}$ cells (Figure 3.11A), we observed the normal immune shift from Ly6C^{High} pro-inflammatory macrophages to Ly6C^{Low} pro-repair macrophages after 16h. To better visualize this, we used the ratio Ly6C^{Low}/Ly6C^{High} that increases as more transition occurs (Figure 3.11C).

MANF deficient mice revealed a significant reduction in the emergent population of anti-inflammatory Ly6C^{Low} cells when compared to the control mice (Figure 3.11B). The ratio Ly6C^{Low}/Ly6c^{High} was significantly lower when MANF was ablated in macrophages suggesting a defect in transition, independently of the recruitment factor (Figure 3.11C).

These alterations seem to be related to defects in the early stages of the transition process since the macrophages' population with intermediate levels of Ly6C (Ly6C^{Int}) also appeared to be reduced in the MANF loss condition. The ratio Ly6C^{Int}/Ly6C^{High} after 16h tended to be lower when compared to controls, while the transition between Ly6C^{Int} and Ly6C^{Low} did not seem affected, seeming identical among both conditions (Figure 3.11D-E).

Furthermore, the number of CD11b^{pos} cells in the total cells present in the culture remained relatively constant, not being detected significant differences between the two timepoints in any of the conditions

(Figure 3.11F). This suggests that the defects identified in the phenotypic transition are not attributed to cell death happening during the process.

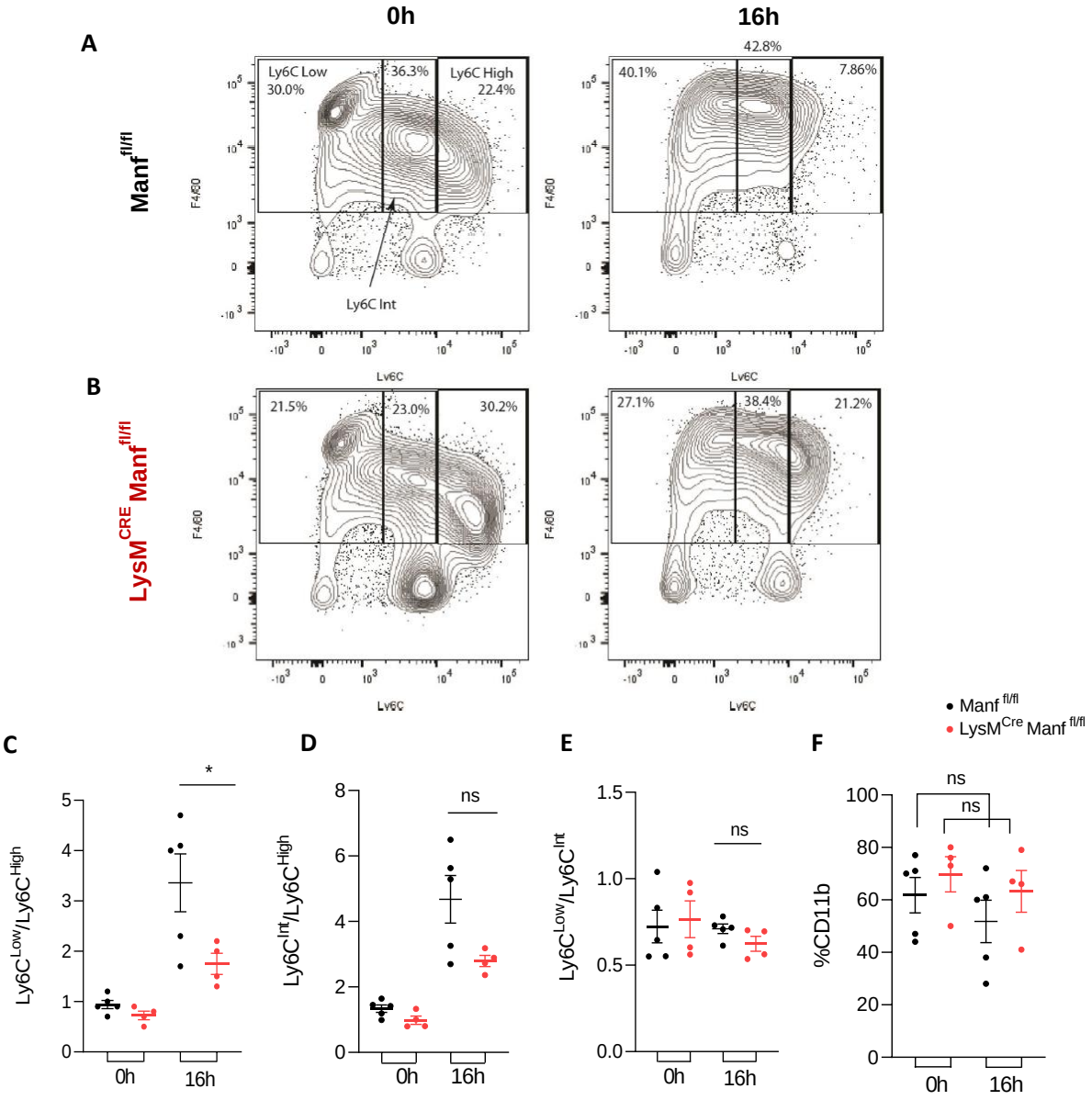

Figure 3.11 - Impact of conditional MANF deletion on the phenotypic transition of cultured macrophages, assessed by Flow Cytometry

A-B. Representative plots obtained by flow cytometry analysis of macrophage subsets at 0h and 16h after culture, gated on the CD11b^{pos} population. Macrophages analysed are originated from cultured single cell suspensions isolated from QC muscles of Manf$^{fl/fl}$ and LysM^{Cre}Manf$^{fl/fl}$ mice at 2dpi. **C-F.** Ratios of (C) pro-repair Ly6C^{Low} to pro-inflammatory Ly6C^{High} macrophages; (D) Ly6C^{Int} to Ly6C^{High} macrophages and (E) Ly6C^{Low} to Ly6C^{Int} macrophages and (F) percentage of myeloid CD11b^{pos} cells quantified by flow cytometry in single cells suspensions isolated from QC muscles from Manf$^{fl/fl}$ and LysM^{Cre}Manf$^{fl/fl}$ mice cultured for 0h and 16h. Data is presented as mean ± SEM and each point represents one animal. *p<0.05, and ns= not significant

Then, we accessed if the phenotypic transition process would be enhanced and restored by MANF supplementation during the incubation time. In this experiment, cells from each LysM$^{CRE/+}$Manf$^{fl/fl}$ mouse were analysed at 0h, 16h and at 16h with rMANF addition to the culture media. The results obtained showed a significant improvement in phenotypic transition since the ratios Ly6C^{Low}/Ly6c^{High} at 16 hours were higher in samples where MANF was added (Figure 3.12).

Therefore, the defects previously detected could be ameliorated by recombinant MANF supplementation, reinforcing the idea that extracellular MANF is involved in the macrophages' shift towards a pro-repair phenotype.

So, here we demonstrated that the absence of MANF in macrophages is sufficient to impair their phenotypic switch and that supplementation with MANF rescue to some extent these defects. Thus, MANF secreted by macrophages is crucial for the phenotypic transition of macrophages into the pro-repair state. In a previous study, it was demonstrated that MANF is specifically induced by pro-repair macrophages during muscle regeneration [80]. Thus, the present results strengthen the hypothesis of a feed-forward mechanism in which MANF induced by pro-repair macrophages facilitate the formation of new ones.

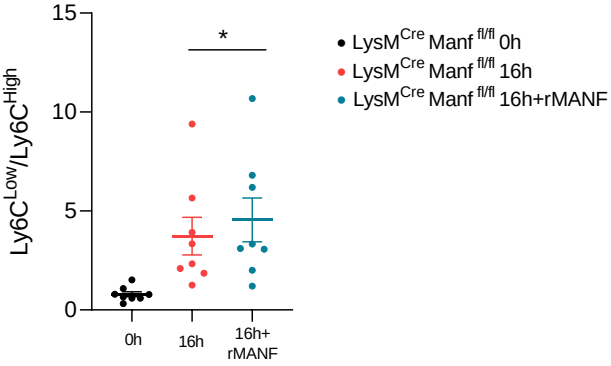

Figure 3.12 - Impact of MANF supplementation on the phenotypic transition of cultured MANF-deficient macrophages analysed by Flow Cytometry

Ratios of pro-repair Ly6C^{Low} to pro-inflammatory Ly6C^{High} macrophages quantified by flow cytometry in single cells suspensions isolated from QC muscles from Manf$^{fl/fl}$ and LysM^{Cre}Manf$^{fl/fl}$ mice after 0h and 16h, with or without recombinant MANF supplementation. Data is presented as mean ± SEM and each point at a certain timepoint represents one animal (n=8). *p<0.05

3.2.4 Pro-repair macrophages alterations upon MANF ablation

Macrophages have a central role in muscle regeneration, and MANF produced by these cells participate in the regulation of their phenotypic transition.

To further investigate the specific role of this protein on macrophages, we tried to characterize the intrinsic alterations of macrophages, zooming in on the pro-repair population, that is particularly responsible for the MANF induction after muscle injury, through transmission electron microscopy (TEM).

For that, we used the genetic mouse model Cx3cr1$^{CRE-ER/+,}$ Manf$^{fl/fl}$, that enables the conditional ablation of MANF upon tamoxifen injection only in the pro-repair population of macrophages and whose phenotype during regeneration has been already described[80]. This model reveals defects in immune response and phenotypic transition[80]. Oil-treated mice were used as controls.

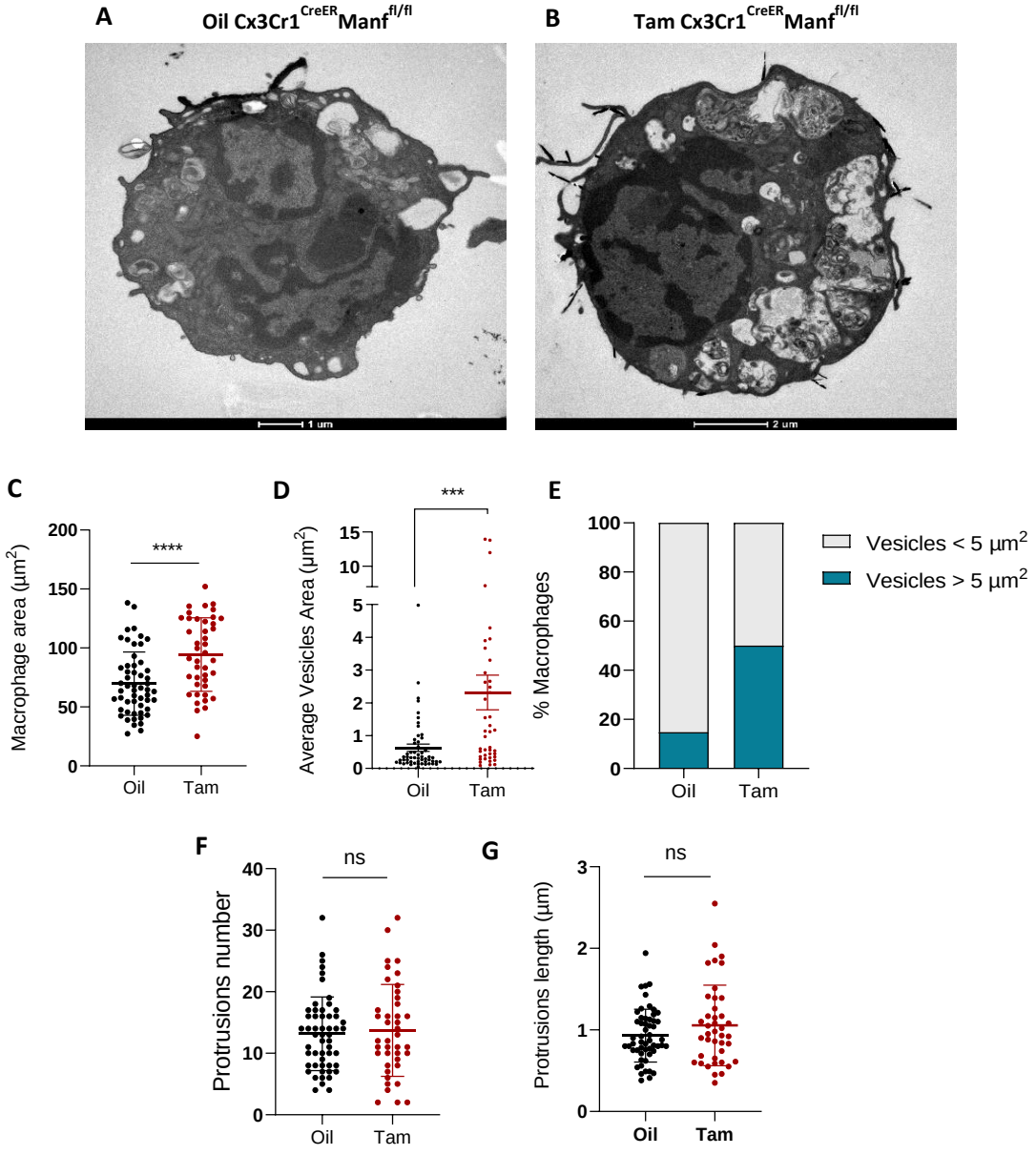

Figure 3.13 - Impact of MANF ablation in pro-repair macrophages evaluated by TEM
A-B. Representative images of F4/80^{pos}Ly6C^{Low} pro-repair macrophages isolated by FACS at 3dpi from QC muscles of Cx3Cr1^{CreER}Manf$^{fl/fl}$ that received (A) oil and (B) tam injections and visualized by TEM. Scale bar (A) 1 µm and (B) 2 µm. **C-G.** Quantifications analyses of these images for independent cells (n=54 macrophages from oil-treated Cx3Cr1^{CreER}Manf$^{fl/fl}$ and n=42 macrophages of tam-treated Cx3Cr1^{CreER}Manf$^{fl/fl}$). Quantification of (C) macrophage area (µm^2) (D), average area of intracellular vesicles (µm^2), (E) percentage of macrophages with at least one vesicle larger than 5 µm^2 and the (F) average number and (G) length (µm) of macrophages protrusions are shown. Data is represented as mean ± SEM and each point represents one macrophage. ****<0.0001, ***p<0.001 and ns= not significant.

F4/80^{pos}Ly6C^{Low} macrophages were isolated from muscle at 3dpi by FACS and further analysed in detail by transmission electron microscopy (TEM).

Comparing both conditions, it was possible to observe marked structural alterations in MANF-deficient pro-repair macrophages. These cells appear to be bigger and exhibited a high number of large vesicular structures, frequently filled with undigested cellular material (Figure 3.13A-B).

Quantification analysis confirmed the significantly increased size of macrophages with MANF ablation (Figure 3.13C). The average area of the vesicular structures was also significantly higher in macrophages from tam-treated mice (Figure 3.13D). In fact, control macrophages displayed on average vesicles with 0.6 μm^2, while the average area in MANF deficient macrophages was 3,8 times bigger. Moreover, 50% of MANF-deficient macrophages exhibited vesicles with more than 5μm^2, while only 14% of control macrophages had these big vesicles (Figure 3.13E). Regarding the number and length of macrophages' protrusions, no significant differences were found (Figure 3.13F-G).

These alterations may be explained by defects in the phagocytic pathway in macrophages with MANF deficiency, specifically in the digestion and intracellular processing of phagocytized cellular material. Phagocytosis involves the engulfment and internalization of fragments of dead cells into phagosomes that further mature and fuse with cellular endosomes and lysosomes[95]. These vesicular compartments carry several proteases, DNases and lipases that allow the elimination of the internalized cellular material[95,96]. Any alteration in this pathway may prevent debris digestion and impair the phagocytic capacity of macrophages.

This idea of an altered phagocytic function correlates with the previous results that reveal an accumulation of necrotic fibres and cell debris within the injury site when MANF is ablated[80].

Literature indicates that the elimination of cell debris by macrophages has immune regulatory roles, in addition to eliminating physical obstacles for regeneration. Previous studies have shown that phagocytosis of muscle debris contributes to macrophages' phenotypic transition and that inhibition of that process prevented the phenotype shift, affecting the regeneration process[42,97].

In addition, the literature points out that phagocytosis by macrophages in aged mice is impaired[98]. Therefore, we hypothesize that MANF loss in the pro-repair population that is also seen in aged animals may be associated with defective phagocytic function and consequent dysregulation of the phenotypic transition. In turn, impairments in the transition towards an anti-inflammatory state impact regeneration and are linked to unsuccessful muscle repair.

However, it is important to have in mind that the current analysis is just descriptive, and the phagocytic pathway must be further examined, for instance, by gene expression changes analysis and/or specific assays that allow quantification of debris ingestion and lysosomal digestion in macrophages.

Macrophages from young and old animals should also be visualized, in the future, by TEM to evaluate if they manifest similar phenotypes.

4

CONCLUSIONS

In this project, we demonstrated that the organismal loss of MANF leads to a severe regenerative failure of injured skeletal muscle (in short and long-term), characterized by dramatic accumulation of cellular debris and failure in the myogenic process. Furthermore, the immune response to damage is significantly impaired, regarding the myeloid infiltration after injury and the phenotypic transition of macrophages towards an anti-inflammatory state. The elevated severity of the regenerative and inflammatory impairments in the full MANF knockout mice, relative to the model of macrophage-specific ablation previously reported, confirmed that **MANF is a crucial factor for muscle regeneration** and indicates that MANF from other cellular sources may impact the regeneration process.

Organismal MANF loss also altered the number of circulating immune cells and disrupted the formation of myeloid progenitors in the bone marrow, uncovering a **potential role of MANF signalling in the hematopoietic process** during a muscular regenerative pressure and unveiling a possible reason for the defective myeloid recruitment identified upon damage.

The current study also strengthens the idea of an **autocrine mechanism of MANF in macrophages' phenotypic transition**. MANF conditional ablation in macrophages resulted in a defect in the phenotypic shift, independently of the defects in cell recruitment during muscle regeneration. Moreover, the transition process could be ameliorated by extracellular MANF supplementation.

Finally, our study points to intrinsic alterations in the macrophage pro-repair population when **MANF** is absent, particularly in the **digestion of engulfed material**, which can be associated with the transition defect identified.

Thus, this project demonstrates that the immune modulator **MANF participates in the muscle regeneration process through the regulation of the inflammatory response** to damage at multiple levels. Moreover, this study contributes to the identification of regenerative and inflammatory dysfunctions that occur as a consequence of MANF loss, enlightening how the age-related decline of MANF may impact the regenerative potential.

4.1 Future Perspectives

In the future, further studies must be performed to assess the resemblance of the results obtained in MANF deletion models to the defects occurring in the elderly. Bone marrow and blood cellular compositions must be evaluated also in aged and young animals during a regenerative pressure to clarify whether the defects that arise from systemic MANF deletion recapitulate (to some extent) defects occurring in aging. In addition, we also intend to analyse the pro-repair population of macrophages from old and young mice by TEM to verify if the intrinsic modifications detected in this study are also present in the aged condition.

Moreover, additional studies must be carried out to understand the role of MANF in emergency hematopoiesis. It would be of great interest to perform BM transplantation experiments. Transplantation of bone marrow from wild-type animals into animals with MANF deletion and vice-versa would help elucidate if the alteration of the bone marrow cells is sufficient to enhance or deteriorate, respectively, the regenerative potential and the immune response. In addition, reintroducing recombinant MANF in animals with MANF ablation would be important to understand if the defects identified in its absence could be rescued.

Importantly, it is necessary to further investigate the MANF mechanism and signalling in immune cells, particularly, in macrophages to comprehend the link between this protein and the regeneration process. Gene expression analysis should be performed in macrophages with MANF deletion for the identification of possible altered biological processes and pathways. Moreover, developing and establishing an *in vitro* model of MANF deletion would be imperative. Bone marrow-derived macrophages from animals with ubiquitous MANF deletion are potential candidates, so an effective protocol must be developed and optimized. After that, it would be possible to study potential impaired pathways in MANF loss conditions, including the phagocytic one. Phagocytic and digestion assays of necrotic and apoptotic material would be of great interest.

All this future work is fundamental to better characterize the relevance of MANF in the immune response during regeneration and its influence on the age-related decline in regenerative capacity. Understanding all this is crucial to translate MANF activities into clinical practice to improve regenerative therapies. Taking into account that immunomodulation has been considered a potential approach for improving stem cell-based therapies, future work may also involve the study of the benefits of MANF administration associated with MuSCs transplantation in the regenerative capacity. Thus, our study may contribute to the identification of MANF as a new candidate to enhance muscle repair in the elderly.

REFERENCES

1. United Nations, Department of Economic and Social Affairs & Population Division. *World Population Prospects 2019: Highlights*. (UN, 2019). doi:10.18356/13bf5476-en.

2. Dao, T. *et al.* Sarcopenia and muscle aging: A brief overview. *Endocrinology and Metabolism* vol. 35 716–732 (2020). https://doi.org/10.3803/EnM.2020.405

3. López-Otín, C., Blasco, M. A., Partridge, L., Serrano, M. & Kroemer, G. The hallmarks of aging. *Cell* vol. 153 1194 (2013). https://doi.org/10.1016/j.cell.2013.05.039

4. Neves, J. & Sousa-Victor, P. Regulation of inflammation as an anti-aging intervention. *FEBS J* **287**, 43–52 (2020).

5. Etienne, J., Liu, C., Skinner, C. M., Conboy, M. J. & Conboy, I. M. Skeletal muscle as an experimental model of choice to study tissue aging and rejuvenation. *Skeletal Muscle* vol. 10, 4 (2020). https://doi.org/10.1186/s13395-020-0222-1

6. World Health Organization. Ageing and health. https://www.who.int/news-room/fact-sheets/detail/ageing-and-health.

7. Franceschi, C. & Campisi, J. Chronic inflammation (Inflammaging) and its potential contribution to age-associated diseases. *Journals of Gerontology - Series A Biological Sciences and Medical Sciences* vol. 69 S4–S9 (2014) doi:10.1093/gerona/glu057.

8. Santoro, A., Bientinesi, E. & Monti, D. Immunosenescence and inflammaging in the aging process: age-related diseases or longevity? *Ageing Research Reviews* vol. 71 (2021). https://doi.org/10.1016/j.arr.2021.101422

9. Teissier, T., Boulanger, E. & Cox, L. S. Interconnections between Inflammageing and Immunosenescence during Ageing. *Cells* vol. 11 (2022). https://doi.org/10.3390/cells11030359

10. Hearps, A. C. *et al.* Aging is associated with chronic innate immune activation and dysregulation of monocyte phenotype and function. *Aging Cell* **11**, 867–875 (2012).

11. Neves, J., Sousa-Victor, P. & Jasper, H. Rejuvenating Strategies for Stem Cell-Based Therapies in Aging. *Cell Stem Cell* vol. 20 161–175 (2017). https://doi.org/10.1016/j.stem.2017.01.008

12. Arnardottir, H. H., Dalli, J., Colas, R. A., Shinohara, M. & Serhan, C. N. Aging Delays Resolution of Acute Inflammation in Mice: Reprogramming the Host Response with Novel Nano-Proresolving Medicines. *The Journal of Immunology* **193**, 4235–4244 (2014).

13. Duong, L. *et al.* Macrophage function in the elderly and impact on injury repair and cancer. *Immunity and Ageing* vol. 18 (2021). https://doi.org/10.1186/s12979-021-00215-2

14. Oishi, Y. & Manabe, I. Macrophages in inflammation, repair and regeneration. *International Immunology* vol. 30 511–528 (2018). https://doi.org/10.1093/intimm/dxy054

15. Yun, M. H. Changes in regenerative capacity through lifespan. *International Journal of Molecular Sciences* vol. 16 25392–25432 (2015). https://doi.org/10.3390/ijms161025392

16. Zhao, A., Qin, H. & Fu, X. What determines the regenerative capacity in animals? *BioScience* vol. 66 735–746 (2016). https://doi.org/10.1093/biosci/biw079

17. Muñoz-Cánoves, P., Neves, J. & Sousa-Victor, P. Understanding muscle regenerative decline with aging: new approaches to bring back youthfulness to aged stem cells. *FEBS Journal* vol. 287 406–416 (2020). https://doi.org/10.1111/febs.15182

18. Tedesco, F. S., Dellavalle, A., Diaz-Manera, J., Messina, G. & Cossu, G. Repairing skeletal muscle: Regenerative potential of skeletal muscle stem cells. *Journal of Clinical Investigation* vol. 120 11–19 (2010). https://doi.org/10.1172/JCI40373

19. Laumonier, T. & Menetrey, J. Muscle injuries and strategies for improving their repair. *Journal of Experimental Orthopaedics* vol. 3 (2016). https://doi.org/10.1186/s40634-016-0051-7

20. Dumont, N. A., Bentzinger, C. F., Sincennes, M. C. & Rudnicki, M. A. Satellite cells and skeletal muscle regeneration. *Compr Physiol* **5**, 1027–1059 (2015).

21. Frontera, W. R. & Ochala, J. Skeletal Muscle: A Brief Review of Structure and Function. *Behavior Genetics* vol. 45 183–195 (2015). https://doi.org/10.1007/s00223-014-9915-y

22. Gayraud-Morel, B., Chrétien, F. & Tajbakhsh, S. Skeletal muscle as a paradigm for regenerative biology and medicine. *Regenerative Medicine* vol. 4 293–319 (2009). https://doi.org/10.2217/17460751.4.2.293

23. Schmidt, M., Schüler, S. C., Hüttner, S. S., von Eyss, B. & von Maltzahn, J. Adult stem cells at work: regenerating skeletal muscle. *Cellular and Molecular Life Sciences* vol. 76 2559–2570 (2019). https://doi.org/10.1007/s00018-019-03093-6

24. Maynard, R. L. & Downes, N. The Musculature of the Rat. in *Anatomy and Histology of the Laboratory Rat in Toxicology and Biomedical Research* 57–76 (Elsevier, 2019). doi:10.1016/b978-0-12-811837-5.00006-x.

25. Yang, W. & Hu, P. Skeletal muscle regeneration is modulated by inflammation. *Journal of Orthopaedic Translation* vol. 13 25–32 (2018). https://doi.org/10.1016/j.jot.2018.01.002

26. Wang, X. & Zhou, L. The Many Roles of Macrophages in Skeletal Muscle Injury and Repair. *Frontiers in Cell and Developmental Biology* vol. 10 (2022). https://doi.org/10.3389/fcell.2022.952249

27. Karalaki, M., Fili, S., Philippou, A. & Koutsilieris, M. Muscle regeneration: cellular and molecular events. *In Vivo (Brooklyn)* **23**, (2009).

28. Dort, J., Fabre, P., Molina, T. & Dumont, N. A. Macrophages Are Key Regulators of Stem Cells during Skeletal Muscle Regeneration and Diseases. *Stem Cells International* vol. 2019 (2019). https://doi.org/10.1155/2019/4761427

29. Ceafalan, L. C., Popescu, B. O. & Hinescu, M. E. Cellular Players in Skeletal Muscle Regeneration. *Biomed Res Int* **2014**, 1–21 (2014).

30. Henze, H., Jung, M. J., Ahrens, H. E., Steiner, S. & von Maltzahn, J. Skeletal muscle aging – Stem cells in the spotlight. *Mech Ageing Dev* **189**, (2020).

31. Yin, H., Price, F. & Rudnicki, M. A. Satellite Cells and the Muscle Stem Cell Niche. *Physiol Rev* **93**, 23–67 (2013).

32. Lukjanenko, L. *et al.* Aging Disrupts Muscle Stem Cell Function by Impairing Matricellular WISP1 Secretion from Fibro-Adipogenic Progenitors. *Cell Stem Cell* **24**, 433-446.e7 (2019).

33. Yamakawa, H., Kusumoto, D., Hashimoto, H. & Yuasa, S. Stem cell aging in skeletal muscle regeneration and disease. *International Journal of Molecular Sciences* vol. 21 (2020). https://doi.org/10.3390/ijms21051830

34. Aurora, A. B. & Olson, E. N. Immune modulation of stem cells and regeneration. *Cell Stem Cell* vol. 15 14–25 (2014). https://doi.org/10.1016/j.stem.2014.06.009

35. Chazaud, B. Inflammation and Skeletal Muscle Regeneration: Leave It to the Macrophages! *Trends in Immunology* vol. 41 481–492 (2020). https://doi.org/10.1016/j.it.2020.04.006

36. Tidball, J. G. Regulation of muscle growth and regeneration by the immune system. *Nature Reviews Immunology* vol. 17 165–178 (2017). https://doi.org/10.1038/nri.2016.150

37. Ziemkiewicz, N., Hilliard, G., Pullen, N. A. & Garg, K. The role of innate and adaptive immune cells in skeletal muscle regeneration. *International Journal of Molecular Sciences* vol. 22 (2021). https://doi.org/10.3390/ijms22063265

38. Peiseler, M. & Kubes, P. More friend than foe: The emerging role of neutrophils in tissue repair. *Journal of Clinical Investigation* vol. 129 2629–2639 (2019). https://doi.org/10.1172/JCI124616

39. Kratofil, R. M., Kubes, P. & Deniset, J. F. Monocyte conversion during inflammation and injury. *Arteriosclerosis, Thrombosis, and Vascular Biology* vol. 37 35–42 (2017). https://doi.org/10.1161/ATVBAHA.116.308198

40. Novak, M. L. & Koh, T. J. Phenotypic transitions of macrophages orchestrate tissue repair. *American Journal of Pathology* vol. 183 1352–1363 (2013). https://doi.org/10.1016/j.ajpath.2013.06.034

41. Lu, H. *et al.* Macrophages recruited via CCR2 produce insulin-like growth factor-1 to repair acute skeletal muscle injury. *The FASEB Journal* **25**, 358–369 (2011).

42. Arnold, L. *et al.* Inflammatory monocytes recruited after skeletal muscle injury switch into antiinflammatory macrophages to support myogenesis. *Journal of Experimental Medicine* **204**, 1057–1069 (2007).

43. Saclier, M. *et al.* Differentially Activated Macrophages Orchestrate Myogenic Precursor Cell Fate During Human Skeletal Muscle Regeneration. *Stem Cells* **31**, 384–396 (2013).

44. Perdiguero, E. *et al.* p38/MKP-1–regulated AKT coordinates macrophage transitions and resolution of inflammation during tissue repair. *Journal of Cell Biology* **195**, 307–322 (2011).

45. Tidball, J. G., Flores, I., Welc, S. S., Wehling-Henricks, M. & Ochi, E. Aging of the immune system and impaired muscle regeneration: A failure of immunomodulation of adult myogenesis. *Exp Gerontol* **145**, (2021).

46. Xu, Y., Murphy, A. J. & Fleetwood, A. J. Hematopoietic Progenitors and the Bone Marrow Niche Shape the Inflammatory Response and Contribute to Chronic Disease. *International Journal of Molecular Sciences* vol. 23 (2022). https://doi.org/10.3390/ijms23042234

47. Gomes, A. C., Saraiva, M. & Gomes, M. S. The bone marrow hematopoietic niche and its adaptation to infection. *Seminars in Cell and Developmental Biology* vol. 112 37–48 (2021). https://doi.org/10.1016/j.semcdb.2020.05.014

48. Lee, J. Y. & Hong, S. H. Hematopoietic stem cells and their roles in tissue regeneration. *Int J Stem Cells* **13**, (2020).

49. Bonaud, A., Lemos, J. P., Espéli, M. & Balabanian, K. Hematopoietic Multipotent Progenitors and Plasma Cells: Neighbors or Roommates in the Mouse Bone Marrow Ecosystem? *Frontiers in Immunology* vol. 12 (2021). https://doi.org/10.3389/fimmu.2021.658535

50. Cheng, H., Zheng, Z. & Cheng, T. New paradigms on hematopoietic stem cell differentiation. *Protein and Cell* vol. 11 34–44 (2020). https://doi.org/10.1007/s13238-019-0633-0

51. Seita, J. & Weissman, I. L. Hematopoietic stem cell: Self-renewal versus differentiation. *Wiley Interdisciplinary Reviews: Systems Biology and Medicine* vol. 2 640–653 (2010). https://doi.org/10.1002/wsbm.86

52. Pietras, E. M. *et al.* Functionally Distinct Subsets of Lineage-Biased Multipotent Progenitors Control Blood Production in Normal and Regenerative Conditions. *Cell Stem Cell* **17**, 35–46 (2015).

53. Iwasaki, H. & Akashi, K. Myeloid Lineage Commitment from the Hematopoietic Stem Cell. *Immunity* vol. 26 726–740 (2007). https://doi.org/10.1016/j.immuni.2007.06.004

54. Fuchs, A. *et al.* Trauma Induces Emergency Hematopoiesis through IL-1/MyD88–Dependent Production of G-CSF. *The Journal of Immunology* **202**, 3020–3032 (2019).

55. Distefano, G. & Goodpaster, B. H. Effects of exercise and aging on skeletal muscle. *Cold Spring Harb Perspect Med* **8**, (2018).

56. Pacifico, J. *et al.* Prevalence of sarcopenia as a comorbid disease: A systematic review and meta-analysis. *Experimental Gerontology* vol. 131 (2020). https://doi.org/10.1016/j.exger.2019.110801

57. Aversa, Z., Zhang, X., Fielding, R. A., Lanza, I. & LeBrasseur, N. K. The clinical impact and biological mechanisms of skeletal muscle aging. *Bone* **127**, 26–36 (2019).

58. Domingues-Faria, C., Vasson, M. P., Goncalves-Mendes, N., Boirie, Y. & Walrand, S. Skeletal muscle regeneration and impact of aging and nutrition. *Ageing Research Reviews* vol. 26 22–36 (2016). https://doi.org/10.1016/j.arr.2015.12.004

59. Sousa-Victor, P. *et al.* Geriatric muscle stem cells switch reversible quiescence into senescence. *Nature* **506**, 316–321 (2014).

60. Conboy, I. M. *et al.* Rejuvenation of aged progenitor cells by exposure to a young systemic environment. *Nature* **433**, 760–764 (2005).

61. Sinha, M. *et al.* Restoring systemic GDF11 levels reverses age-related dysfunction in mouse skeletal muscle. *Science (1979)* **344**, 649–652 (2014).

62. Brack, A. S. *et al.* Increased Wnt signaling during aging alters muscle stem cell fate and increases fibrosis. *Science* **317**, 807–810 (2007).

63. Wang, Y. *et al.* Aging of the immune system causes reductions in muscle stem cell populations, promotes their shift to a fibrogenic phenotype, and modulates sarcopenia. *FASEB Journal* **33**, 1415–1427 (2019).

64. Sousa-Victor, P., Neves, J. & Muñoz-Cánoves, P. Muscle stem cell aging: identifying ways to induce tissue rejuvenation. *Mech Ageing Dev* **188**, (2020).

65. Yagi, T. *et al.* Neuroplastin Modulates Anti-inflammatory Effects of MANF. *iScience* **23**, (2020).

66. Sousa-Victor, P., Jasper, H. & Neves, J. Trophic factors in inflammation and regeneration: The role of ManF and CDNF. *Frontiers in Physiology* vol. 9 (2018). https://doi.org/10.3389/fphys.2018.01629

67. Yang, S., Li, S. & Li, X. J. MANF: A New Player in the Control of Energy Homeostasis, and Beyond. *Frontiers in Physiology* vol. 9 (2018). https://doi.org/10.3389/fphys.2018.01725

68. Petrova, P. S. *et al.* MANF A New Mesencephalic, Astrocyte-Derived Neurotrophic Factor with Selectivity for Dopaminergic Neurons. *Journal of Molecular Neuroscience* vol. 20 (2003).

69. Lindahl, M., Saarma, M. & Lindholm, P. Unconventional neurotrophic factors CDNF and MANF: Structure, physiological functions and therapeutic potential. *Neurobiology of Disease* vol. 97 90–102 (2017). https://doi.org/10.1016/j.nbd.2016.07.009

70. Danilova, T. & Lindahl, M. Emerging Roles for Mesencephalic Astrocyte-Derived Neurotrophic Factor (MANF) in Pancreatic Beta Cells and Diabetes. *Front Physiol* **9**, (2018).

71. Lindholm, P. *et al.* MANF is widely expressed in mammalian tissues and differently regulated after ischemic and epileptic insults in rodent brain. *Molecular and Cellular Neuroscience* **39**, 356–371 (2008).

72. Lindahl, M. *et al.* MANF Is Indispensable for the Proliferation and Survival of Pancreatic β Cells. *Cell Rep* **7**, 366–375 (2014).

73. Kim, Y., Park, S. J. & Chen, Y. M. Mesencephalic astrocyte-derived neurotrophic factor (MANF), a new player in endoplasmic reticulum diseases: structure, biology, and therapeutic roles. *Translational Research* vol. 188 1–9 (2017). https://doi.org/10.1016/j.trsl.2017.06.010

74. Manf mesencephalic astrocyte-derived neurotrophic factor [Mus musculus (house mouse)] - Gene - NCBI. https://www.ncbi.nlm.nih.gov/gene?Db=gene&Cmd=DetailsSearch&Term=74840.

75. Voutilainen, M. H. *et al.* Mesencephalic Astrocyte-Derived Neurotrophic Factor Is Neurorestorative in Rat Model of Parkinson's Disease. *Journal of Neuroscience* **29**, 9651–9659 (2009).

76. Neves, J. *et al.* Immune modulation by MANF promotes tissue repair and regenerative success in the retina. *Science (1979)* **353**, (2016).

77. Tadimalla, A. *et al.* Mesencephalic Astrocyte-Derived Neurotrophic Factor Is an Ischemia-Inducible Secreted Endoplasmic Reticulum Stress Response Protein in the Heart. *Circ Res* **103**, 1249–1258 (2008).

78. Sousa-Victor, P. *et al.* MANF regulates metabolic and immune homeostasis in ageing and protects against liver damage. *Nat Metab* **1**, 276–290 (2019).

79. Chen, L. *et al.* Mesencephalic Astrocyte-Derived Neurotrophic Factor Is Involved in Inflammation by Negatively Regulating the NF-κB Pathway. *Sci Rep* **5**, (2015).

80. Simões de Sousa, N. S. Regulation of skeletal muscle repair by mesencephalic astrocyte-derived neurotrophic factor *[Master's thesis]*. (2021). http://hdl.handle.net/10362/134442

81. Shi, J., Hua, L., Harmer, D., Li, P. & Ren, G. Cre driver mice targeting macrophages. in *Methods in Molecular Biology* vol. 1784 263–275 (Humana Press Inc., 2018).

82. Bournazos, S., Wang, T. T. & Ravetch, J. v. The Role and Function of Fcγ Receptors on Myeloid Cells. *Microbiol Spectr* **4**, (2016).

83. Fischer, A. H., Jacobson, K. A., Rose, J. & Zeller, R. Hematoxylin and Eosin Staining of Tissue and Cell Sections. *Cold Spring Harb Protoc* **2008**, pdb.prot4986 (2008).

84. Fortes, M. A. S. *et al.* Housekeeping proteins: How useful are they in skeletal muscle diabetes studies and muscle hypertrophy models? *Anal Biochem* **504**, 38–40 (2016).

85. Bencze, M., Periou, B., Baba-Amer, Y. & Authier, F. J. Immunolabelling myofiber degeneration in muscle biopsies. *Journal of Visualized Experiments* **2019**, (2019).

86. Lu, H., Huang, D., Ransohoff, R. M. & Zhou, L. Acute skeletal muscle injury: CCL2 expression by both monocytes and injured muscle is required for repair. *The FASEB Journal* **25**, 3344–3355 (2011).

87. Bryer, S. C., Fantuzzi, G., van Rooijen, N. & Koh, T. J. Urokinase-Type Plasminogen Activator Plays Essential Roles in Macrophage Chemotaxis and Skeletal Muscle Regeneration. *The Journal of Immunology* **180**, 1179–1188 (2008).

88. van de Vlekkert, D., Machado, E. & D'azzo, A. Analysis of Generalized Fibrosis in Mouse Tissue Sections with Masson's Trichrome Staining. *Bio Protoc* **10**, (2020).

89. Urao, N., Liu, J., Takahashi, K. & Ganesh, G. Hematopoietic Stem Cells in Wound Healing Response. *Adv Wound Care (New Rochelle)* **11**, 598–621 (2022).

90. Kovtonyuk, L. v., Fritsch, K., Feng, X., Manz, M. G. & Takizawa, H. Inflamm-aging of hematopoiesis, hematopoietic stem cells, and the bone marrow microenvironment. *Frontiers in Immunology* vol. 7 (2016). https://doi.org/10.3389/fimmu.2016.00502

91. Lee, J., Yoon, S., Choi, I. & Jung, H. Causes and Mechanisms of Hematopoietic Stem Cell Aging. *Int J Mol Sci* **20**, 1272 (2019).

92. Broxmeyer, H. E. *et al.* Fate of Hematopoiesis During Aging. What Do We Really Know, and What are its Implications? *Stem Cell Rev Rep* **16**, 1020–1048 (2015).

93. Dykstra, B., Olthof, S., Schreuder, J., Ritsema, M. & Haan, G. de. Clonal analysis reveals multiple functional defects of aged murine hematopoietic stem cells. *Journal of Experimental Medicine* **208**, 2691–2703 (2011).

94. Pang, W. W. *et al.* Human bone marrow hematopoietic stem cells are increased in frequency and myeloid-biased with age. *Proc Natl Acad Sci U S A* **108**, 20012–20017 (2011).

95. Rosales, C. & Uribe-Querol, E. Phagocytosis: A Fundamental Process in Immunity. *Biomed Res Int* 1–18 (2017) doi:10.1155/2017/9042851.

96. Westman, J., Grinstein, S. & Marques, P. E. Phagocytosis of Necrotic Debris at Sites of Injury and Inflammation. *Front Immunol* **10**, (2020).

97. Zhang, J. *et al.* Phagocytosis mediated by scavenger receptor class BI promotes macrophage transition during skeletal muscle regeneration. *Journal of Biological Chemistry* **294**, 15672–15685 (2019).

98. Li, W. Phagocyte dysfunction, tissue aging and degeneration. *Ageing Res Rev* **12**, 1005–1012 (2013).

99. Nguyen, J. H., Chung, J. D., Lynch, G. S. & Ryall, J. G. The Microenvironment Is a Critical Regulator of Muscle Stem Cell Activation and Proliferation. *Front Cell Dev Biol* **7**, (2019).

A

APPENDIX

A.1 Recipes

- **Tragacanth Gum**: 5g of Tragacanth (Sigma-Aldrich), 50ml of Milli-Q® water, 500µl of 16% (w/v) Formaldehyde solution Methanol free (Thermo Scientific).
- **Separating gel (12%):** 3.2ml of Acrylamide 30%; 2.6ml Milli-Q® water; 2ml Tris 1.5M ph8.8; 80µl of sodium dodecyl sulfate (SDS) 10%; 80µl of Ammonium persulphate (APS) 10%; 8µl of Tetramethylethylenediamine (TEMED).
- **Stacking gel** (2 gels): 1ml of Acrylamide 30%; 2.6ml Milli-Q® water; 1.25ml Tris 0.5M ph6.8; 50µl SDS 10%, 50µl APS 10%, 5µl TEMED.